Institutionen för systemteknik
Department of Electrical Engineering

Examensarbete

Charging Cost Optimization of Plug-in Hybrid Electric Vehicles

Master's thesis performed in Vehicular Systems
at Linköping Institute of Technology
by

Markus Knutfelt

LiTH-ISY-EX--15/4829--SE

Linköping 2015

Linköpings universitet
TEKNISKA HÖGSKOLAN

Department of Electrical Engineering
Linköpings universitet
SE-581 83 Linköping, Sweden

Linköpings tekniska högskola
Linköpings universitet
SE-581 83 Linköping, Sweden

Charging Cost Optimization of Plug-in Hybrid Electric Vehicles

Master's thesis performed in Vehicular Systems
at Linköping Institute of Technology
by

Markus Knutfelt

LiTH-ISY-EX--15/4829--SE

Supervisor: Martin Sivertsson, ISY, Linköping University

Examiner: Mattias Krysander, ISY, Linköping University

Linköping 2015-06-11

Presentation Date

2015-06-11

Publishing Date (Electronic version)

2015-06-22

Linköping University
Department of Electrical Engineering
Division of Vehicular Systems
SE-581 83 Linköping
SWEDEN

Language

_X_ English
___ Other (specify below)

Number of Pages
98

Type of Publication

___ Licentiate thesis
_X_ Degree thesis
___ Thesis C-level
___ Thesis D-level
___ Report
___ Other (specify below)

ISBN (Licentiate thesis)

ISRN: LiTH-ISY-EX--15/4829--SE

Title of series (Licentiate thesis)

Series number/ISSN (Licentiate thesis)

URL, Electronic Version
http://www.ep.liu.se

Publication Title
Charging Cost Optimization of Plug-in Hybrid Electric Vehicles

Author(s)
Markus Knutfelt

Abstract

The future success of chargeable vehicles will, among other factors, depend on their charging costs and their ability to charge with minimal disturbances to the national, local and household electrical grid. To be able to minimize costs and schedule charging sessions, there has to be knowledge of how the charging power varies with time. This is called charging profile. A number of charging profiles for a Volvo V60 plug-in hybrid electric vehicle have been recorded. For charging currents above 10 A they prove to be more complex than are assumed in most current research papers.

The charging profiles are used together with historical electricity prices to calculate charging costs for 2013 and 2014. Charging is assumed to take place during the night, between 18:00 and 07:00, with the battery being totally depleted at 18:00. By using a timer to have the charging start at 01:00, instead of immediately at 18:00, annual charging costs are reduced by approximately 7 to 8%. By using dynamic programming to optimize the charging sessions, annual charging costs are reduced by approximately 10 to 11%. An interesting issue regarding dynamic programming was identified, namely when using a limited set of predetermined discrete control signals, interpolation returns unrealizable cost-to-go values. This occurs specifically for instances crossing the zero cost-to-go area boundary.

It is concluded that the mentioned savings are realizable, via implementing timers or optimization algorithms into consumer charging stations. Finally, by using these decentralized charging planning tools and seen from a power usage perspective, at least 30% of the Swedish vehicle fleet could be chargeable and powered by the electrical grid.

Keywords
charging cost optimization profiles dynamic programming electric vehicles

Abstract

The future success of chargeable vehicles will, among other factors, depend on their charging costs and their ability to charge with minimal disturbances to the national, local and household electrical grid. To be able to minimize costs and schedule charging sessions, there has to be knowledge of how the charging power varies with time. This is called charging profile. A number of charging profiles for a Volvo V60 plug-in hybrid electric vehicle have been recorded. For charging currents above 10 A they prove to be more complex than are assumed in most current research papers.

The charging profiles are used together with historical electricity prices to calculate charging costs for 2013 and 2014. Charging is assumed to take place during the night, between 18:00 and 07:00, with the battery being totally depleted at 18:00. By using a timer to have the charging start at 01:00, instead of immediately at 18:00, annual charging costs are reduced by approximately 7 to 8%. By using dynamic programming to optimize the charging sessions, annual charging costs are reduced by approximately 10 to 11%. An interesting issue regarding dynamic programming was identified, namely when using a limited set of predetermined discrete control signals, interpolation returns unrealizable cost-to-go values. This occurs specifically for instances crossing the zero cost-to-go area boundary.

It is concluded that the mentioned savings are realizable, via implementing timers or optimization algorithms into consumer charging stations. Finally, by using these decentralized charging planning tools and seen from a power usage perspective, at least 30% of the Swedish vehicle fleet could be chargeable and powered by the electrical grid.

To MSOSM

Acknowledgement

This thesis finalizes my Master of Science (Civilingenjör) degree in Applied Physics and Electrical Engineering (Teknisk Fysik och Elektroteknik - Y) at Linköping University.

I've written this master's thesis at Vehicular Systems at Linköping University from December 2014 to June 2015. It has been a great time thanks to the people working there. I would especially like to thank Christofer Sundström, my supervisor Martin Sivertsson, and my examiner Mattias Krysander.

Linköping, June 2015

Markus Knutfelt

If you have any comments or questions, please don't hesitate to contact me via email:
MARKUS@KNUTFELT.SE

Table of Contents

1 Introduction 1
  1.1 Motivation 1
  1.2 Purpose 2
  1.3 Problem statements 2
  1.4 Delimitations 3
  1.5 Miscellaneous 4
2 Background 5
  2.1 The charging station 5
  2.2 The vehicle 8
    2.2.1 Specifications 8
    2.2.2 Charging the vehicle 10
    2.2.3 Driving modes 11
    2.2.4 Preconditioning of the cabin 12
    2.2.5 Conditioning of the battery 12
    2.2.6 Fully charged and totally depleted battery 13
    2.2.7 Totally depleting the battery 14
  2.3 System overview 15
3 Theory 17
  3.1 Vehicle charging profile logging and analysis 17
    3.1.1 Power factor 17
    3.1.2 Vehicle charging 18
    3.1.3 Lithium-ion batteries 20
    3.1.4 The vehicle / charging station relation 24
  3.2 Micro and macro perspective on vehicle charging 24
  3.3 Dynamic Programming 25
    3.3.1 Formal description of dynamic programming 27
4 Measurements 31
  4.1 Considerations 31
  4.2 Measurement equipment 31
  4.3 Measurements overview 33
  4.4 Thermal battery aspects 33
  4.5 Charging sessions 34
    4.5.1 Charging session 1 35

4.5.2 Charging session 2 36
4.5.3 Charging session 3 37
4.5.4 Charging session 4 38
4.5.5 Charging session 5 39
4.6 Summary 40
5 Charging cost simulations 41
5.1 Electricity prices 41
5.2 Timer started charging session 42
5.3 Timer start at cheapest hour for each individual night 44
5.4 Simulation results 47
6 Charging scheduling with dynamic programming 49
6.1 The grid and matrix setup 49
6.2 Cost-to-go 51
6.3 New state calculation and interpolation 51
6.4 Calculating the cost-to-go matrix 54
6.5 Finding the optimal state trajectory 57
6.6 Results 58
7 Dynamic programming boundary issues 63
7.1 Issues introduction 63
7.2 Formal issues description 64
7.3 Current research 67
7.4 Solutions 67
7.4.1 Negative cost-to-go values 67
7.4.2 Change the interpolation function 68
7.4.3 Add an extra row to the grid 71
8 Discussion 75
8.1 Charging profiles 75
8.1.1 Ambient temperature 75
8.1.2 Thermal battery aspects 75
8.1.3 Ramp down 76
8.1.4 Battery capacity available to the driver 77
8.1.5 Measurements versus specifications 78
8.2 Charging cost: simulation vs optimization 79
8.3 What can be done short term? 79
8.4 What can be done long term? 80

8.5 Dynamic programming issues 80
8.6 The power gap 80
8.7 Swedish energy taxation issues 83
8.8 Method 84
9 Conclusions 87
9.1 Key findings and main conclusions 87
9.2 Future work 88
9.2.1 Immediate accessible range 88
9.2.2 The buffer battery 88
9.2.3 Battery state of health impact on charging energy consumption 88
9.2.4 Charging indoors and outdoors 88
9.2.5 Post charging cooling 88
9.2.6 Charging current ramp down 89
9.2.7 Solving the boundary crossing issues 89
9.2.8 Improvements on the timer started charging session 89
9.2.9 Charging efficiency and ambient temperature 89
9.2.10 Optimization made easy 89
Appendix 91
A Dynamic programming settings 91
B Brennenstuhl PM 231 E power meter 92
C Electricity prices import routine 93
D Volvo V60 PHEV specifications 94
Bibliography 95

Notation

Abbreviation	Meaning
AC	alternating current
BEMS	building energy management system
CC	constant current
CtG	cost-to-go
CV	constant voltage
DC	direct current
DP	dynamic programming
EV	electric vehicle
EVSE	electric vehicle supply equipment (i.e. a charging station)
GPS	global positioning system
ICE	internal combustion engine
inf	infinity
Li-ion	lithium-ion (battery)
MPC	model predictive control
OCV	open circuit voltage
PF	power factor
PHEV	plug-in hybrid electric vehicle
SOA	safe operating area
SoC	state of charge
SoH	state of health
TPoE	total price of electricity
VAT	value added tax
VIN	vehicle identification number

1 Introduction

People like to move around, not only for fun but also to make a society function and be successful. Walking or riding a bike only uses foodstuff as energy source. But what happens if people want to move quickly, long distances, or are just lazy? Then there's need for some kind of transportation. Nonscheduled personal transportation has now for many years almost exclusively been powered by oil, or sometimes gas, in rich countries. Today, 2015, there are many environmental, political, economic and national safety related reasons to end this habit.

So, what could be done? One idea is to do research on how a transition away from oil and gas could be executed. This master's thesis can be seen as a part of the research project *Investigation of user behavior for partially electrified environmentally adopted carpool*, and its work package *Charging scenarios and smart energy usage in "Smart Post Carbon Cities"*.

1.1 Motivation

To protect the environment and save energy increased efforts are put into the development of electric and hybrid vehicles. Electricity is getting more and more important in the transportation sector. (Diallo, Benbeouzid and Masrur, 2013, p. 962)

One of the main consequences of this is the need for injecting and storing externally generated electrical energy in vehicles, commonly known as charging. Plug-in hybrid electric vehicles (PHEV) and pure electric vehicles (EV) thus need to be charged, primarily from the electrical grid. A PHEV has got a battery and an "ordinary" internal combustion engine (ICE), that use e.g. gasoline. An EV has a battery as its only source of energy.

Thus to be able to move away from fossil fuels as energy sources in vehicles, the process of charging has to be studied and refined. It must become easy and cheap for consumers to use a chargeable vehicle.

1.2 Purpose

Most people with a driving license know what to expect from a vehicle with an internal combustion engine. For example the need to go to the gas station or change engine oil once in a while.

Owning a chargeable vehicle introduces a large spectrum of new challenges quite different from the simple chore of going to the gas station. But what are the challenges owning a chargeable vehicle?

1.3 Problem statements

Charging is mainly done at the homes of people and at their workplaces. But there is also a need for "public" charging, of which there are mainly two types (Lindergren 2014). The first one is activity based charging. This means that one takes the opportunity to charge one's vehicle while one does an activity away from home, such as shopping, practice sports or go to the cinema. The other type of public charging is when one takes a break during a road trip with the main purpose of charging one's vehicle. This is most often done where there are fast chargers using a much higher power output than ordinary chargers. Fast chargers can today mostly be found in larger cities and along "electrical corridors". Simply put, electrical corridors are fast chargers strategically positioned along main roads between larger cities.

One important detail is that the non-fast chargers of today does not get information about state of charge (SoC), i.e. how fully charged the battery is, from the vehicle (Lindergren 2014). This can make it difficult to plan a charging session, if there is no method to know how long it will last. According to Lindergren one method to get SoC could be for the charging station to connect to the vehicle's manufacturer, who in turn could get the SoC using the vehicle's built in telematics.

This thesis will mainly investigate charging in the home environment. One main issue is the maximum current limit set by the home's electrical service. A household has many other needs for electrical power than charging a vehicle, especially if it is heated by electric energy. Computers, air conditioning equipment, dish washers, washing machines etc. all consume electric energy. Therefore, if a vehicle's charging can be moved to a point in time when other energy usage in the household might be low, a household may both save money and be rid of issues regarding reaching power usage limits.

This thesis will answer the following questions:

- How does a vehicle consume electric energy when it is charged? This is called charging profile.
- Since energy prices fluctuate during the day, how to minimize the cost of charging the vehicle? Are any charging cost savings possible to realize?

Further, what are the challenges on a macro (regional / national) level of having a large fleet of chargeable vehicles? Are there solutions on the micro (household) level that might solve those on the macro level?

Thus this thesis is expected to find what vehicle charging profiles look like, and use that information as an input when optimizing charging sessions. Can optimized vehicle charging coexist with a family living in a household, with minimal lifestyle changes?

The realization aspect involves factors such as if equipment that saves money can be manufactured and sold for less money than they aim to save. Handling a large fleet of chargeable vehicles involves questions such as how the charging could be coordinated, to minimize strains on the electric grid. Is there potential, from a national power supply perspective, to have a large fleet of chargeable vehicles in Sweden?

1.4 Delimitations

This thesis will mainly be focused on charging a vehicle during the night between 18:00 and 07:00; every day of the year. This is to simulate a vehicle e.g. used to commute during the workweek, and used for pleasure during the weekend. The battery will be assumed to be depleted at the beginning of each charging session. Please note that the optimization algorithm used can handle any valid SoC level as an initial condition.

With an electric range of approximately 40 km for the vehicle used in the thesis, these criteria means a reasonable total yearly driving distance of 14 600 km.

SoC will thus be considered as known to the algorithm, and state of health (SoH), i.e. how "worn" the battery is, will be assumed as constant, even if a battery actually deteriorates with time, between charging sessions. In this case the timeframe is so short and the vehicle usage so low that this shouldn't be a problem. The exact same vehicle has been used for all measurements, done within a month, to minimize SoH impact.

1.5 Miscellaneous

To better understand the plots in this thesis, it might be handy to keep in mind that there are 8760 hours in one year. A plot of one year often has hours of the year on the x-axis. The first hour of the year, hour 1, begins at 00:00 January the 1st and ends at 01:00 that same day.

On the same theme, a plot might run from the 19th to the 36th hour. Hour 19 (18:00-19:00) to 24 (23:00-00:00) belongs to the first day (of the year), and hour 25 to 36 is hour 1 to 12 on the second day (of the year).

In a few instances the first hour, 00:00 to 01:00, is labelled hour 0, etc. These cases are clearly pointed out to the reader.

Further, in some cases there are "wrapping issues". Electricity prices are given and imported into Matlab on a year by year basis, and only two years are available, 2013 and 2014. For example, assume a vehicle charging is started at 23:00 December 31st 2014. What electricity price are to be used for hour 2 and forward of that charging? In these cases the Matlab code written usually copies the results from 30th December into 31st December; the equations given in this thesis doesn't regard these "wrapping issues".

Why can it be OK to copy the costs like this? Firstly the cost of one day only represents circa 1/365th of the total cost for a year. Secondly, assume that day 365 actually was 10% more expensive than day 364, then the error is close to 1/3650th, which is negligible.

For the international reader, it might be interesting to know that as of June 2015
1 SEK ≈ 0.11 USD ≈ 0.12 EUR.

2 Background

Since the oil based vehicle energy infrastructure is so dominant today, the vehicle charging infrastructure is somewhat unknown to most people. This chapter briefly outlines how it works.

2.1 The charging station

A charging station is a device used to connect a vehicle to a source of electric energy. An example can be seen in Figure 1. Though "charger" is in most cases a somewhat misleading term. To be precise, for non-fast charging the vehicle's charger is found on board the vehicle. That charger takes the alternating current (AC) from the electrical grid and converts it to direct current (DC), which then charges the battery. Thus the charging station, in its simplest form (say for home use), is not a "charger". It is only a rather simple box that supplies the electrical energy from the grid to the vehicle. This box, cord and plug has a formal name, electric vehicle service equipment (EVSE) (PluginCars.com, 2014).

Some non-fast charging stations, often for public usage, are more advanced. They might contain a small computer, can be remote controlled and has the ability to control the vehicle charging current (Lindergren, 2014).

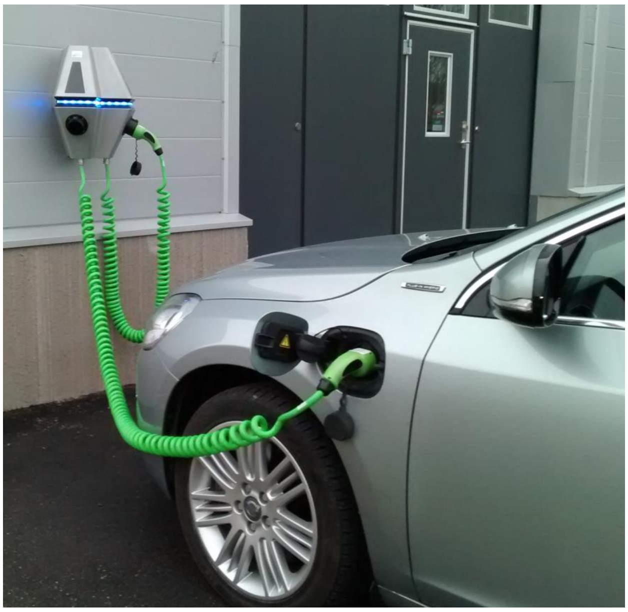

Figure 1: Chargestorm's CSR100 charging station, connected to a Volvo V60 PHEV, outside the L-building, Linköping University.

Fast charging stations, e.g. those of the CHAdeMO standard, deliver DC to the vehicle, and thus are more deserving of their name. This thesis will with very few exceptions focus on non-fast charging stations. Figure 2 shows a fast charging station.

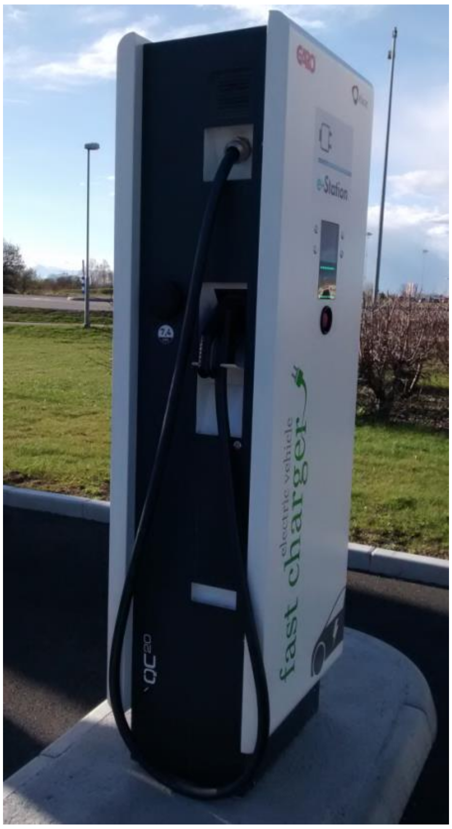
GARO
e-Station
electric vehicle
fast charger
QC20

Figure 2: The Garo QC20 fast charging station, outside Engströms Bil, Linköping.

For the charging measurements in this thesis, a Mennekes 35084 portable charging station was used. This charging station is supplied together with Volvo V60 PHEVs, and the user manual of the vehicle even details how to use the charging station.

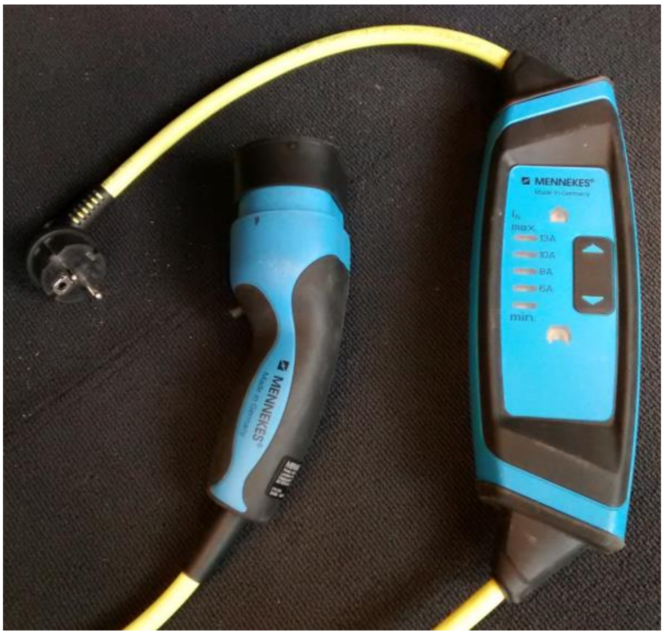

Figure 3: The Mennekes 35084 portable charging station used in this thesis.

As can be seen in the Figure 3, The Mennekes 35084 connects to the electrical grid using a standard single phase 230 V Schucko plug. On the vehicle side it has a type 2 mode 3 connector. The charging station allows the user to set a preferred charging current, 6, 8, 10, or 13 A. Most Schucko wall sockets in Sweden are rated for a maximum of 10 A. Therefor an adapter that converts a 16 A 3-phase IEC 60309 wall socket to a 16 A single phase Schucko socket was used to do the 13 A measurement.

2.2 The vehicle

The division of Vehicular Systems has access to two plug-in hybrid electric vehicles. They are pre-production versions of the Volvo V60 D6 AWD PHEV.

All measurements were done on the Volvo V60 PHEV with registration plate MHP509, manufactured in 2012. It has a mileage of approximately 20 000 km, and can be seen in Figure 4.

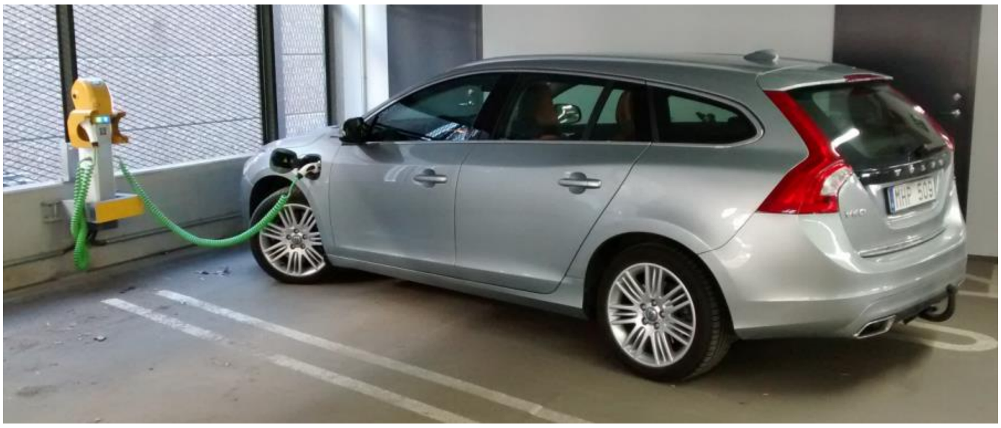

Figure 4: Volvo V60 PHEV charging with a Garo charger at the Linköping University Hospital parking garage.

2.2.1 Specifications

Selected data from the specifications for the production version of the vehicle (Volvo Cars, n.d.):

- Hybrid system: PHEV
- Combustion engine: 2.4 l, five cylinder diesel (215 hp, 440 Nm)
- Transmission: 6-speed automatic
- Electric motor / final drive: Synchronous AC (50 kW / 70 hp, 200 Nm) / 9.16
- Battery: Lithium-ion, 400 V, 11.2 kWh
- Weight compared to ordinary front-wheel drive V60: +300 kg (weight of battery: 150 kg)
- Acceleration: 0-100 km/h: 6.1 s
- Top speed: 230 km/h (actively limited)
- Top speed with only electric motor active: 120 km/h (actively limited)
- Charging times (empty to full):
    - 16 A: 3.5 h
    - 10 A: 4.5 h
    - 6 A: 7.5 h

For more information and specifications, see Appendix D.

Using the charging times (empty to full) from the specifications gives the following intervals for theoretical energy usage (assuming e.g. constant current charging etc.):

- 16 A: **3.5** h $\Rightarrow\ 230 \cdot 16 \cdot [3.25\ \mathbf{3.5}\ 3.74] = [11.96\ \ \mathbf{12.880}\ 13.76]$ kWh
- 10 A: **4.5** h $\Rightarrow\ 230 \cdot 10 \cdot [4.25\ \mathbf{4.5}\ \ 4.74] = [9.76\ \mathbf{10.350}\ 10.90]$ kWh
- 6 A: **7.5** h $\Rightarrow\ 230 \cdot 6 \cdot [7.25\ \mathbf{7.5}\ \ 7.74] = [10{,}01\ \ \mathbf{10.350}\ \ 10.69]$ kWh

As with most chargeable vehicles, the full battery capacity, here 11.2 kWh, isn't available to the driver. This can easily be understood by comparing 11.2 kWh with the energy usage calculations above, which in some cases are below 11.2 kWh. To preserve the battery SoH, the driver has access to approximately 80% of total battery capacity. From 10% of real SoC to 90% of real SoC. Since this real interval is hidden from the driver, when SoC is mentioned in this thesis, it is in reference to the capacity available to the driver. The energy available to the driver could therefore be approximated as

$$0.8 \cdot 11.2 = 8.96\ \text{kWh}$$

This hints at a charging losses of

$$\frac{10.35 - 8.96}{10.35} \approx 13\%$$

at best, if all assumptions are correct.

The V60 PHEV is a "through the road hybrid", with the diesel engine driving the front wheels, and the electric motor driving the rear wheels. The lithium-ion (Li-ion) battery is located below the luggage compartment.

2.2.2 Charging the vehicle

Charging the vehicle is easy, open the cap and insert the connector. Once connected, the vehicle uses the charging current and SoC of the vehicle to calculate and show an estimation of when the vehicle will be fully charged in the dashboard. This can be seen in Figure 5.

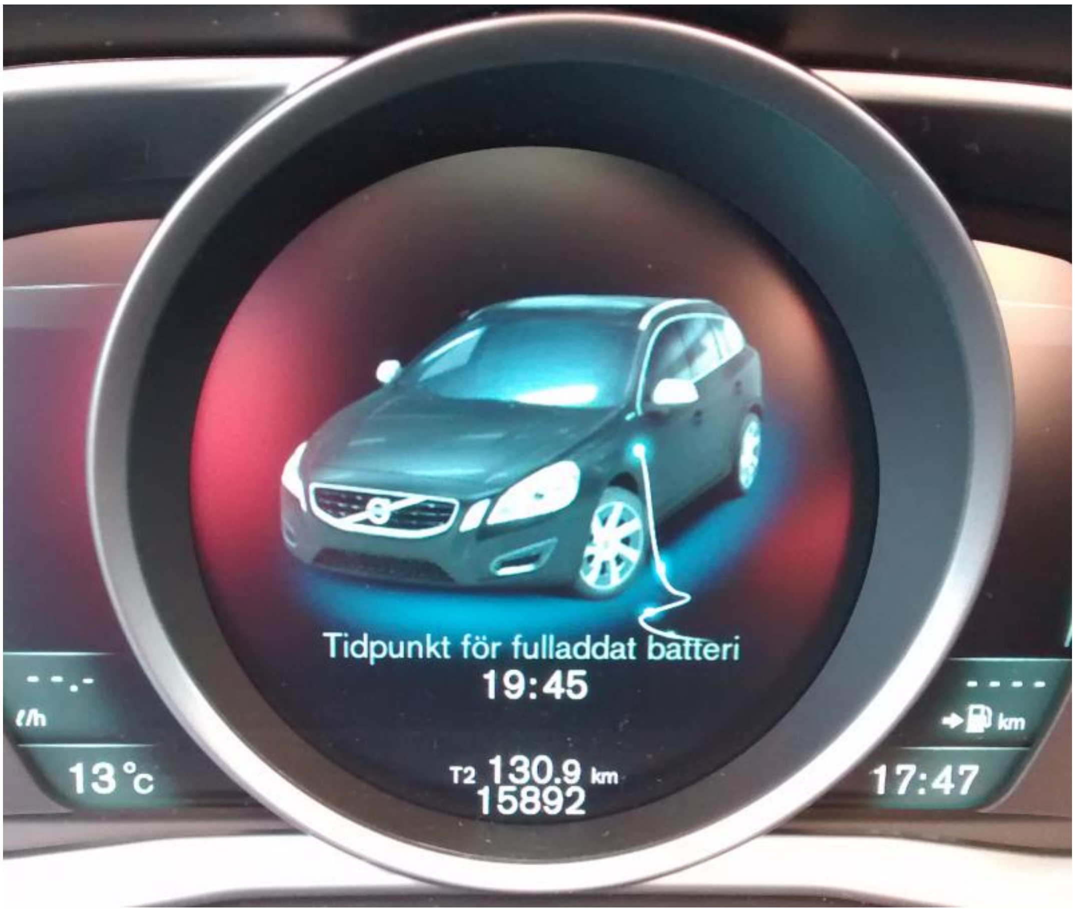
Tidpunkt för fulladdat batteri
19:45
- - . -
ℓ/h
13 °c
T2 130.9 km
15892
- - - -
km
17:47

Figure 5: The Volvo V60 PHEV charging and showing an estimation of when the battery will be fully charged in the dashboard.

2.2.3 Driving modes

Many modern vehicles offer the driver to choose between different driving modes, for example sport, normal, and economy. With the diesel electric hybrid powertrain in the Volvo V60 PHEV, even more combinations of different characteristics are possible.

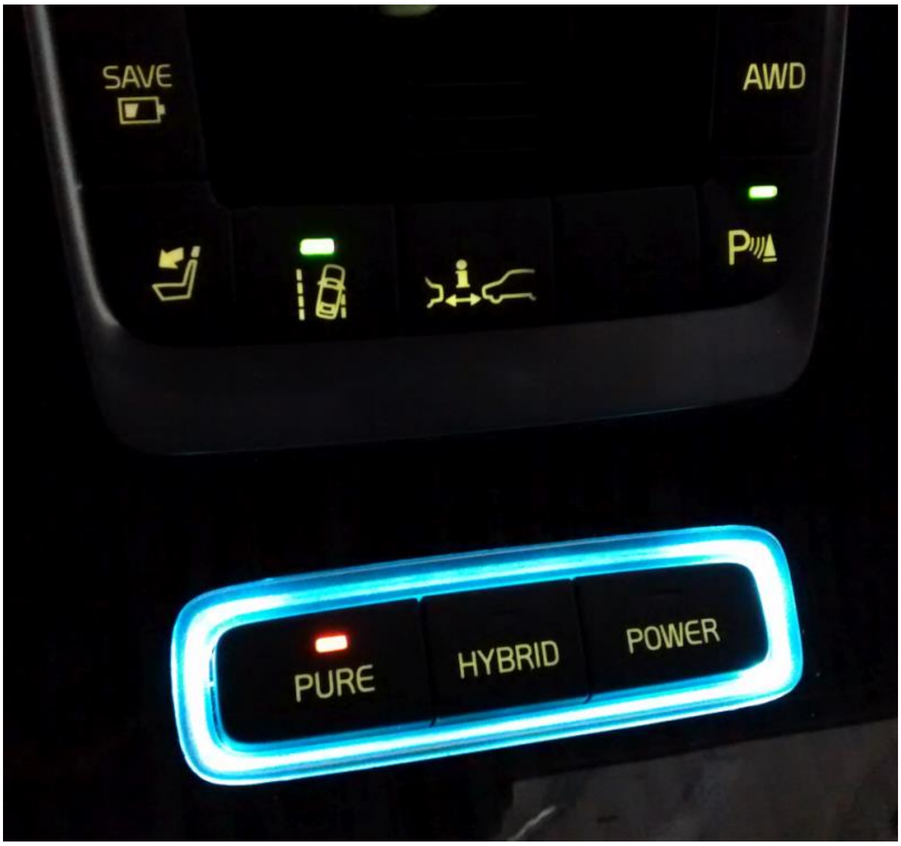

Figure 6: Driving mode buttons on the Volvo V60 PHEV.

The Volvo V60 PHEV offers 3 main and 2 specialty driving modes, which are selected by pressing the buttons seen in Figure 6.

- **Pure -** Drive the vehicle in pure electric mode, range is approximately 40-50 km. The diesel engine will only be activated if the driver, by pressing the throttle deep enough, demands more power than the electric motor can deliver. The dashboard clearly shows how close to the power limit of the electric motor the current driving situation is, and if the diesel engine is started, a drop of oil symbol becomes solid in color. Also, as seen in the specifications, there is a top speed of using the vehicle in pure driving mode.
- **Hybrid** - This mode lets the vehicle decide when to use which power source.
- **Power** - This is the sport mode. The throttle is remapped to be more aggressive, the diesel engine is constantly running and the electric motor provides extra power and fast throttle response.
- **Save** - This mode prioritizes to use the diesel engine to charge the battery. It could be used if one e.g. is driving on the highway and is heading to a city center.
- **AWD** - Activates all-wheel drive if the battery has enough energy. This mode is intended for low speeds in slippery conditions.

2.2.4 Preconditioning of the cabin

One detail that has to be taken into consideration measuring charging sessions with the Volvo V60 PHEV is its many cabin preconditioning settings. Perhaps most important, if one has the vehicle inside a building, is to turn on the indoors setting. This disables the diesel cabin heater. There are also options to heat the cabin and the front seats with electric energy, or cool the cabin with electric energy. This heating and cooling use energy from the battery or if available from the electrical grid.

2.2.5 Conditioning of the battery

In the measurements chapter, preconditioning, e.g. heating the battery when it is cold outside, will be discussed. In hot climates on the other hand, it is likely that the battery has to be cooled while charging. Even when charging the battery at 20°C ambient temperature, some kind of postconditioning, probably cooling of the battery or charging electronics, was noticed. For more details see section 9.2.5 Post charging cooling. Energy for these different conditioning activities probably comes from the electrical grid.

2.2.6 Fully charged and totally depleted battery

The most detailed view of the vehicles SoC can be found on the infotainment display, see Figure 7 and 8.

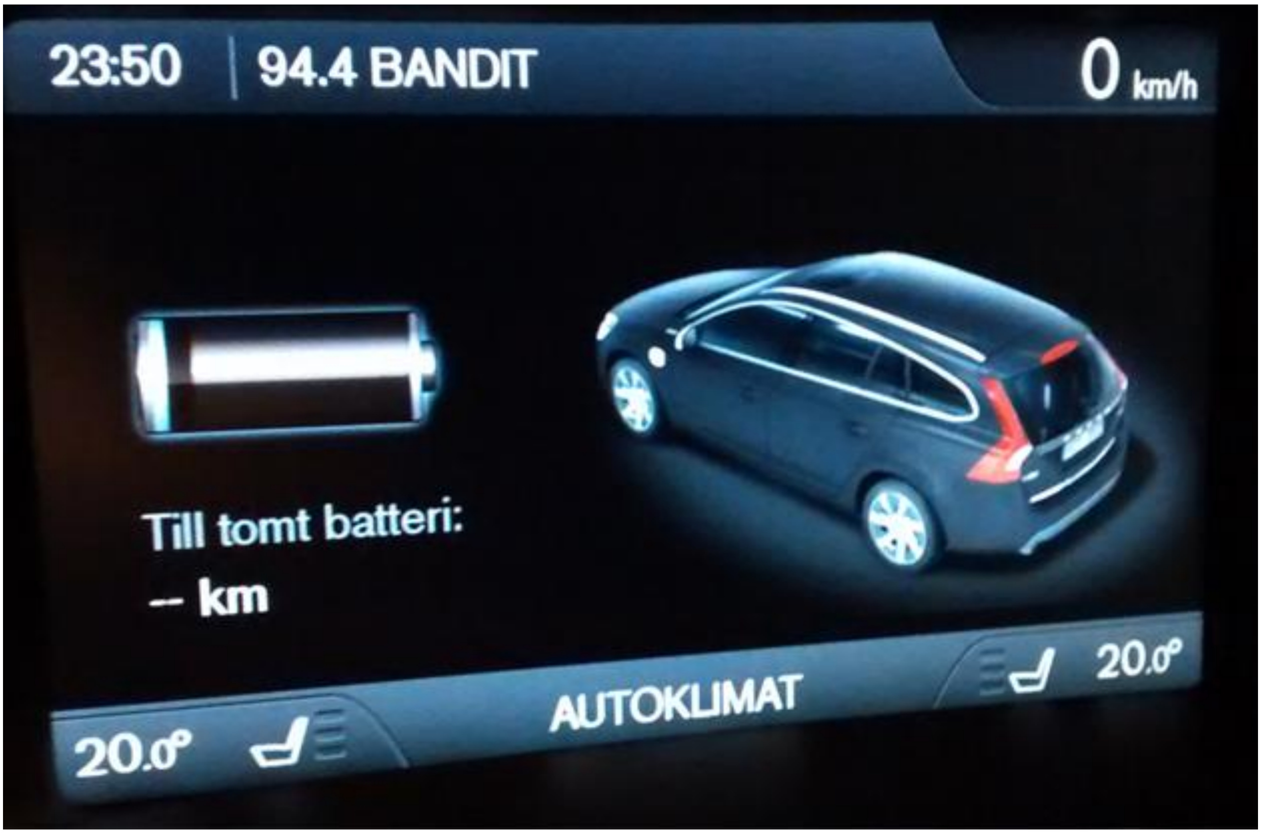
23:50
94.4 BANDIT
0 km/h
Till tomt batteri:
-- km
AUTOKLIMAT
20.0°
20.0°

Figure 7: The infotainment display showing a totally depleted battery.

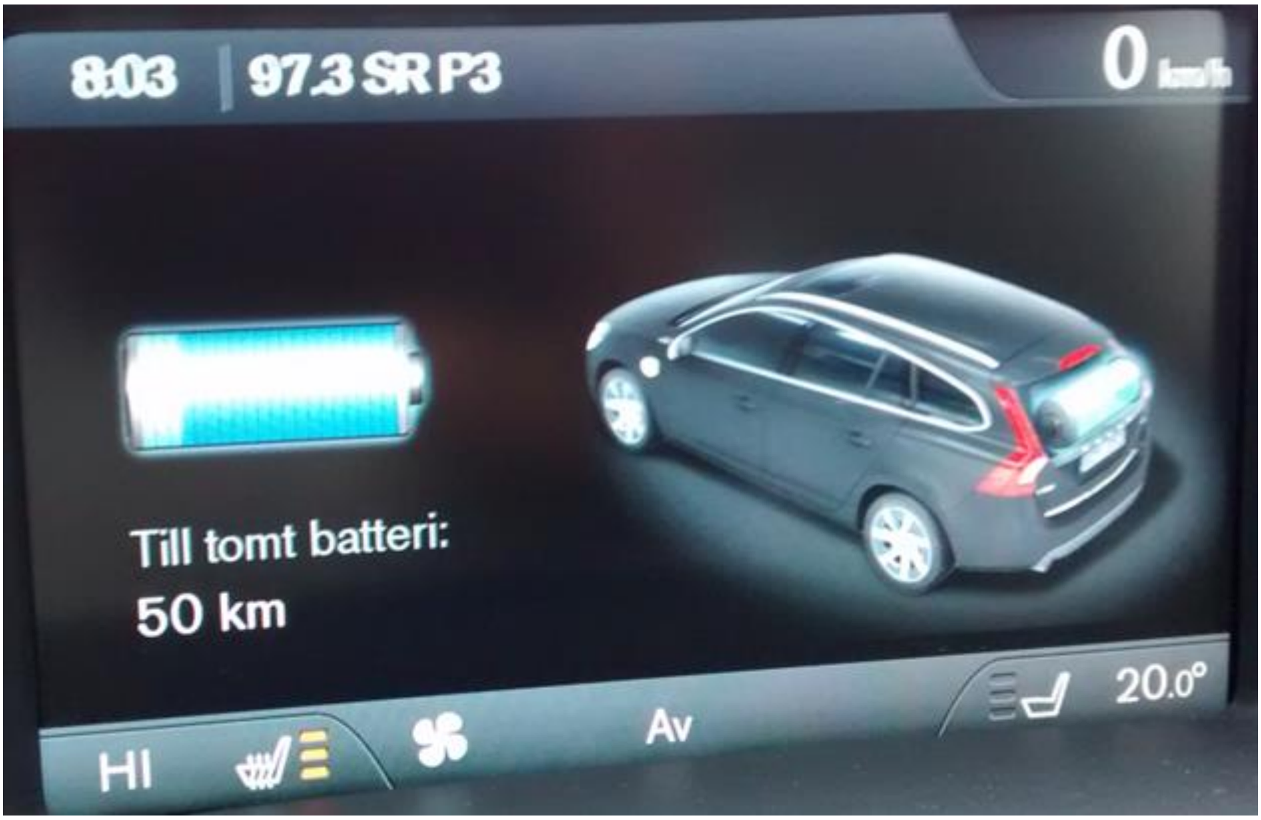

Figure 8: The infotainment display showing a fully charged battery.

The battery graphics always has two grey bars on the far left and far right. These do not indicate SoC, they are only there to illustrate the limits of the battery. Between these two grey bars, the vehicle will display one to 20 bars. One bar means that the battery is totally depleted, 20 bars mean fully charged.

2.2.7 Totally depleting the battery

Because repeatability in the charging profile measurements is very important, the vehicle must reach the same, or as identical as possible, state before each charging session.

Getting the battery to be fully charged is easy, simply charge the vehicle. Totally depleting the battery is a little bit more difficult. The quickest method to get the vehicle down from 20 bars (full) to two or three bars is to drive it in Pure driving mode. But often the vehicle will switch into Hybrid driving mode and start the diesel engine before one bar is reached, refusing to switch back to Pure. Thus to reach one bar, the vehicle has to be driven in Hybrid driving mode, and be coaxed to drive with the diesel engine turned off. This is done by driving really slow, ≈10 km/h, for a kilometer or two.

Adding to this, the timing of reaching one bar has to be right. If the vehicle isn't at the place where it is intended to be charged and can be turned off, the diesel engine will turn on and start charging the battery, quickly gaining one or two extra bars.

2.3 System overview

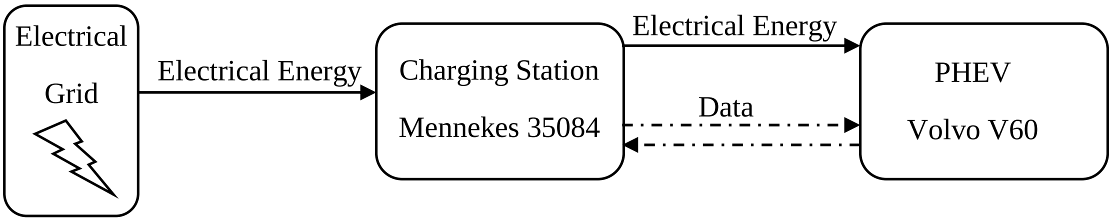
Electrical
Grid
Electrical Energy
Charging Station
Mennekes 35084
Electrical Energy
Data
PHEV
Volvo V60

Figure 9: Vehicle charging system overview.

The data exchange between the vehicle and the non-fast charging station is very limited. E.g. a decision about charging current is made at the beginning of the charging session. No advanced information, such as SoC, is transmitted. Figure 9 has a vehicle charging system overview.

3 Theory

This chapter presents the theoretical foundation for three important parts of this thesis:

- different aspects of vehicle charging and the recording of charging profiles.
- micro and macro perspective on vehicle charging, e.g. electrical grid peak capacity.
- dynamic programming, an optimization algorithm used for determining a charging strategy and planning the charging sessions.

Sheiki, et al (2013, p. 500) claims that there are three main categories of plug-in hybrid vehicles charging literature.
a) How vehicle charging impact the electrical grid (loads, frequency stability, peak capacity, grid usage of energy stored in vehicle batteries, etc.).
b) How the different properties of batteries affect charging behavior (charging with minimal energy usage, battery lifetime, etc.).
c) Charging strategies and optimization (smart load management, peak demand shaving, minimizing cost considering real time pricing, queue management at charging stations, etc.)

3.1 Vehicle charging profile logging and analysis

A charging profile describes how the power consumed by a vehicle that's being charged changes during the charging session. This section describes a number of things that should be considered when recording charging profiles.

A charging session is defined as the *"time between the beginning (connection of the cable) and the end (disconnection of the cable) of a charging process" ... "During a charging session the EV may have none, one, or many periods of charging the battery, doing pre-conditioning or post-conditioning."* (ISO, 2013)

3.1.1 Power factor

When measuring power consumption for an AC load it is important to consider the power factor. The power factor (PF) is defined as

$$PF = \frac{P}{S} \tag{1}$$

where P is the real power and S is the apparent power. The PF stems from the phase angle φ between the current and voltage, where

$$\frac{|P|}{|S|} = \cos\varphi \tag{2}$$

or

$$|P| = |S| \cos \varphi = U \cdot I \cdot \cos(\varphi) \tag{3}$$

The PF is important, since only if PF=1 all energy supplied by the source is consumed by the load, as is the case for a purely resistive load. Thus it is not enough to only measure the voltage U or current I for an AC load if the PF isn't one. In those cases the phase angle φ or PF also has to be recorded.

3.1.2 Vehicle charging

Concerning charging profile logging and analysis, not much relevant prior research was to be found. Kumar, et al. (2012) present an interesting model of the charging profile. But a verification of the model, or any reference to where it was found, is missing. Presented in the article is an interesting and rather grand scheme where charging profiles of vehicles are logged and stored in a building energy management system (BEMS). They also claim that they will use historic charging profiles in their charging control strategy. But in the end, they claim that they lack real historic data of charging profiles, and revert to using a model.

Further Kumar, et al. (2012) claims that no available battery management system stores charging profiles to use for approximation of future ones. They also claim that apart from Qian, et al. (2011), research doesn't consider initial state of charge and battery type to predict vehicle charging profiles. It is also important to take battery aging, SoH, into account, and to improve the accuracy of charging profile prediction by using not one but a few previous charging profiles (Kumar, et al., 2012). Thus charging profiles can't be seen as static in a real application.

Perhaps the best analysis of charging profiles, looking at recent research articles, can be found in Qian, et al. (2011). In their paper "Modeling of Load Demand Due to EV Battery Charging in Distribution Systems" they show the charging profile of the GM EV1 (lead-acid battery) and the Nissan Altra (lithium-ion battery).

As Qian, et al. (2011, p. 803) notes, the charging profiles, and thus power demands, are rather different between the lead-acid and the lithium-ion (Li-ion) batteries. The lead-acid battery has a relatively constant charging phase for 2.5 h with approximately 6 kW charging power. This is followed by a ramp down phase until the end of the 7th hour. The Li-ion battery's charging profile is almost flat and constant at 6.5 kW for 5 hours. The durations thus differs, with 7 h for the lead-acid and 5 h for the lithium-ion battery. Though both have an almost identical capacity, 27.19 kWh (lead-acid) and 29.07 kWh (Li-ion).

These charging profiles in Qian, et al. (2011) were originally published by Southern California Edison, a large electrical utility company in Southern California, in two corporate research reports (Mendoza and Arguetta, 2000; Madrid, Arguetta and Smith, 1999). During the charging of the lead-acid vehicle (GM EV1) the PF was 0.99 and for the Li-ion vehicle (Nissan Altra) the PF was 0.99 (Mendoza and Arguetta, 2000; Madrid, Arguetta and Smith, 1999). Their methodology for measuring charging profiles is very straightforward. Simplified, first they note some relevant data, such as ambient temperature and SoC. Then with the measurement equipment set up, they start charging the vehicle. Figure 10 shows how a charging profile generally might look.

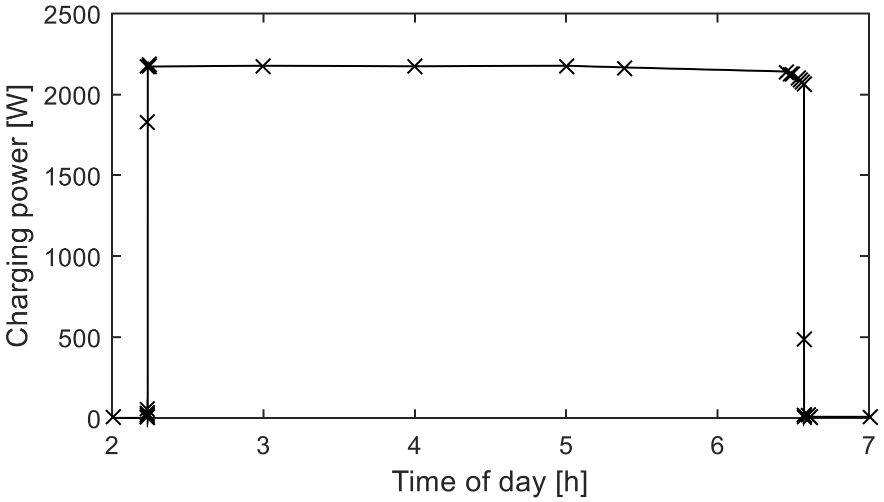

Figure 10: An example of a charging profile.

Outside the scope of this thesis, but broadening one's horizons, is the information about fast charging in Bai and Lukic (2013). The DC fast charging charging profile of a Nissan Leaf EV is pictured in their paper. The vehicle has a 25 kWh Li-ion battery. In the described charging session, lasting between 30 and 35 minutes, the battery's state of charge is increased from 15% to 80%. The charger used is a CHAdeMO compatible Terra 51 made by ABB. How does this charging profile compare to non-fast Li-ion charging? It's not completely different, but it has a much more prominent ramp down. In a way rather similar to the lead-acid battery in the GM EV1, but with the entire charging session lasting half an hour instead of 7 hours. With such a peaky charging profile, it would probably be even more difficult to manage on both a micro and macro perspective. The paper also mentions that researchers at ABB envision charging vehicles with power levels in the range of 125 to 300 kW. Compare that to the charging in this thesis, using approximately 3 kW.

Pashajavid and Golkar (2014, p. 199) go as far as saying that most studies of how vehicle charging creates load demands on the electrical grid assumes an absolutely constant charging profile versus time. They also note that aggregated, this may create huge estimation errors of the power and energy demands. Therefore they present a theoretical state transition model that describes the charging process.

To summarize, only one example of original research regarding actual vehicle charging profiles has been found.

Jiang, et al (2014) discusses a model of the charging current rate (p. 357) and charging strategies (p. 362). Ashtari, et al. (2012) suggests using the global positioning systems (GPS) in vehicles to be able to predict their upcoming charging profiles. For example, if the vehicle is being driven long distances one day, the house could potentially be preheated to the maximum allowed indoor temperature, using the indoor air as buffer. When the vehicle arrives at the house, the heating system can be turned off completely for a while.

3.1.3 Lithium-ion batteries

Different battery terms are used in different literature. In this thesis:

- a cell is the most basic element of a battery (having 3 to 4 V in the case of Li-ion) (Andrea, 2010, p. 1).
- a battery or battery pack are used interchangeable and means a (often huge) collection of cells wired and packaged together. A battery can e.g. be installed in a vehicle.

Since charging often is done outdoors, in non-managed temperatures, different aspects of battery behavior including its dependence on temperature is of interest. Marra, et al. (2010) look into this, including considering the temperatures experienced in Scandinavian countries.

Battery University (n.d.) claims the following for Li-ion batteries:

- Should not be charged below 0°C.
- Can be charged between 0°C and 45°C.
- Allow fast-charging between 5°C to 45°C.
- Can be discharged between -20°C and 60°C.
- Some cells developed for vehicles can be charged down to -10°C at a reduced rate.
- May have to be heated if the temperature is too low, vehicles can use:
  - an electric heating blanket
  - hot cabin air
  - a hot liquid agent
- Cold temperature increases the internal resistance.

According to Andrea (2010, p. 4) *"Li-Ion cells perform magnificently, but are rather unforgiving if operated outside a rather tight safe operating area (SOA), with consequences ranging from the annoying to the dangerous."*. Figure 11 shows the SOA for a certain battery cell. The data in the figure more or less match those stated by Battery University (n.d.).

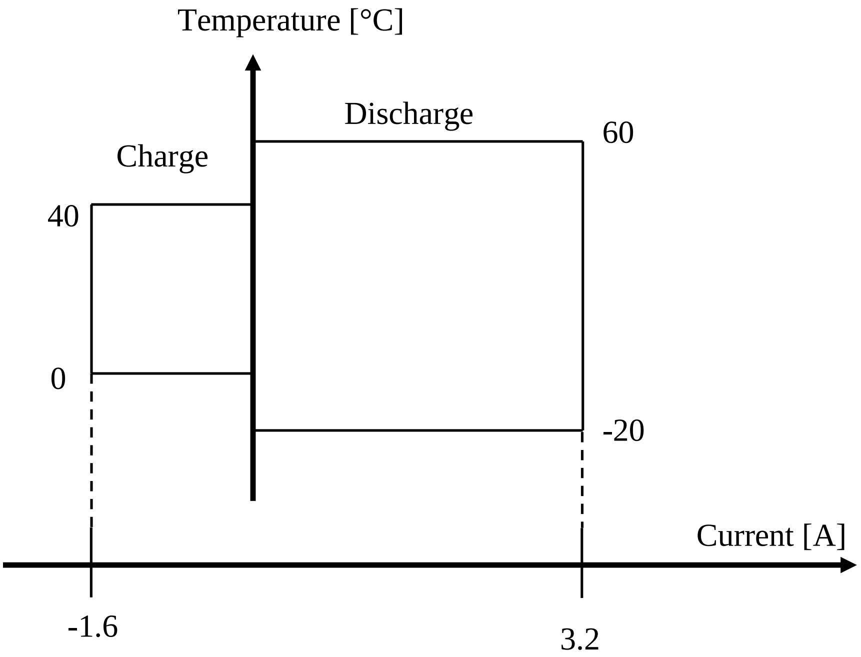

Figure 11: SOA of a $LiFePO_4$ cell. Data from Andrea (2010, p. 7).

According to Marra, et al. (2012) the standard charging algorithm of a Li-ion battery includes two separate phases. First one with constant current (CC), this is kept until an upper limit on battery voltage is reached. Then the charging is done with constant voltage (CV), until the state of charge reaches 100%. Please note that these details can't be monitored directly in the measurements in this thesis, since these factors will be handled by the vehicle's internal battery management system, leaving only the power and power factor transferred at 230 V to be measured. Still, the shift from CC to CV might be possible to identify indirectly by looking at the power usage.

To be able to do this, the Li-ion cell has to be understood on a somewhat deeper level. Figure 12 shows a simple electrical equivalent model of a Li-ion cell.

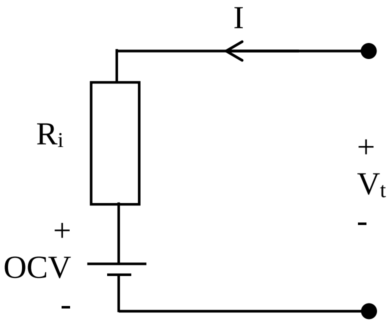

Figure 12: Simple electrical equivalent model of a Li-ion cell.

Open circuit voltage (OCV) is essentially the same as terminal voltage (V_t) at minimal discharge current (Andrea, 2010, p. 20). At higher currents, the two voltages differ.

$$I = \frac{I \cdot R_i}{R_i} = \frac{V_t - OCV}{R_i} \Rightarrow \tag{4}$$

$$OCV + I \cdot R_i = V_t \tag{5}$$

$$OCV < V_t \leq V_{max} \tag{6}$$

During charging, the battery can be damaged and catch fire if OCV exceeds V_{max}. The battery charging algorithm as defined by cell manufacturers, including the CC and the CV phases, is illustrated in Figure 13. Andrea's (2010, p. 21) description of the standard charging algorithm for Li-ion batteries is similar to Marra, et al. (2012). Andrea claims that manufacturers specify that cells should be charged at CC until V_t reaches V_{max}. This is followed by charging at CV until the current drops below a certain level, C_{cutoff}. Note that CC and CV can be seen as two different control strategies in the charger.

Looking at Figure 13, and remembering what was mentioned earlier, the current flowing into the battery can be approximated by looking at the power usage of the vehicle, since the voltage is close to constant. Thus it can be expected that the power usage will fall considerably in the final stages of the charging session. Also, looking at the SoC curve, it can be noted that charging in the CV phase has a considerably smaller (and constantly decreasing) derivative compared to charging in the CC phase.

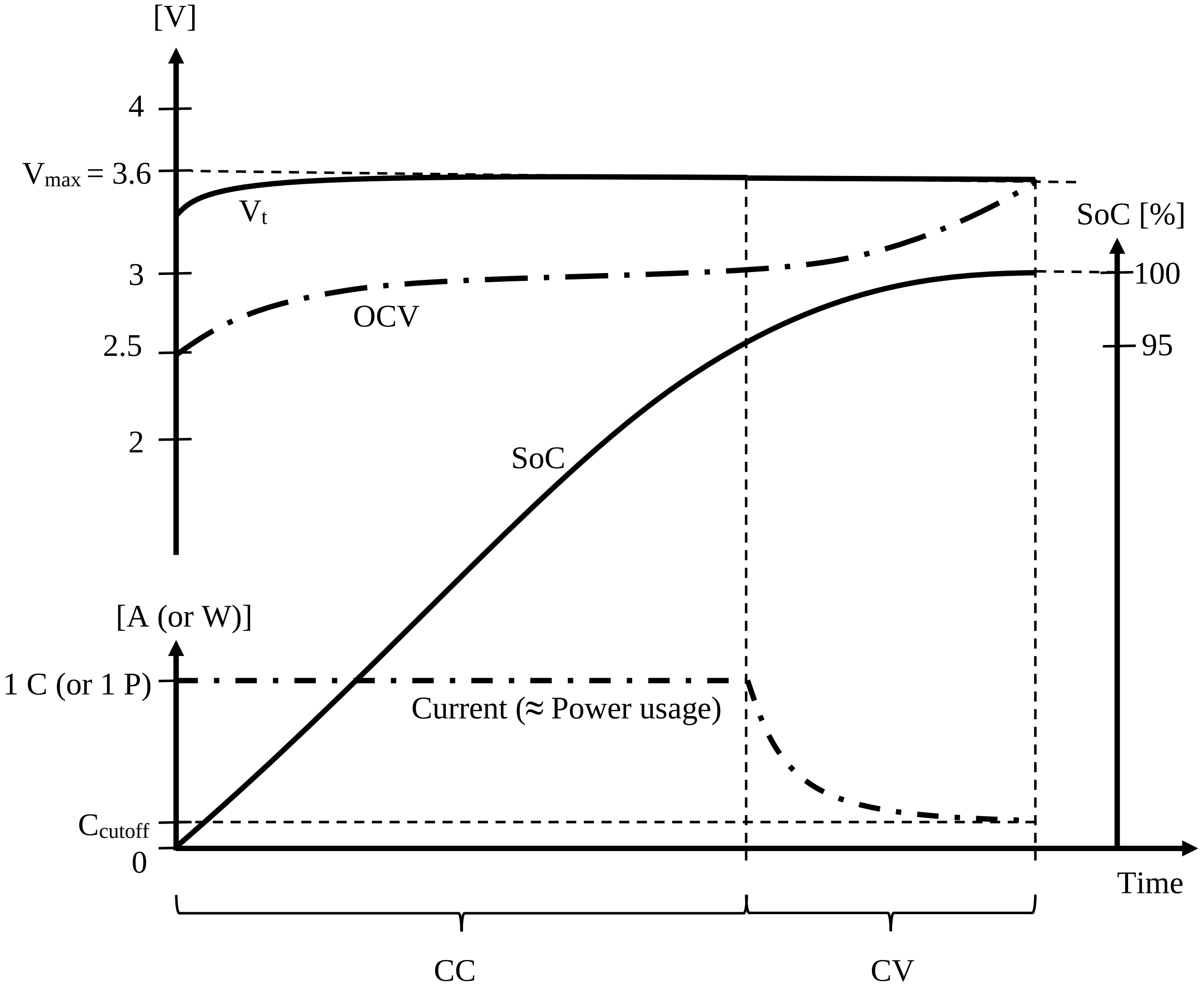

Figure 13: Charging algorithm as defined by cell manufacturer (Andrea, 2010, p. 22).

The real charging algorithm used by the Volvo V60 PHEV is not published and probably considered a company secret by Volvo Cars.

Gao, et al. (2011) claims (without immediate apparent reference) that it is recommended that vehicles are charged with constant current and constant voltage. They also include a figure showing the charging profile, detailing how the SoC depend on time.

Marra, et al. (2010) claims that drivers of PHEV usually have access to 60% of their true rated battery capacity, while the number for EVs is 80%. More about this number will follow.

It is also worth noting that lithium has a very high heat capacity. It thus requires almost seven to eight times more energy per mass unit to heat up 1°C than iron and steel. Since Li-ion batteries are composed of different materials, not only lithium, the heat capacity for Li-ion battery has to be determined. Maleki, et al. (1999) puts it at approximately 0.96 J/K/g, compare this to 0.450 for iron and 3.58 for pure lithium. See section 4.4 Thermal battery aspects for calculations using this data.

3.1.4 The vehicle / charging station relation

The vehicle to charging station communication is covered in detail in ISO (2013). According to Lindergren (2015), the charging current in non-fast charging stations can be set between 6 and 63 A, with intermediary steps of 0.1 A. In line with this, the Mennekes portable charging station supplied with the Volvo V60 PHEV allows charging current to be set at 6, 8, 10, or 13 A.

Lindergren also claims that some vehicles can't handle this 0.1 A resolution, for example the Kia Soul. Furthermore some vehicles can't charge below 13 A.

3.2 Micro and macro perspective on vehicle charging

Most research papers concerning vehicle charging discuss the macro perspective of vehicle charging, e.g. how the large scale electrical grids handle a large number of charging vehicles. Few include the micro perspective, e.g. how to handle the power limitations of a household or how to minimize a family's charging cost. A good example of these macro studies is Weiller (2011). Many macro studies are concerned with the effects unscheduled vehicle charging might have on the electrical grid. Mohsenian Rad, et al. (2010a) use game theory to even out loads on a macro perspective. One advantage with this method is that it decentralizes the decisions and that the households don't have to reveal any specific details of their energy consumption – except for how much they consume in total.

Qian, et al. (2011, p. 804), mentioned in an earlier section, has some discrete time models for the power demand during battery charging, and many interesting theories regarding for example how variable electricity rates can place vehicle charging at a more optimal time of day. In their words they compare "uncontrolled charging" and "smart charging". Other papers use the terms "unmanaged" and "managed" charging.

The article by Di Giorgio, Liberati and Canale (2013) describes how to use model predictive control (MPC) to handle charging operations in a smart grid, and includes a neat comparison of several different control strategies: MSS scheduling, Linear programming, AIMD, Sliding mode control, Congestion pricing and (proposed by them) Event driven MPC.

Sarabi and Kefsi (2014) use dynamic programming to schedule vehicle charging concerning the macro perspective.

Mohsenian-Rad and Leon-Garcia (2010b) apply linear programming to help an "Energy Scheduler" prioritize between e.g. vehicle charging, appliances, and air conditioning.

Using quadratic programming Jian, et al. (2013) details how by managing the charging profile of PHEVs, the variance of power usage can be reduced. They also write about the "microgrid" of the household, and vehicle-to-grid (V2G), i.e. when the vehicle sends power to the public electrical grid. Adding to that they look into how the battery capacity of the vehicle affects mean load power.

All of these research papers don't fit the content of this thesis perfectly, but reading them offers a width of up to date information in related areas.

3.3 Dynamic Programming

One main interest in this thesis is to plan, i.e. schedule, a charging session. What charging powers should be used at different points in time to minimize cost?

Dynamic programming (DP) is an optimization algorithm, developed by Richard Bellman in the 1950's (Guzzella and Sciarretta, 2013, p. 367), which can be used to minimize charging cost. The standard texts on DP are Bellman (1957) and Bertsekas (2005) according to Guzzella and Sciarretta. While the book by Bellman is the original work, Bertsekas' book is much more accessible and uses a more current notation.

Generally, DP implementations use a cost-to-go (CtG) matrix. In this thesis:
- moving upwards in the matrix, i.e. vertically, the state, SoC, grows.
- moving to the right in the matrix, i.e. horizontally, time increases.

This matrix is first filled with costs to reach the final time and sought state by traversing the matrix backwards in time, starting at the end. Then the matrix is traversed a second time, this time in forward order, finding the optimal control policy.

Employing the optimal control policy results in an optimal state trajectory, which can be seen as a path through the CtG matrix, see Figure 14. Therefore the terms optimal control policy and optimal state trajectory can almost be used interchangeable, even if they mean different things.

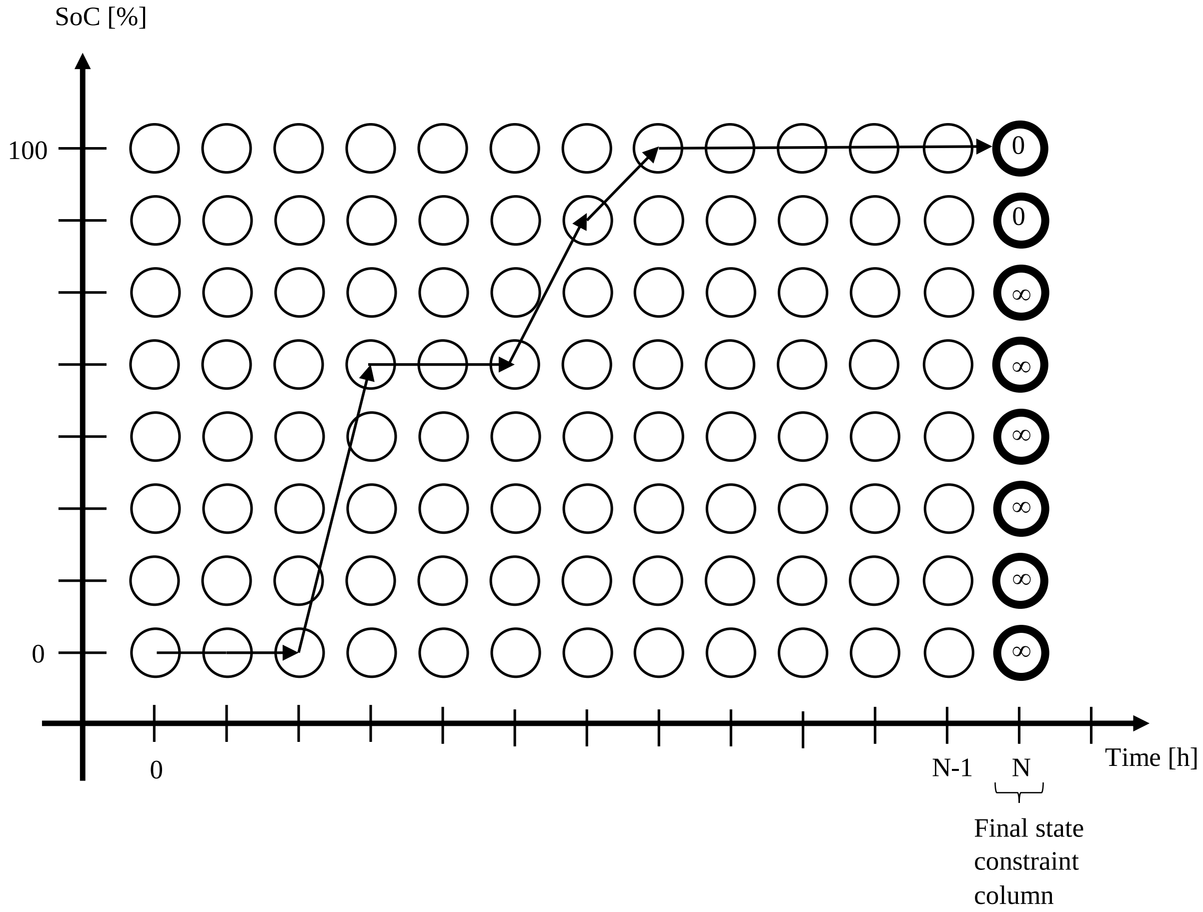

Figure 14: A simplified view of an optimal state trajectory.

Guzzella and Sciarretta (2013) further states that some of the benefits of DP is that it can handle multiple complex constraints on both states and inputs - and at the same time requires relatively few computation cycles. The disadvantage with DP is how to handle disturbances. If the stochastic properties of disturbances are known, stochastic DP can be used. If there are no disturbances, as in this thesis, or if they are known in the beginning, deterministic DP can be used. Deterministic DP will henceforward be referred to as DP.

Next up is a formal description of the DP algorithm implemented in such a way that it is suitable to solve the optimization problem in this thesis. This is followed later by a more lucid explanation of how the DP algorithm works, using the vehicle charging scheduling problem as a base, in chapter 6.

3.3.1 Formal description of dynamic programming

The charging planning problem can be described as having:

- fixed final time
- partially constrained final state
- state constraints
- input constraints
- single state variable
- disturbances none-existent

Thus the problem can be described as an optimal control problem (Sundström, Ambühl and Guzzella, 2010)

$$\min_{u(t)} J\big(u(t)\big) \tag{7}$$

$$\text{subject to (s.t.)}$$

$$\dot{x} = F(x(t), u(t), t) \tag{8}$$

$$x(0) = x_0 \tag{9}$$

$$x\big(t_f\big) \in [x_{f,\min}, x_{f,max}] \tag{10}$$

$$x(t) \in \mathcal{X}(t) \tag{11}$$

$$u(t) \in \mathcal{U}(t) \tag{12}$$

$$J\big(u(t)\big) = G\left(x\big(t_f\big)\right) + \int_0^{t_f} H(x(t), u(t), t)dt \tag{13}$$

where J is the cost function, u is the control signal, x is the state, and t is the time.

Since our problem is discrete in time, and DP requires discretization to work, we must discretize, giving

$$x_{k+1} = F_k(x_k, u_k), \qquad k = 0,1, \dots, N-1 \tag{14}$$

Therefore, the state variable and control signal also have to be discrete in time

$$x_k \in \mathcal{X}_k$$

$$u_k \in \mathcal{U}_k$$

With this in place, we can define the DP algorithm (Sundström, Ambühl and Guzzella, 2010) as follows

$$J_\pi(x_0) = g_N(x_N) + \phi_N(x_N) + \sum_{k=0}^{N-1} \Big(h_k\big(x_k, \mu_k(x_k)\big) + \phi_k(x_k)\Big) \tag{15}$$

where:

- $\pi = \{\mu_0, \mu_1, \dots, \mu_{N-1,}\}$ is the control policy.
- the first final cost term $g_N(x_N)$ matches the final cost in equation (13).
- the second final cost term $\phi_N(x_N)$ corresponds to the partially constrained final state in equation (10).
- $h_k\big(x_k, \mu_k(x_k)\big)$ is the cost of $\mu_k(x_k)$ at x_k, following $H(x(t), u(t), t)$ in equation (13).
- $\phi_k(x_k)$ is a penalty function that applies the state constraint in equation (11) for $k = 0,1, \dots, N-1$.

The optimal control policy is π^0, which minimizes J_π

$$J^0(x_0) = \min_{\pi \in \Pi} J_\pi(x_0) \tag{16}$$

Π is the set of allowed control policies.

The following conclusions rest upon the *principle of optimality*. First described by Bellman (1957), it is defined and explained by Bertsekas (2005, p. 18) in the following way:

> Principle of Optimality
> Let $\pi^* = \{\mu_0^*, \mu_1^*, \dots, \mu_{N-1}^*\}$ be an optimal policy for the basic problem, and assume that when using π^*, a given state x_i occurs at time i with positive probability. Consider the subproblem whereby we are at x_i at time i and wish to minimize the "cost-to-go" from time i to time N
>
> $$E\left\{g_n(x_N) + \sum_{k=i}^{N-1} g_k(x_k, \mu_k(x_k), \omega_k)\right\}.$$
>
> Then the truncated policy $\{\mu_i^*, \mu_{i+1}^*, \dots, \mu_{N-1}^*\}$ is optimal for this subproblem.
>
> ...
> For an auto travel analogy, suppose that the fastest route from Los Angeles to Boston passes through Chicago. The principle of optimality translates to the obvious fact that the Chicago to Boston portion of the route is also the fastest route for a trip that starts from Chicago and ends in Boston.

Please note that since there are no disturbances in the DP implementation in this thesis, ω_k is zero and thus the encapsulating function E, as in expected cost, isn't really needed.

As a result of the principle of optimality, the DP algorithm will by proceeding backwards in time through every node in the discretized state-time space, calculate the optimal cost-to-go function $\mathcal{J}_k(x^i)$ at every said node (Sundström, Ambühl and Guzzella, 2010).

1. Calculations for the end cost step

$$\mathcal{J}_N(x^i) = g_N(x^i) + \phi_N(x^i) \tag{17}$$

2. Calculations for every step $k = N - 1$ to 0

$$\mathcal{J}_k(x^i) = \min_{u_k \in \mathcal{U}_k} \left\{ h_k(x^i, u_k) + \phi_k(x^i) + \mathcal{J}_{k+1}\left(F_k(x^i, u_k)\right) \right\} \tag{18}$$

Minimizing the right hand side of equation (18), $\forall\ x_i$ for all time index k in the discretized state-time space, results in optimal control.

4 Measurements

This chapter describes the charging profile measurements that have been done with the Volvo V60 PHEV.

4.1 Considerations

When logging the charging sessions it is important to record and consider the ambient temperature surrounding the vehicle, and to which extent the vehicle has adapted this temperature. For example, it might be that a cold battery takes a longer time to charge, and perhaps the vehicle will even preheat the battery before real charging, i.e. storing energy, begins (Battery University, n.d.). It's important to identify if a vehicle preheats the battery, and compensate for this, otherwise the logged vehicle charging profiles won't be accurate. In addition to battery preheating, one has to be on the lookout for cabin preconditioning.

To increase the reliability of the charging sessions, they could have been done in a controlled repeatable temperature, i.e. indoors, and first after the vehicle and battery have adapted to the ambient temperature.

Will it be possible to determine what power consumption goes to battery heating and what goes to battery charging? Can high validity be achieved?

For the charging sessions logging of the Volvo V60 PHEV it is important to record the state of charge before the charging session is started. In a real life situation a DP charging optimization would need to know the SoC and the SoH of the vehicles battery pack. Otherwise it will have a hard time optimizing the timing and profile of the charging session.

Since so little time and few charge–discharge cycles will pass between different charging session measurements, SoH will be assumed to be unchanged.

4.2 Measurement equipment

The Mennekes portable charging station was used together with a power meter. The power meter is an ordinary consumer grade unit, a Brennenstuhl PM 231 E seen in Figure 15, which was connected between the power grid and the portable charging station. It has a power measuring accuracy of ± 1% or ± 0.2 W, according to its specifications. See Appendix B for full specifications. If those specifications are correct, the accuracy has negligible impact on the recorded data, and conclusions drawn upon the recorded data.

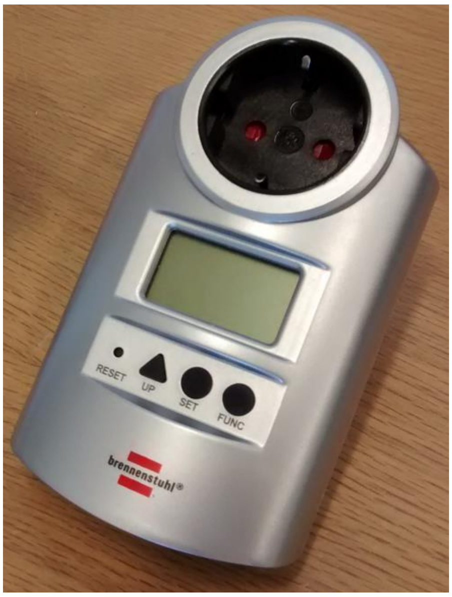
RESET
UP
SET
FUNC
brennenstuhl®

Figure 15: The Brennenstuhl
PM 231 E power meter.

To capture the charging profiles, the power meter display was recorded with an ordinary webcam, see Figure 16.

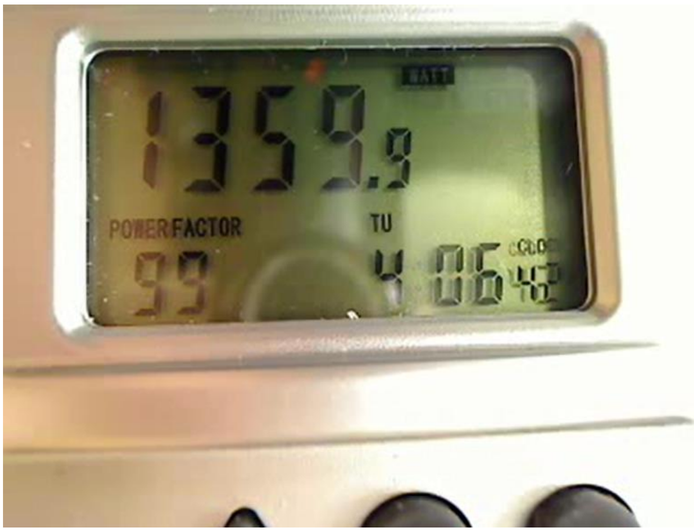
WATT
1359.9
POWER FACTOR
99
TU
4:06 42
CLOCK

Figure 16: Frame from a movie recording a
charging profile.

4.3 Measurements overview

The setup used to record charging sessions is presented in Figure 17.

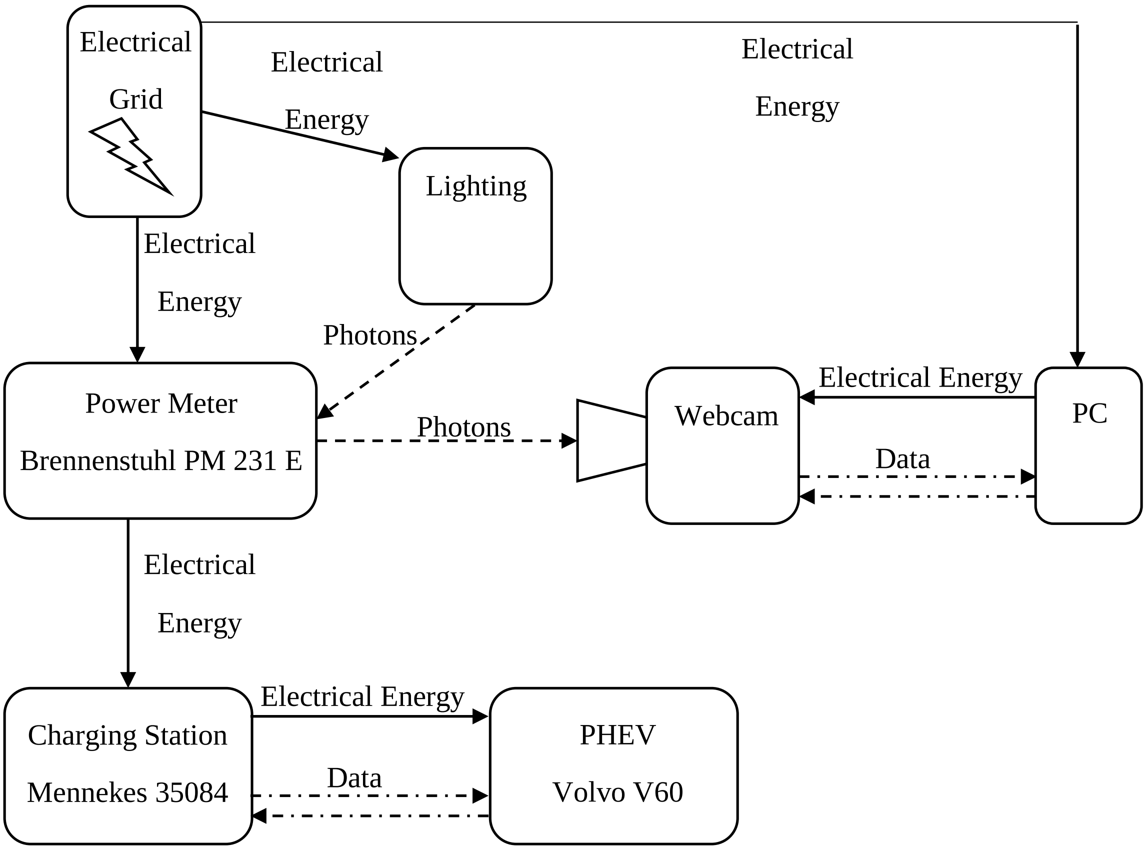

Electrical Grid
Electrical Energy
Electrical Energy
Lighting
Electrical Energy
Photons
Power Meter
Brennenstuhl PM 231 E
Photons
Webcam
Electrical Energy
PC
Data
Electrical Energy
Charging Station
Mennekes 35084
Electrical Energy
Data
PHEV
Volvo V60

Figure 17: Measurements overview. Since the power meter has no light source of its own, only a non-backlit LCD, the webcam recording relies on an external light source.

4.4 Thermal battery aspects

To protect the battery from overheating, cooling might be needed. During cold winter nights in Sweden temperatures below -20°C is not uncommon, and by then the battery will need some preheating. As mentioned earlier, the battery must be preheated to -10°C (or perhaps 0°C). Using battery data from sections 2.2.1 Specifications and 3.1.3 Lithium-ion batteries, this would require the following amount of energy

$$Q_{preheating} = m_{battery} \cdot C_{p_{battery}} \Delta T \ \Rightarrow$$

$$Q_{preheating} = 150\,000 \cdot 0.96 \cdot 10 = 1.44 \text{ MJ} = \ 0.4 \text{ kWh}$$

Compare this with the approximate number of how much energy is available to be used by the driver, 8.96 kWh. If the battery instead has to be heated an additional 20 K, then the preheating energy usage reaches approximately 10% of the energy storage capacity of the battery.

4.5 Charging sessions

All charging sessions begin with a totally depleted (1 bar in the display) battery. The battery is then charged until fully charged (20 bars in the display). The charging sessions were conducted outdoors. This is why the temperature data from SMHI (n.d.) is considered to be the ambient temperature of the vehicle. The Malmslätt weather station is only a few kilometers from the charging location.

Total energy consumption was calculated using the Matlab function trapz on the charging profile data.

4.5.1 Charging session 1

This charging session was run after first totally depleting the battery, and then letting the battery and vehicle cool down for about 2 hours in an ambient temperature of approximately -7°C. Two hours may be too short a time for cooling down, see section 9.2.4 Charging indoors and outdoors. The power factor was shown to be 1.00. Charging with the 10 A setting.

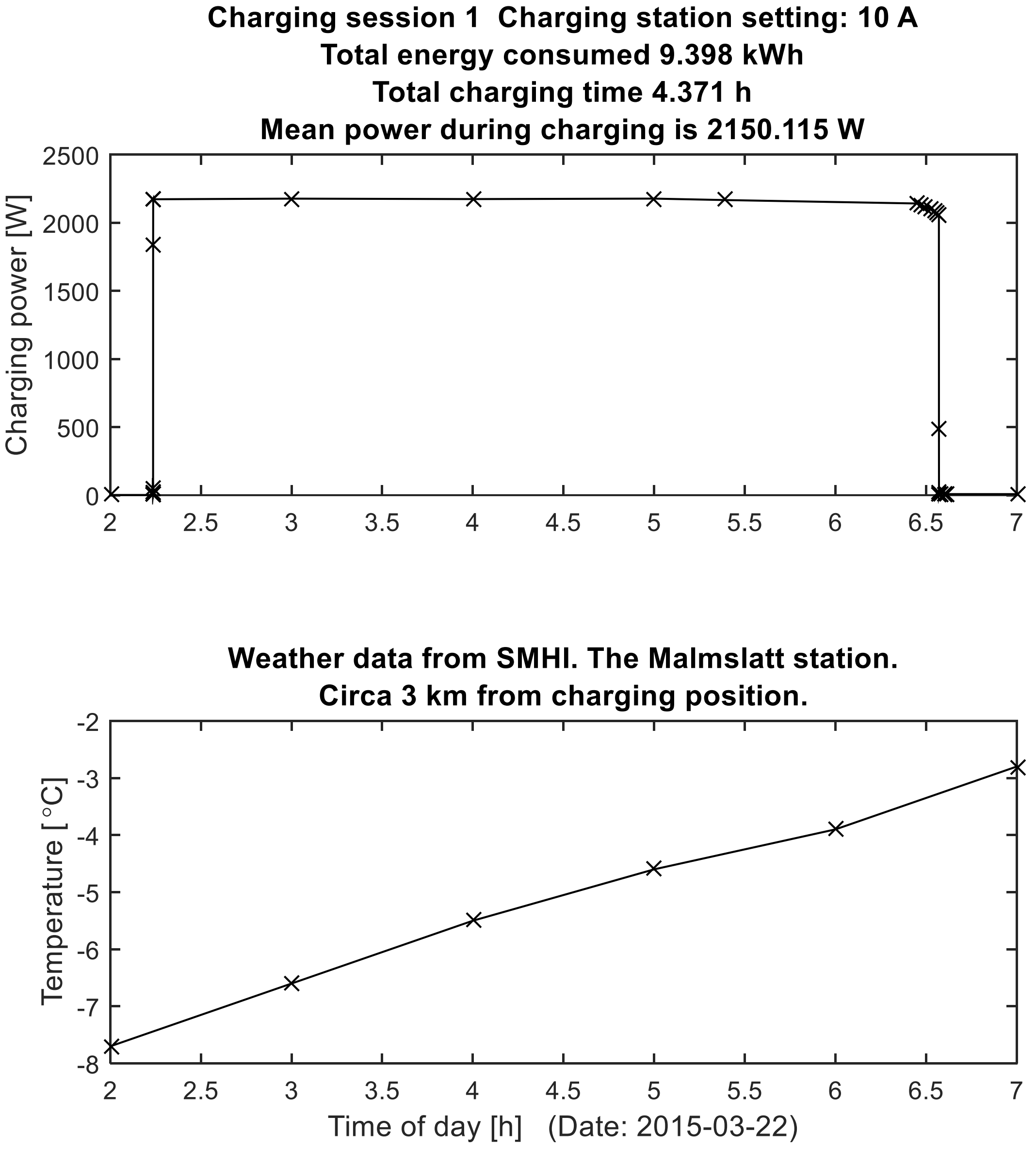

Figure 18: Charging session 1. Charging setting: 10 A.

A tiny ramp down can be seen at the end of the charging session.

4.5.2 Charging session 2

This charging session was done immediately after depleting the battery, thus the battery probably was hotter than in charging session 1. The power factor was shown to be 1.00. Charging with the 10 A setting just like in charging session 1, with the objective of seeing how similar the results will be.

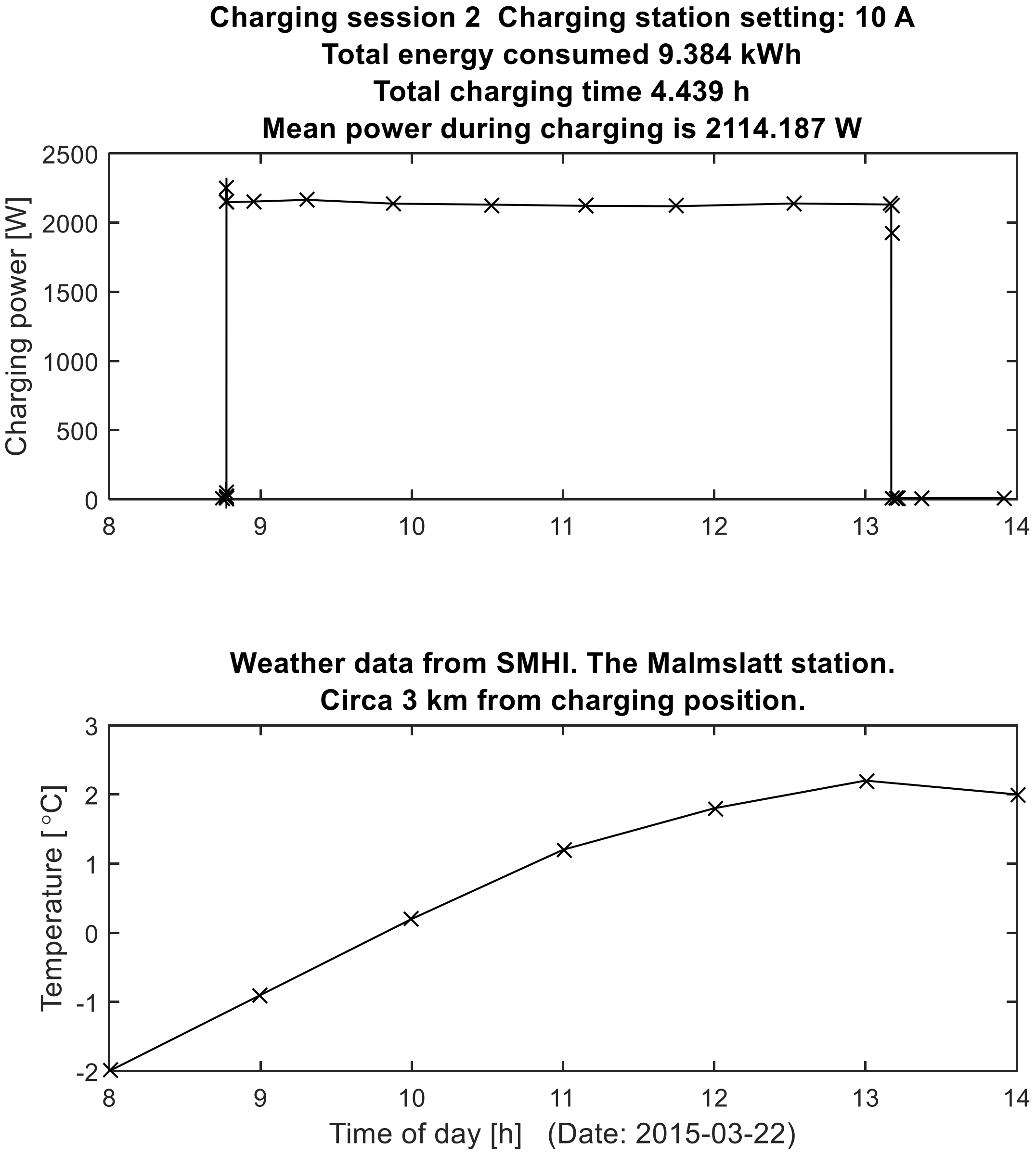

Figure 19: Charging session 2. Charging setting: 10 A.

No tiny ramp down as in charging Session 1. Very similar total energy usage as compared to charging session 1.

4.5.3 Charging session 3

This charging session was done immediately after depleting the battery. The power factor was shown to be 0.99. Charging with the 6 A setting.

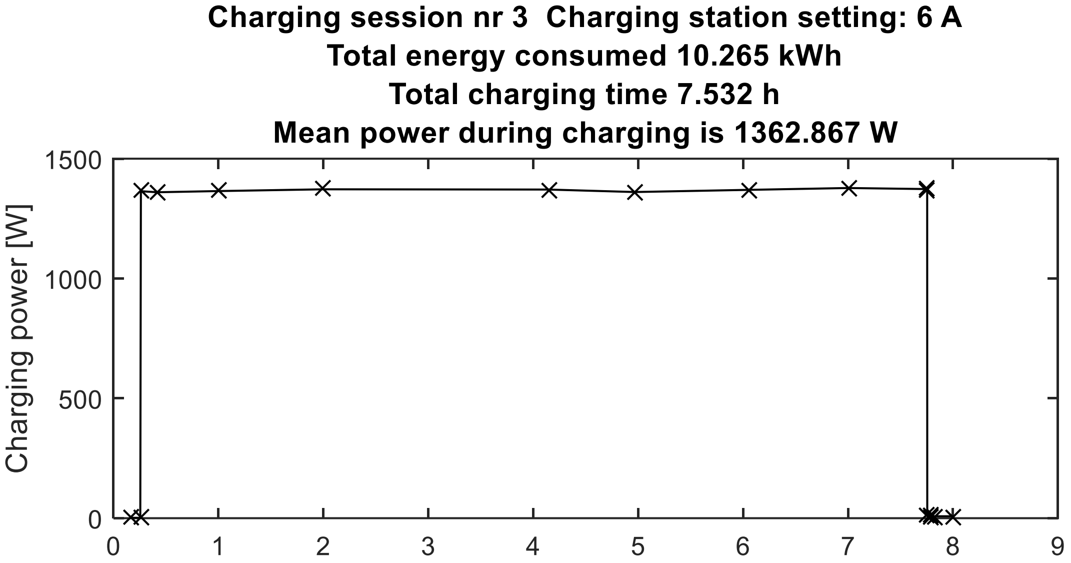

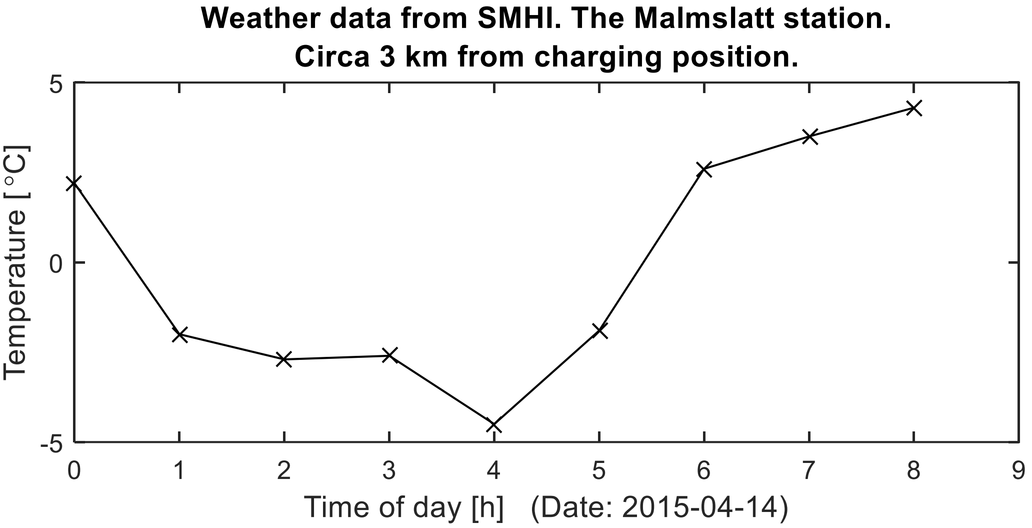

Figure 20: Charging session 3. Charging setting: 6 A.

The total energy consumption calculation result given above is supported by the power meter's built in function, which in this case claimed a total consumption of 10.2 kWh. This value is only 0.6% "too small". Remember that the power meter has a stated power measuring accuracy of ± 1% or ± 0.2 W. In this case we are within the stated 1%. The power meter's energy consumption meter wasn't recorded for the other charging sessions.

4.5.4 Charging session 4

This charging session was done immediately after depleting the battery. The power factor was shown to be 1.00 (except see note below). Charging with the 13 A setting.

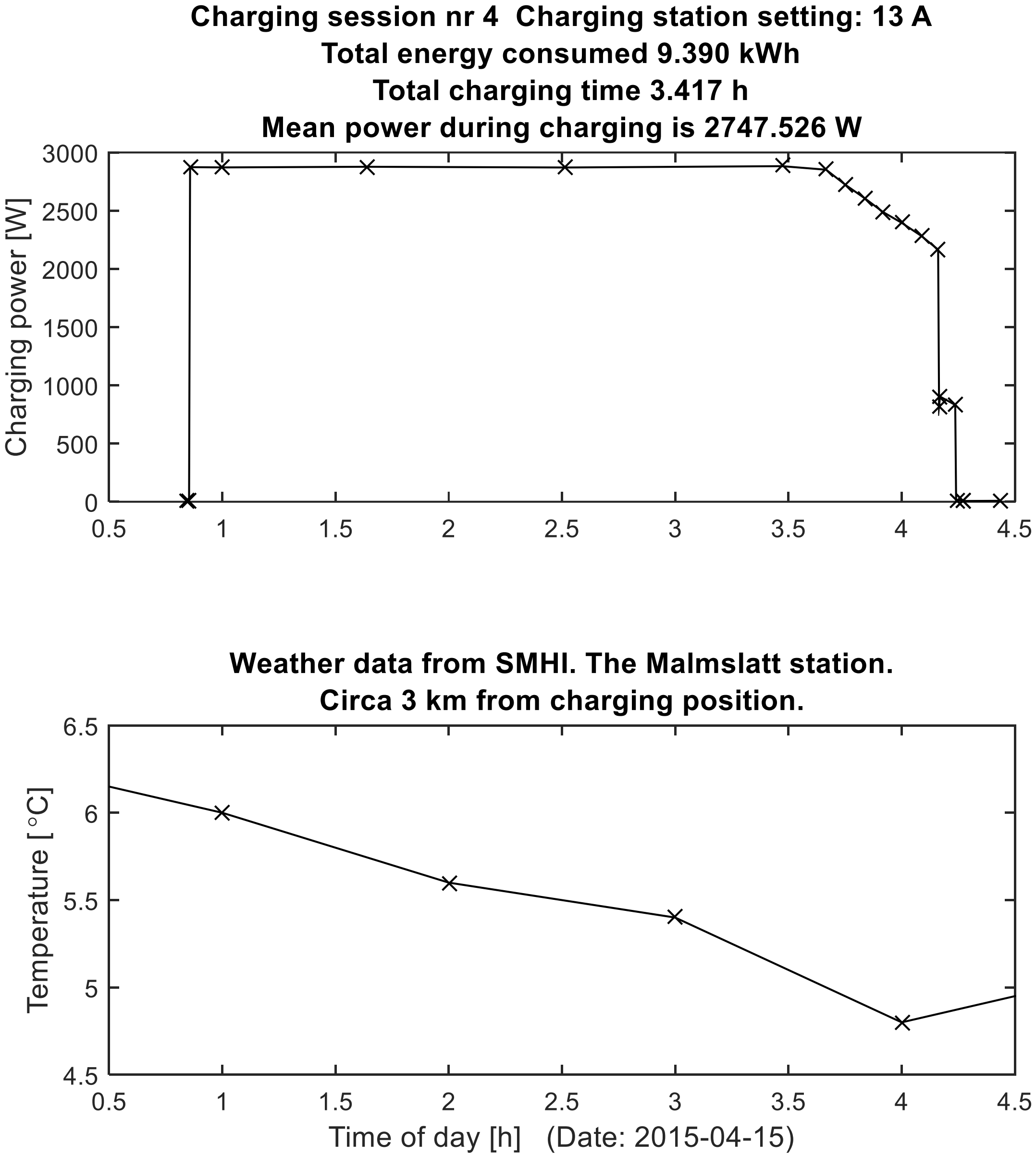

Figure 21: Charging session 4. Charging setting: 13 A.

A visible ramp down begins at 3.5 hours. At around 4:10 the load changes into approximately 800 to 900 W with PF 0.97. This might be the cooling fan and cooling system running, doing postconditioning.

4.5.5 Charging session 5

This charging session was done immediately after depleting the battery. The power factor was shown to be 1.00. Charging with the 8 A setting.

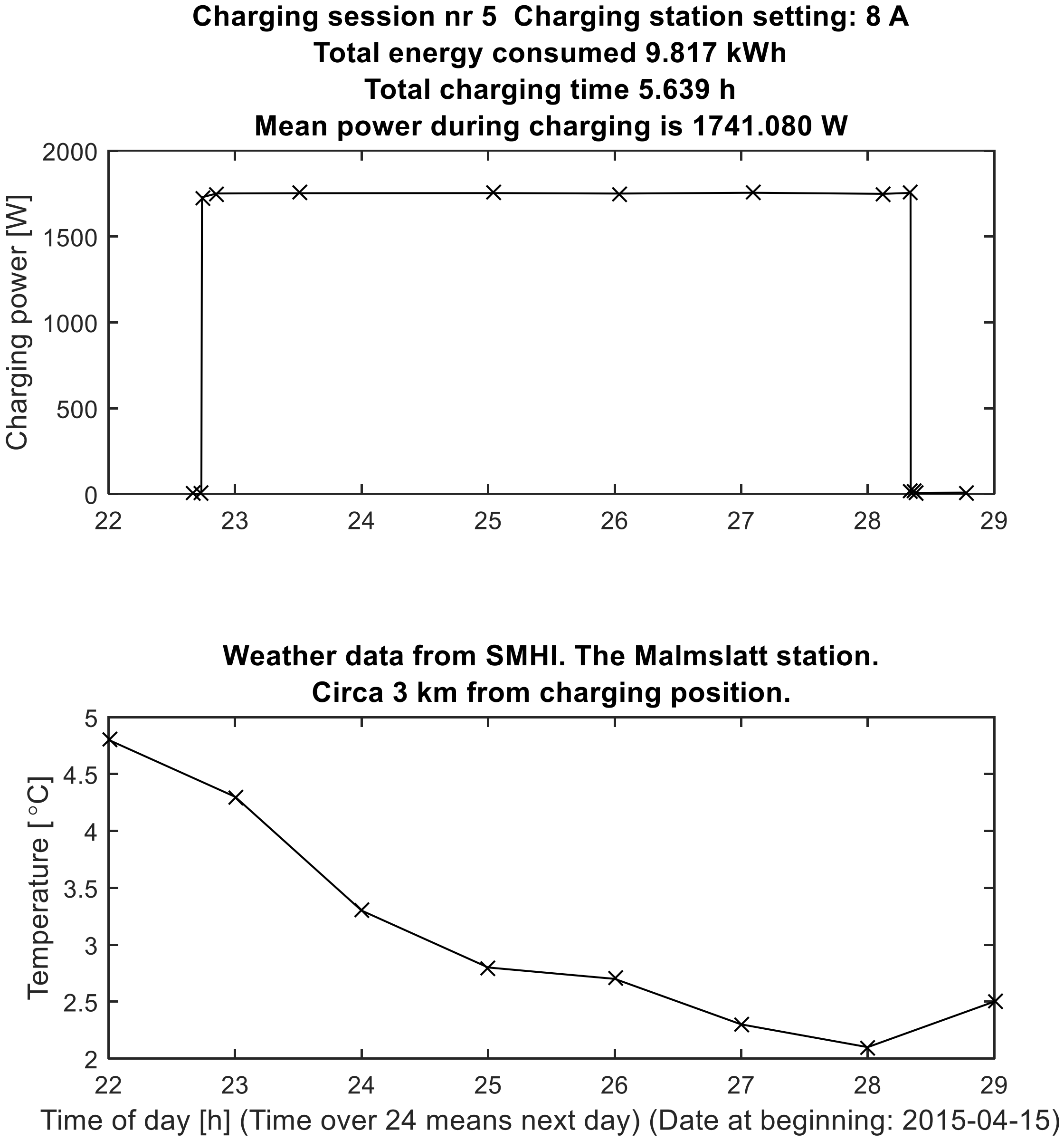

Figure 22: Charging session 5. Charging setting: 8 A.

4.6 Summary

Table 1 shows a summary of the results of the charging sessions together with approximations calculated from the specifications.

Charging session	**Current [A]**	**Total energy consumption [kWh]**	**Duration [h]**	**Mean power [W]**	**Average ambient temperature [°C]**
3	6	10.265	7.532	1363	-0.12
specs	6	a 10.350	s 7.500		
5	8	9.817	5.639	1741	3.10
1	10	9.398	4.371	2150	-5.46
2	10	9.384	4.439	2114	0.84
specs	10	a 10.350	s 4.500		
4	13	9.390	3.417	2748	5.53
***specs**	13	*a 11.615	*s 4.000		
specs	16	a 12.880	s 3.500		

Table 1: A summary of the five charging sessions. "*" indicates that a value was calculated with interpolation. "s" indicates a value from the specifications. "a" indicates an approximated value calculated from data in the specifications.

While the 10 A and the 13 A charging sessions have similar total energy usage, the lower the charging current, the higher the total energy consumption seems to become. This table will be further analyzed in section 8.1.2 Thermal battery aspects.

Note: Average temperature for the entire year of 2014 for the Malmslätt weather station is 8.13°C (SMHI, n.d.).

5 Charging cost simulations

Since the price of electricity isn't constant during the day, it might be a good idea to charge the vehicle when electricity is cheap. As stated in 1.4 Delimitations, this thesis is focused on charging a vehicle during the night between 18:00 and 07:00, assuming the battery to be totally depleted at 18:00. Thus since the only firm requirement is that the vehicle is fully charged at 07:00 the next morning, the exact timing of the charging is irrelevant to the vehicle user.

5.1 Electricity prices

A nightly charging session in Sweden can be planned and optimized fully, since the electricity prices are known in advance. Between 12:00 and 13:00 CET electricity prices for the entire 24 hours of the next day are bid upon and decided (Nord Pool Spot, n.d.-a).

Figure 23 and 24 show plots of the electricity prices (Nord Pool Spot, n.d.-b) from 2014, with all Swedish taxes included, to give the reader an idea how they generally fluctuate during the day and the year. Prices are constant for one hour at a time.

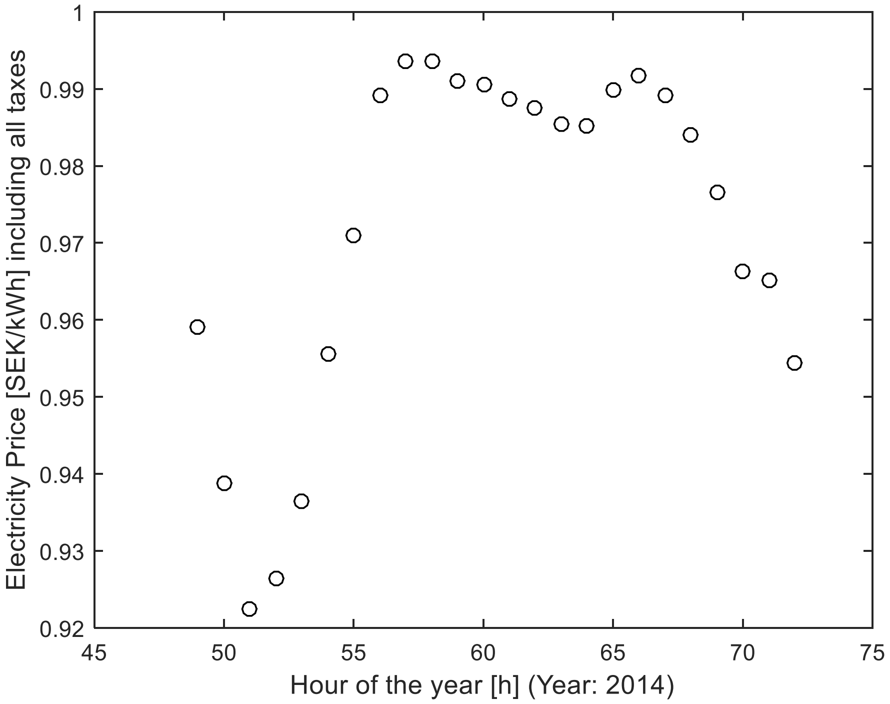

Figure 23: Electricity prices including all taxes for January 3rd 2014, in the price area SE3, where Linköping is located.

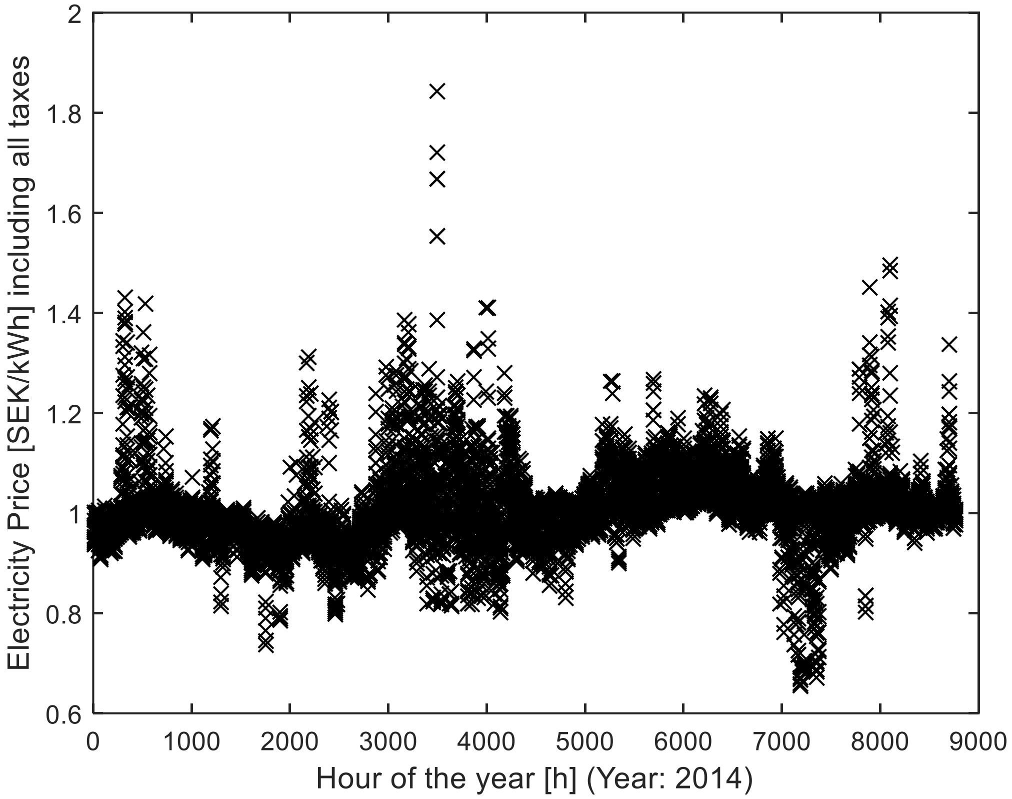

Figure 24: Electricity prices including all taxes for 2014,
in the price area SE3, where Linköping is located.

When importing the electricity prices from Excel files into Matlab, careful attention was put into getting the shifts to summer time and away from summer time correct. Energy usage patterns, and consequently electricity prices, rather strictly follow local time. When later calculating the optimal starting hour for a charging session, it is important that the prices are imported correctly. See Appendix C for parts of the used import routine.

Hourly electricity prices for 2013 and 2014 were available, and have been used.

Since this chapter mostly relies on summations and minimizations, the term simulations has been chosen, while the term optimization is reserved for DP, used later.

5.2 Timer started charging session

Let's assume that a timer is available to start the charging session at a certain time of the day, every day of the year. What hour is the optimal starting hour for the charging session? How much money can for example be saved compared to starting the charging directly when returning home from work or leisure activities, assumed to happen at 18:00 every day of the year?

As basis for these calculations the measured data from charging session 2 was used. Charging session 2 was done at 10 A. Reasons to choose charging session 2 and 10 A are:

- Charging at lower currents than 10 A only increase total energy usage.
- Charging at lower currents increases the total charging time, and thus leaves less options of placing the charging session in time. A longer charging session will also be more difficult to place in the deepest part of the valley in the electricity pricing.
- Charging at 13 A gave a comparable total energy consumption, but since ordinary Swedish household wall sockets rarely are rated at more than 10 A, this alternative was ruled out.
- Charging session 1 and 2 were so similar, that one of them was chosen at random.

The main characteristics of charging session 2 is:

- Charging current: 10 A
- Total energy consumed: 9.384 kWh
- Mean power during charging: 2.114 kW

To compute the charging cost, start by establishing the charging vector, ChV. This vector details how much energy is consumed each hour

$$ChV = [E_1, E_2, \dots, E_k, \dots, E_i] \tag{19}$$

In this instance we have

$$ChV = [2114, 2114, 2114, 2114, 928] \tag{20}$$

with i=5.

Please note that in a real application, almost any energy amount E_k can be reached by running power P for a specific part of an hour, as long as P>E.

Let the energy price [SEK/Wh] for a certain hour t of the year be e(t). The formula for calculating the cost of a charging session starting hour t thus becomes

$$C_{charging}(t) = \sum_{j=1}^{i} e(t + j - 1) \cdot ChV(j) \tag{21}$$

This formula is run for every hour of the year, storing the results in a vector in Matlab. With a simple routine using the modulo operator with the number 24 in Matlab, the cost of starting charging a certain time of the day for every day an entire year can be calculated.

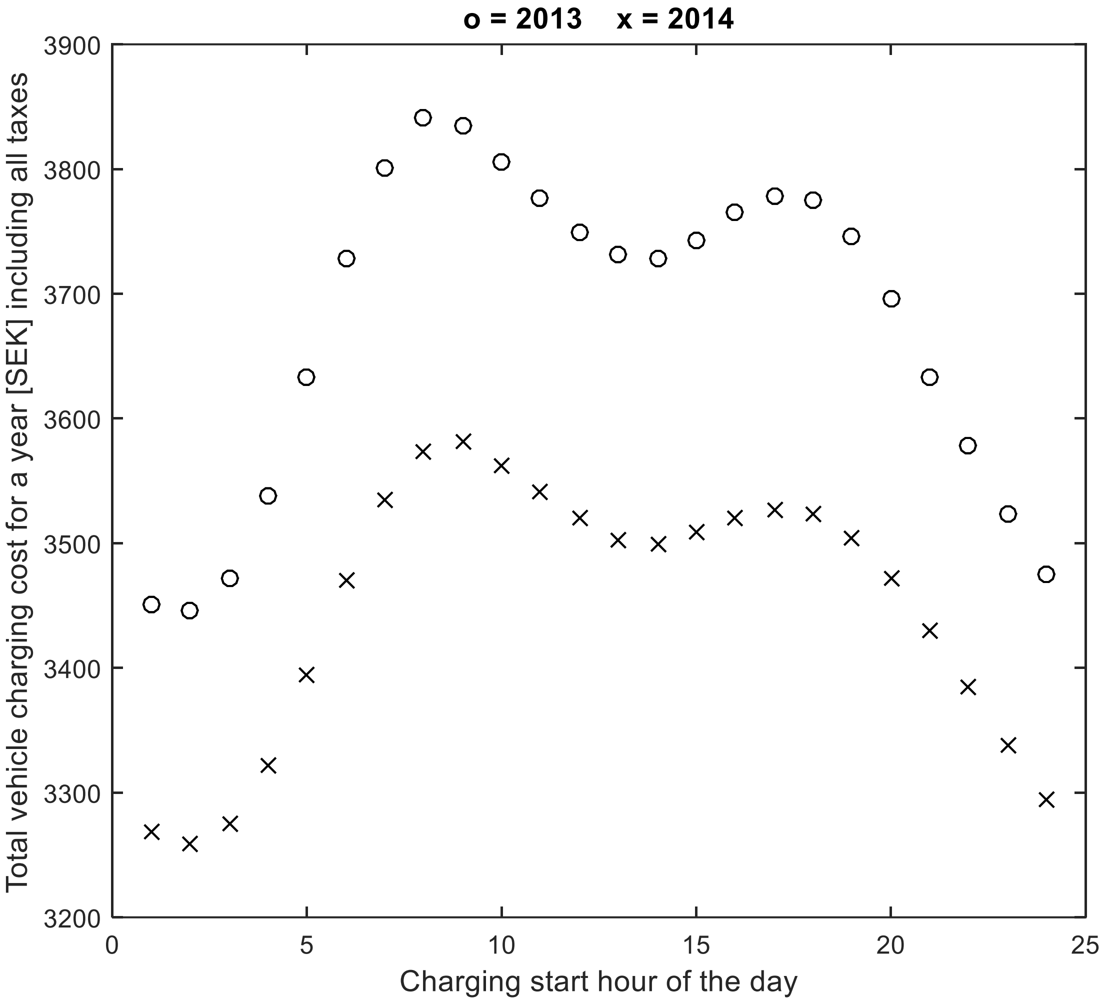

Figure 25: The cost of starting the charging of a vehicle at a certain time of the day for an entire year. Hour 2, i.e. 01:00-02:00, is the cheapest hour to start charging the vehicle for both 2013 and 2014. (Hour 1 is 00:00 to 01:00.)

As can be seen in Figure 25, there is a clear saving potential of using a timer. While clearly having different energy price situations, both 2013 and 2014 display similar price patterns. Starting charging at the beginning of hour 2, at 01:00, is the cheapest. The savings compared to hour 19, that is 18:00, is approximately 250 to 300 SEK. Meanwhile starting a charging session at around 08:00, when arriving at work, would be the most expensive option.

5.3 Timer start at cheapest hour for each individual night

It is important to remember that 01:00 isn't always the cheapest point in time to start the charging. Figure 25 only shows a sum of the charging costs for an entire year for each starting hour. For many nights, another charging start time than 01:00 gives the minimal charging cost.

So how can the cheapest charging start hour be found for each "charging night"? Charging night can be defined as beginning at 18:00 (hour 19) the first day, and ending at 07:00 the following day. I.e. charging can start between 18:00 (hour 19) to at latest 02:00 (hour 27) in the morning the next day, to be fully charged at 07:00, assuming 5 hours charging time.

Using the hour of the year format gives the following set of charging start hours for night n to choose from

$$chargingNight(n) = [19\ 20\ 21\ 22\ 23\ 24\ 25\ 26\ 27] + (n-1) * 24 \tag{22}$$

Again, note that charging can't start later than 02:00 (hour 27) with a charging duration of 5 hours, since charging has to be finished at 07:00.

Now calculate the cost for the entire year. Combining equation (21) and equation (22) and adding the sum for the entire year yields

$$C_{year} = \sum_{n=1}^{365} \min_{t \in chargingNight(n)} C_{charging}(t) \tag{23}$$

which looks at each charging night, and selects the charging start hour with minimal cost, and summarizes all these costs for the entire year. Figure 26 shows which hours that was chosen.

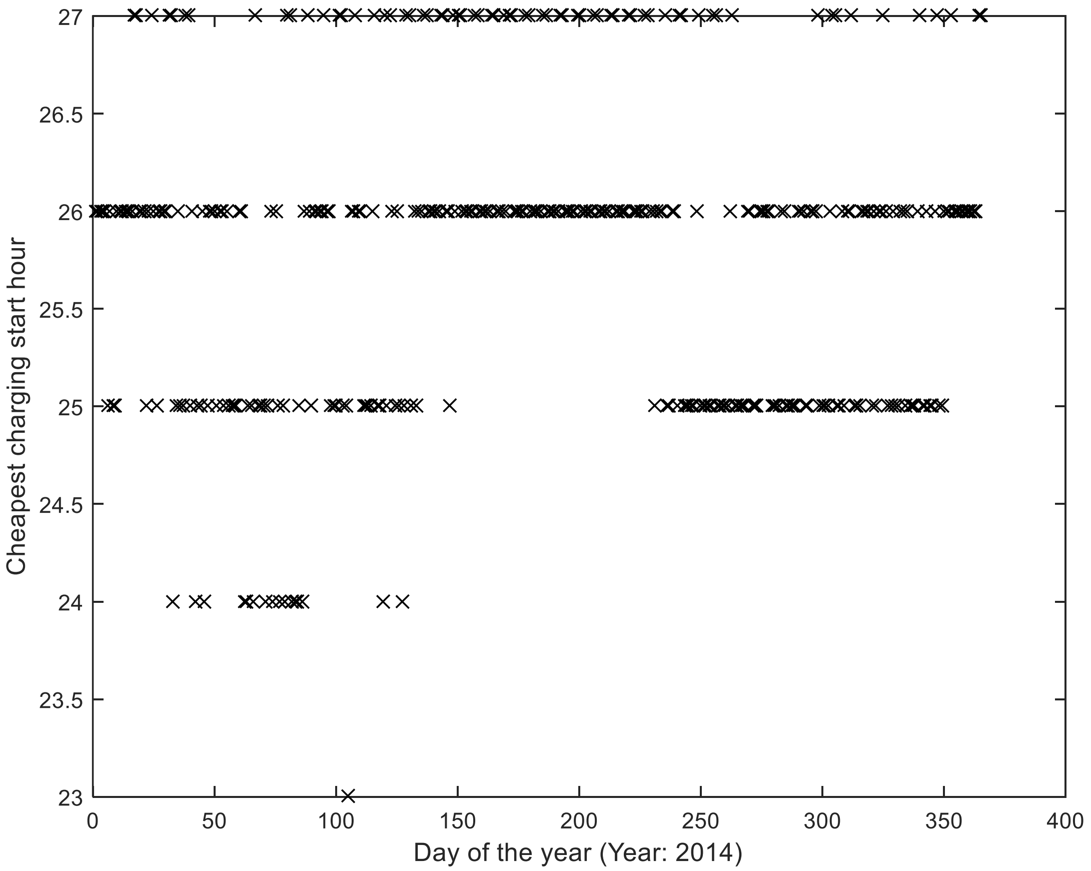

Figure 26: Which charging start hour that is the cheapest for every charging night (day) of 2014.

Table 2 shows the frequency for each charging start hour. Hour 26 (01:00) has the highest frequency, but hour 25 isn't that far behind.

Hour	**Frequency**
23	1
24	16
25	110
26	171
27	67

Table 2: The frequency of different charging start hours for 2014. 01:00 (hour 26) has the highest frequency.

5.4 Simulation results

The results from the simulations are summarized in Table 3.

[SEK]	**Total yearly cost starting charging at (Savings [SEK] are in relation to start at 18:00)**				
	18:00	**01:00**		**Cheapest hour**	
Year	**Cost**	**Cost**	**Savings**	**Cost**	**Savings**
2013	3746	3446	300	3434	312
2014	3504	3259	245	3252	252

Table 3: Costs of different charging start times

A simple timer set at 01:00 offers a sizeable cost saving compared to simply starting charging at the arrival home from work. Implementing a charging start at the hour optimal for each day would be much more complex, requiring the charger to know future electricity prices, and offers only a very small savings potential.

6 Charging scheduling with dynamic programming

While the previous chapter described charging cost simulations, relying on summations and minimizations mostly, the problem at hand now is to optimize the cost of charging a vehicle by deciding when and at which power to charge using dynamic programming.

This chapter describes an implementation of DP to solve the charging scheduling problem. First the grid and matrix is explained, followed by the cost-to-go concept and how to find the optimal solution. To streamline the explanation, some simplifications have been done.

Seen as an optimal control problem, see section 3.3.1 Formal description of dynamic programming, the SoC of the battery becomes the state x, and the charging power becomes the control signal u. Therefore in this application equation (8) becomes

$$\frac{dx_{SoC}}{dt} = \eta \frac{P_{charge}}{Q} \tag{24}$$

where η is the charging efficiency and Q is the battery capacity. Charging efficiency is considered to be one when using DP in this thesis. Battery capacity is thus assumed to be 9384 Wh, using data from charging session 2, as were the case in the simulations.

6.1 The grid and matrix setup

DP can be used to solve many different problems, and can look somewhat different depending on application. In Guzzella and Sciarretta (2013) a version adapted to solving energy optimization problems in hybrid vehicles is described. A DP framework inspired by this text has been developed at the division of Vehicular Systems at Linköping University, and that has been the starting point for the DP implementation in this thesis. The framework is developed in Mathworks Matlab code, using ordinary matrix manipulation commands. To analyze output, Matlab's plotting features are used.

At the core of DP is the "grid". In this application it looks very much like a two dimensional coordinate system, as can be seen in Figure 27. On the x-axis is time in hours and on the y-axis is SoC in %. The grid points are positioned at the intersections of the integer values (0, 1, 2, 3, ...,) of the x- and y-axis.

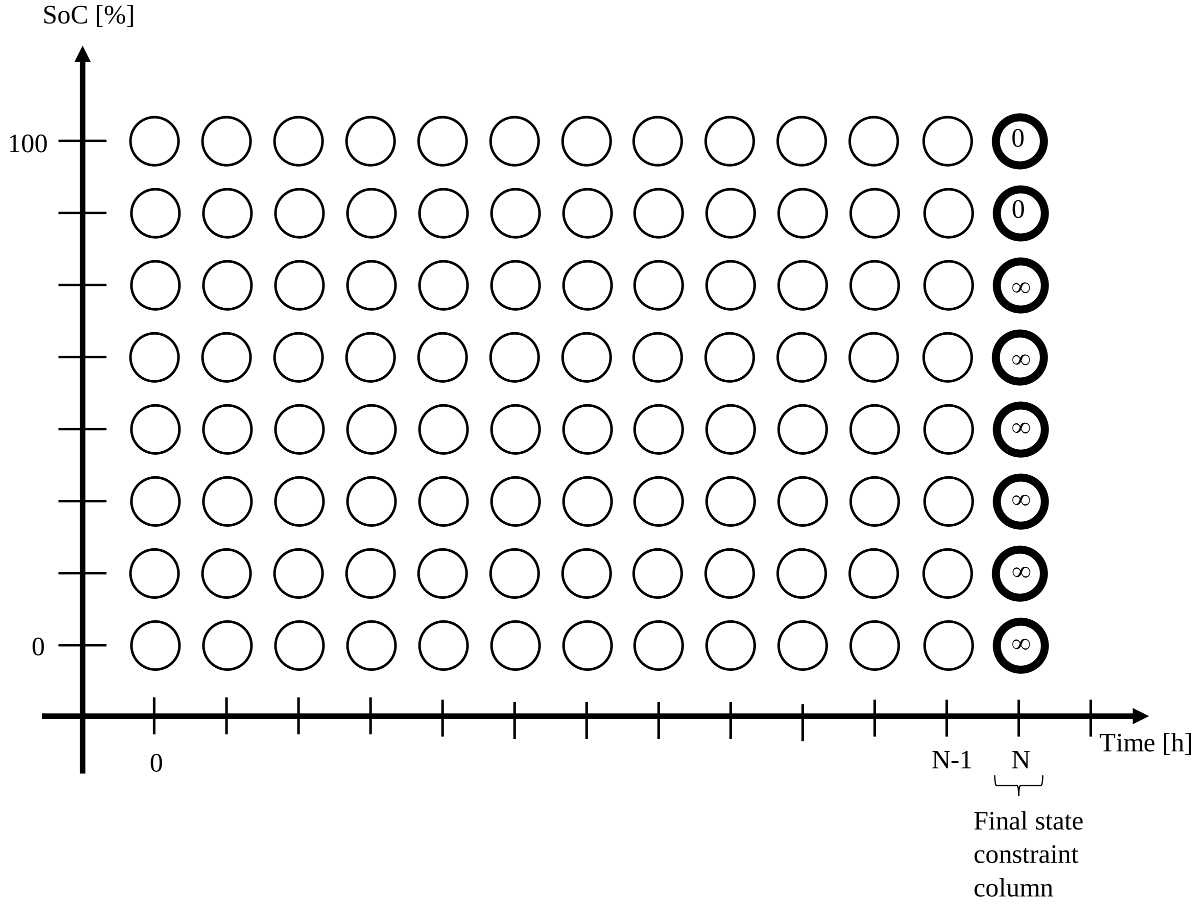

Figure 27: The state-time grid, simplified, having much fewer elements than the actual grid, for illustrational purposes.

To be able to do computations on this grid, the grid is mapped onto a matrix. Every grid point is mapped onto a single matrix element. Just as in the coordinate system, time increases going to the right, and SoC increases going upwards in the matrix. To optimize charging for a day, one might choose to have 24 columns, since the day has 24 hours, and 101 cells vertically, representing the integer values of SoC zero to 100%. Total grid size 101*24 = 2 424 cells. (Note: Increasing the size of the grid can improve the optimization results.)

To determine what shall be accomplished with the optimization, a final state constraint is defined. This tells the algorithm which levels of SoC are sought and accepted at the end of the last hour. Assume SoC = 100% is wanted, then an interval of for example 97-100% will have to be accepted, because of how DP is implemented in this thesis. Otherwise we might run the risk of not finding a solution. The final state constraint is in this instance effected by creating a column vector, 1 element wide and 101 cells high, each element representing a specific integer value of SoC, 0 to 100, with 0% at the bottom. In the unwanted cells numbered 0 to 96, infinity (inf) or a very large number, is stored. In the matrix elements representing acceptable SoC levels 0 is stored. Finally this column is added at the end of the matrix, like if it was a 25th hour. The column that implements the final state constraint is known as the final cost.

6.2 Cost-to-go

Cost-to-go is, simply put, how much it will cost in some currency unit from "now" to get to the end. Let's assume that we are at the beginning of the last hour of a charging session. The battery is missing 1 kWh of energy. Then we will have to charge the battery with 1 kW for that hour. Thus the cost-to-go is simply 1 kWh times the current energy price. The unit of cost-to-go in this example is SEK, Swedish krona. A cost-to-go matrix is a matrix filled with pre-calculated costs. In this case the matrix will contain the cheapest way to meet the final constraints for every level of SoC for every step in time. That way, one can look up a certain element in the cost-to-go matrix, say SoC 50% at 20:00, and find how much it will cost to get to the predefined 97-100% SoC target interval at 07:00.

6.3 New state calculation and interpolation

Interpolation is important in this thesis, since:

- it is used in the DP implementation described in this thesis.
- it is the cause of interesting issues, described in Chapter 7.

Assume a level of SoC of say 40% at time k, as can be seen in Figure 28, for which CtG is not known. Now calculate the SoC at time k+1. If a certain charging power is applied, say 1 kW, what will the SoC be at the end of that hour? Since it's assumed that battery doesn't lose any energy by itself, add the integral of equation (24) to the current SoC

$$SoC_{k+1} = SoC_k + \frac{P_{charge}}{Q} 100 \tag{25}$$

thus

$$SoC_{k+1} = 40 + \frac{1000}{9300} 100 \approx 50.75\% \tag{26}$$

But what is the cost-to-go for SoC = 50.75% at time k+1? The grid only has cost-to-go for integer values of SoC, so interpolation has to be used. Assume that CtG is known for all ordinary fixed grid points at k+1.

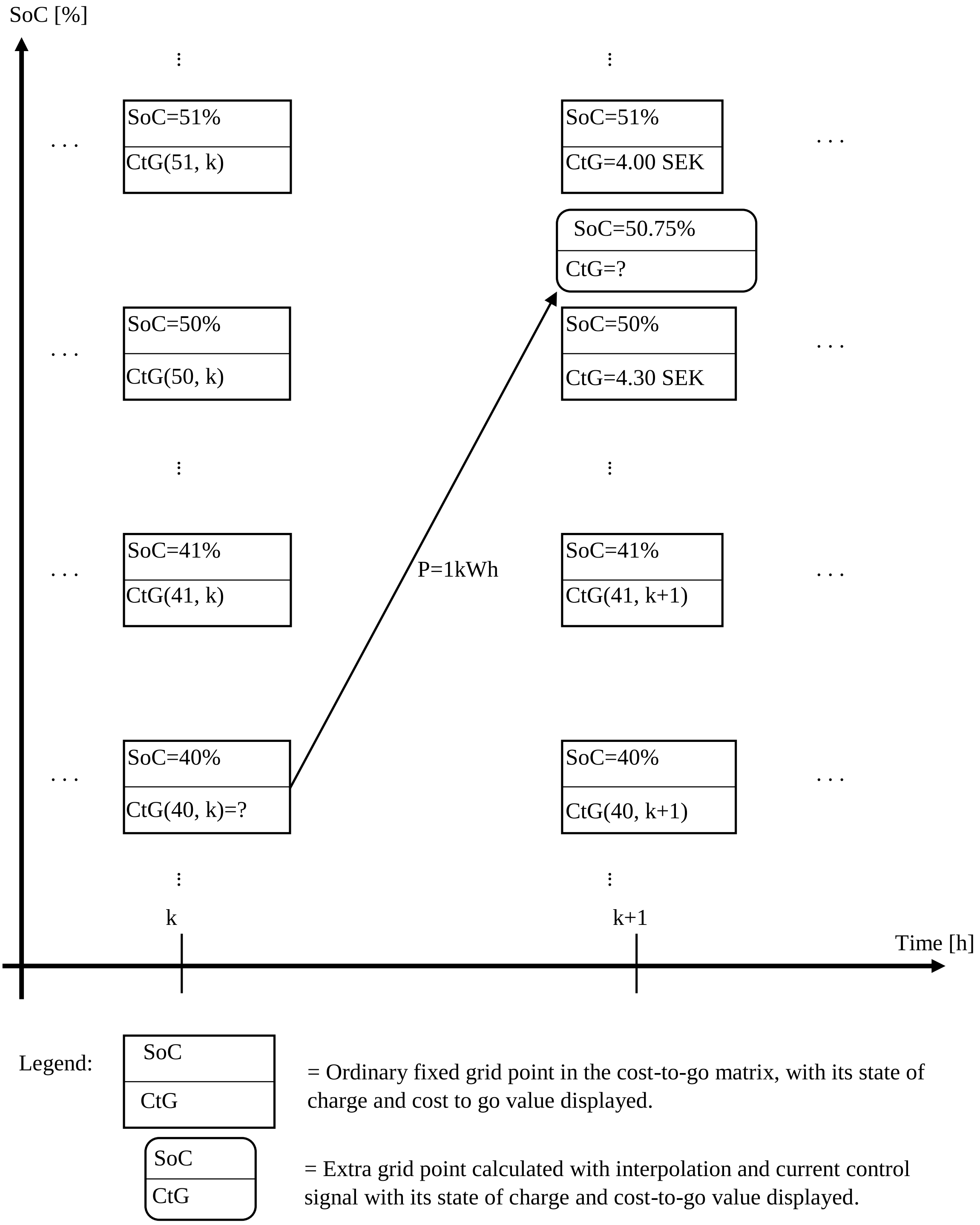
SoC [%]
SoC=51%
CtG(51, k)
SoC=51%
CtG=4.00 SEK
SoC=50.75%
CtG=?
SoC=50%
CtG(50, k)
SoC=50%
CtG=4.30 SEK
SoC=41%
CtG(41, k)
P=1kWh
SoC=41%
CtG(41, k+1)
SoC=40%
CtG(40, k)=?
SoC=40%
CtG(40, k+1)
k
k+1
Time [h]
Legend:
SoC
CtG
= Ordinary fixed grid point in the cost-to-go matrix, with its state of charge and cost to go value displayed.
SoC
CtG
= Extra grid point calculated with interpolation and current control signal with its state of charge and cost-to-go value displayed.

Figure 28: Detail of CtG matrix. Charging creates a movement in the CtG matrix.

The charging can thus be seen as a "power arrow" creating a movement and a new position in the cost-to-go matrix. The interpolation that shall now be executed is only concerned with some items in the column at time k+1, the new extra calculated grid point and the two adjacent ordinary grid points.

The interpolation is easier understood if we rotate the column -90° and plot the CtG values of the fixed grid points, as seen in Figure 29. SoC is on the x-axis and cost-to-go is on the y-axis.

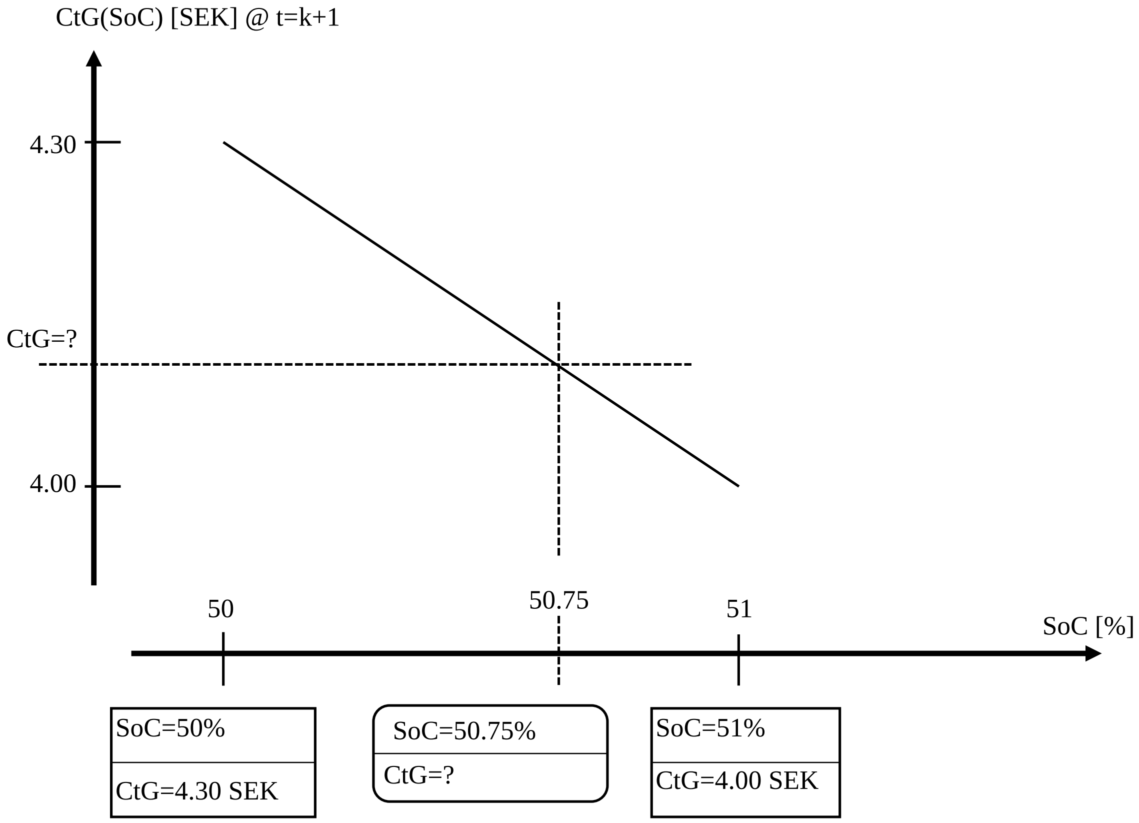

Figure 29: The interpolation to find CtG at a 50.75% SoC at t=k+1

This problem is solved with simple linear interpolation, illustrated in Figure 30.

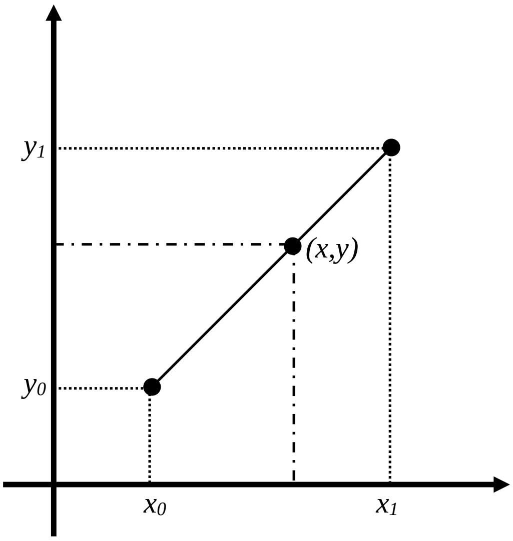

Figure 30: Linear interpolation

$$y = y_0 + \frac{y_1 - y_0}{x_1 - x_0}(x - x_0) \qquad (27)$$

which after numbers have been entered turns into the linear equation

$$y = mx + b \qquad (28)$$

Continuing our example we get

$$CtG_{SoC=50.75,t=k+1} = 4.30 + \frac{4 - 4.3}{51 - 50}(50.75 - 50) \approx 4.075 \text{ SEK} \qquad (29)$$

This is the first step in determining CtG(40, k), the following section will explain this further.

6.4 Calculating the cost-to-go matrix

After covering the basics: the grid, CtG, CtG matrix, new state calculation and interpolation, the reader is now prepared to understand the first phase of DP: calculating the cost-to-go matrix.

In this example, we will use the following notation:

- states: SoC = {0, 1, 2, ..., 100} [%]
- control signals (charging powers): P = {0, 100, 200, ..., 3000} [W]
- points in time: t = {0, 1, 2, 3, ..., N-1} where N = 13
- electricity price: e(t) [SEK/kWh]

Please note, the zeroth hour t = 0 is the first hour, representing for example 18:00 to 19:00. N-1 is the last hour, lasting for example from 06:00 to 07:00. There is no N:th hour, that column in the CtG matrix holds the final cost.

1. Define the grid, as described earlier in section 6.1 The grid and matrix setup. Remember that in this implementation, the calculated extra grid points are always positioned at x-axis-positions (points in time) that they share with a column of fixed pre-calculated grid points. See Figure 28 for reference. The y-axis-position (SoC) of the extra grid points on the other hand, can vary within the limits of possible states, 0-100%.

2. Begin at the far right, at column t = N-1. (Note: The rightmost column N contains the final cost. These values will not be changed, only read.)

3. Now, for every grid point in the N-1:th column (i.e. all different SoC levels), send out a "power arrow" for each of the different charging power levels, see Figure 31.

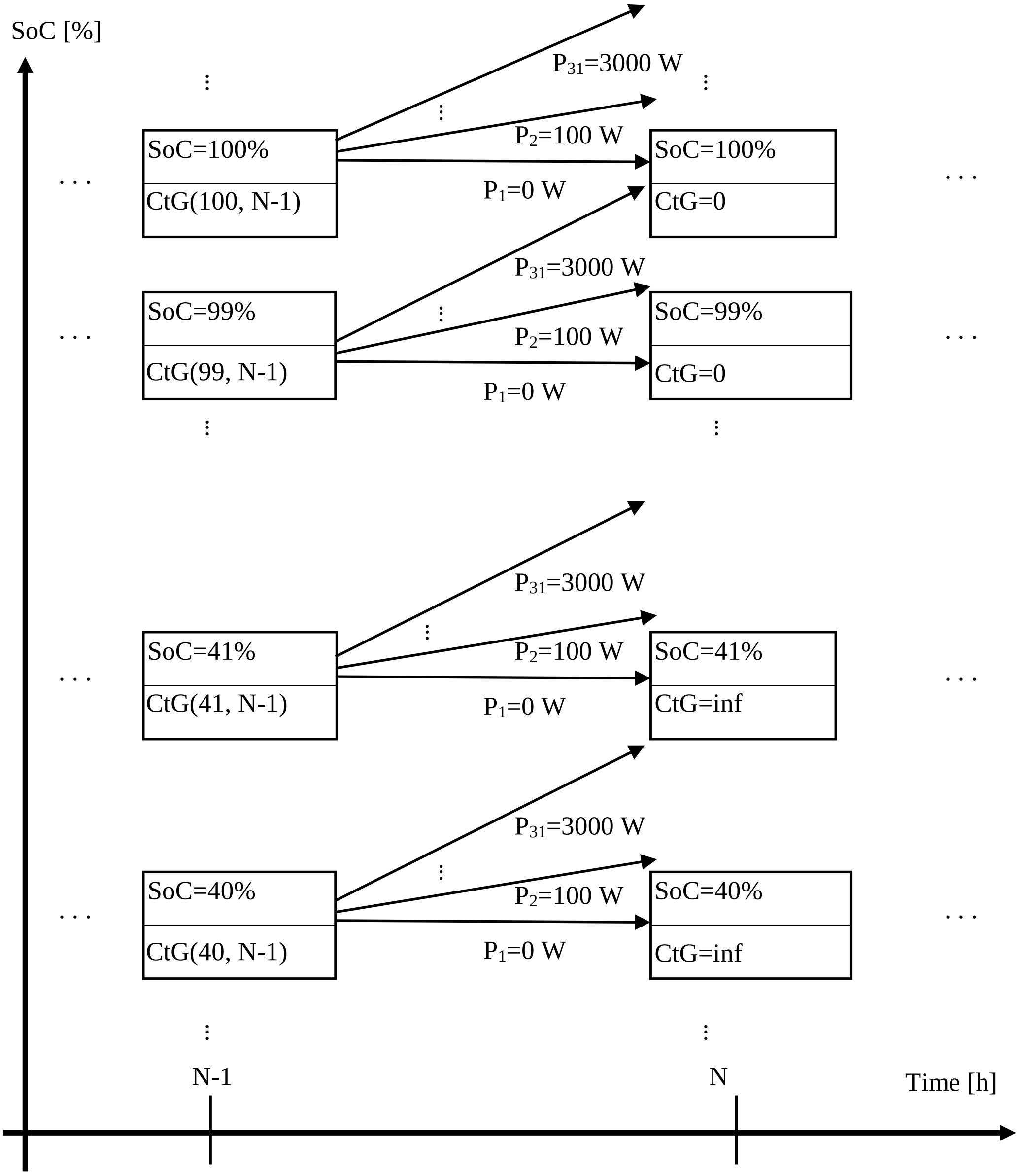
SoC [%]
SoC=100%
CtG(100, N-1)
SoC=99%
CtG(99, N-1)
SoC=41%
CtG(41, N-1)
SoC=40%
CtG(40, N-1)
P_{31}=3000 W
P_2=100 W
P_1=0 W
SoC=100%
CtG=0
SoC=99%
CtG=0
SoC=41%
CtG=inf
SoC=40%
CtG=inf
N-1
N
Time [h]

Figure 31: Send out all possible power arrows for every grid point in the current column.

4. Calculate where every power arrow end up in the (N-1)+1 = N:th column.

5. For every power arrow, look between which precalculated grid points (in this case the grid points of the final cost) they end up. Read the CtG value of these grid points in the N:th column. Use interpolation to calculate the CtG for the power arrows.

6. For each of the grid points in the (t = N-1) CtG matrix column : Take the CtG found for every power arrow starting at said grid point, and to that add the cost of consuming that arrow's power for an hour, using that arrow's power level times e(N-1). Choose the arrow that has the smallest sum of CtG and energy cost. Store that sum in the matrix element corresponding to that grid point.

7. With this column finished, work through the matrix to the left, stepping backwards in time, one column at a time. Repeat point 3 to 6 for every column in the grid., until the CtG matrix is filled.

6.5 Finding the optimal state trajectory

With the CtG matrix finished, we enter the second and last phase of the DP algorithm, finding the optimal state trajectory. Again, the optimal state trajectory is the result of using the optimal control policy, equation (16).

In this specific DP implementation, the optimal state trajectory can be seen as a path through the CtG matrix, from the left to the right, increasing the state SoC (charging) when electrical energy is cheap, and in the end reaching the 97-100% SoC target, see Figure 32.

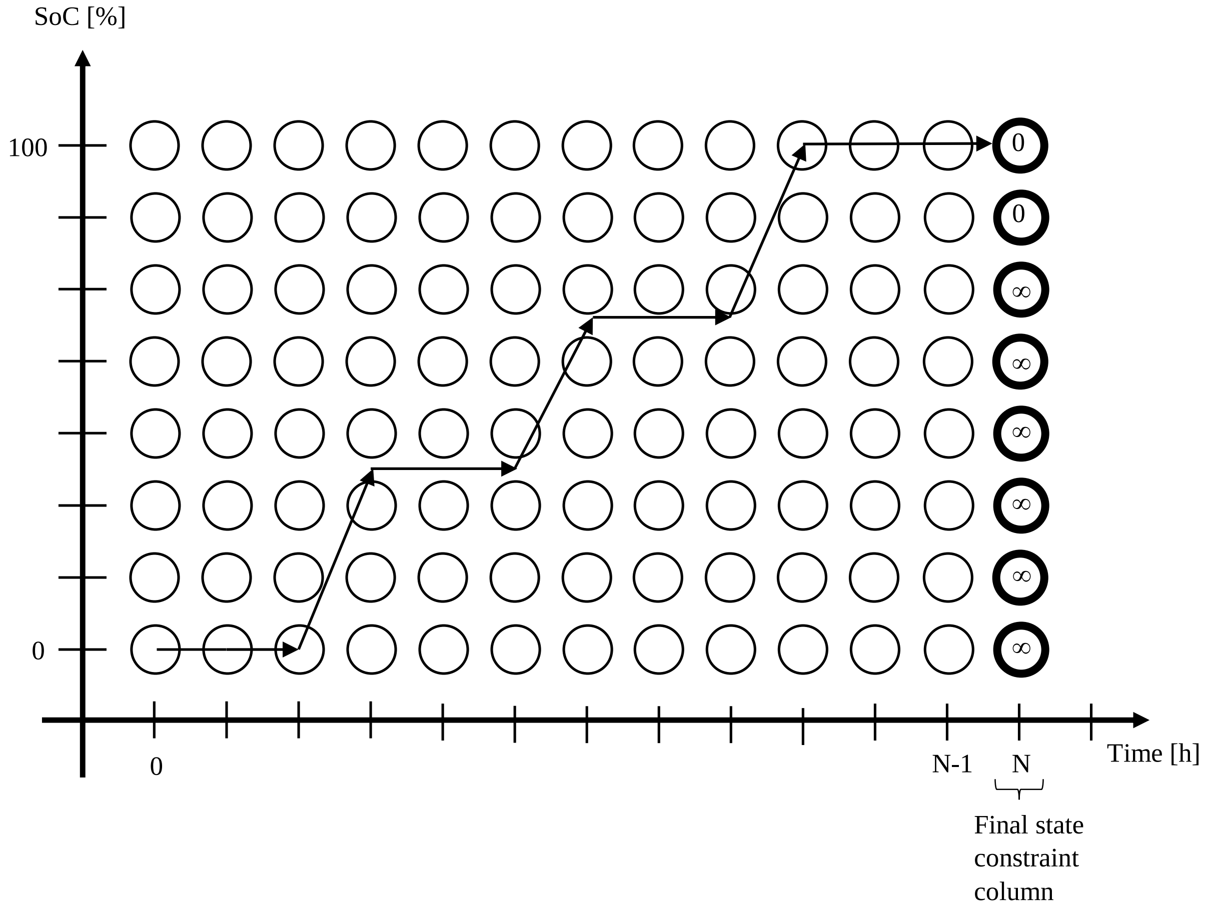

Figure 32: Optimal state trajectory. Simplified figure.

Please note that the initial condition, for SoC, doesn't have to be zero as in this figure. A vehicle can have energy left in the battery when the user wants to charge the vehicle.

Let's continue with the algorithm.

8. Traverse the CtG matrix from left to right, one column at a time. Begin at the preferred initial condition (SoC level) in column t=0. From that point in the grid (and from no other point), send out a power arrow for every available charging power level towards column t=1.

9. As earlier, add the energy cost of the power arrows to the cost-to-go found at the end of the power arrows in column t=1. Choose the arrow with the lowest sum.

10. Store state (SoC), control signal (charging power) and the cost of using said control signal.

11. Now, at t=1, from the SoC position found at point 9, send power arrows from t=1 towards column t=2.

12. Repeat point 9 to 11 until the entire optimal state trajectory is found.

Note: The total cost found using this method should be close to, save for accuracy errors, the value of the grid point where the trajectory starts, at t=0. This is fittingly also the case for the DP implementation in this thesis.

6.6 Results

Total cost including all taxes

- 2013: 3328 SEK
- 2014: 3153 SEK

Please note that these results are based on optimizations with specific settings, see Appendix A. Changing the settings, e.g. grid size, the set of charging powers etc., might give different results.

The results for the first night of 2014 can be seen in Figure 33.

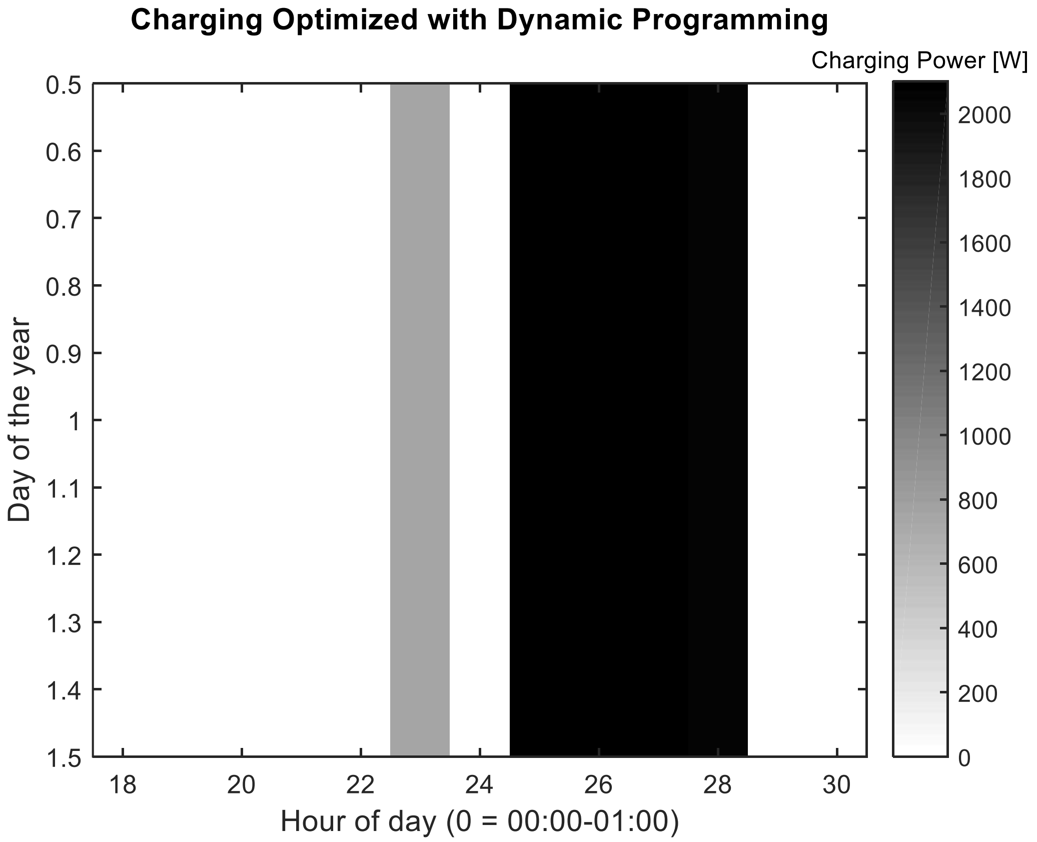

Figure 33: Charging powers for the first night of 2014. Please note that:
A) Only day 1 is shown, thus merely the number "1" on the y-axis is relevant.
B) The tics on the x-axis in this and the following figures of the same type point at the middle of the bars representing each charging hour.

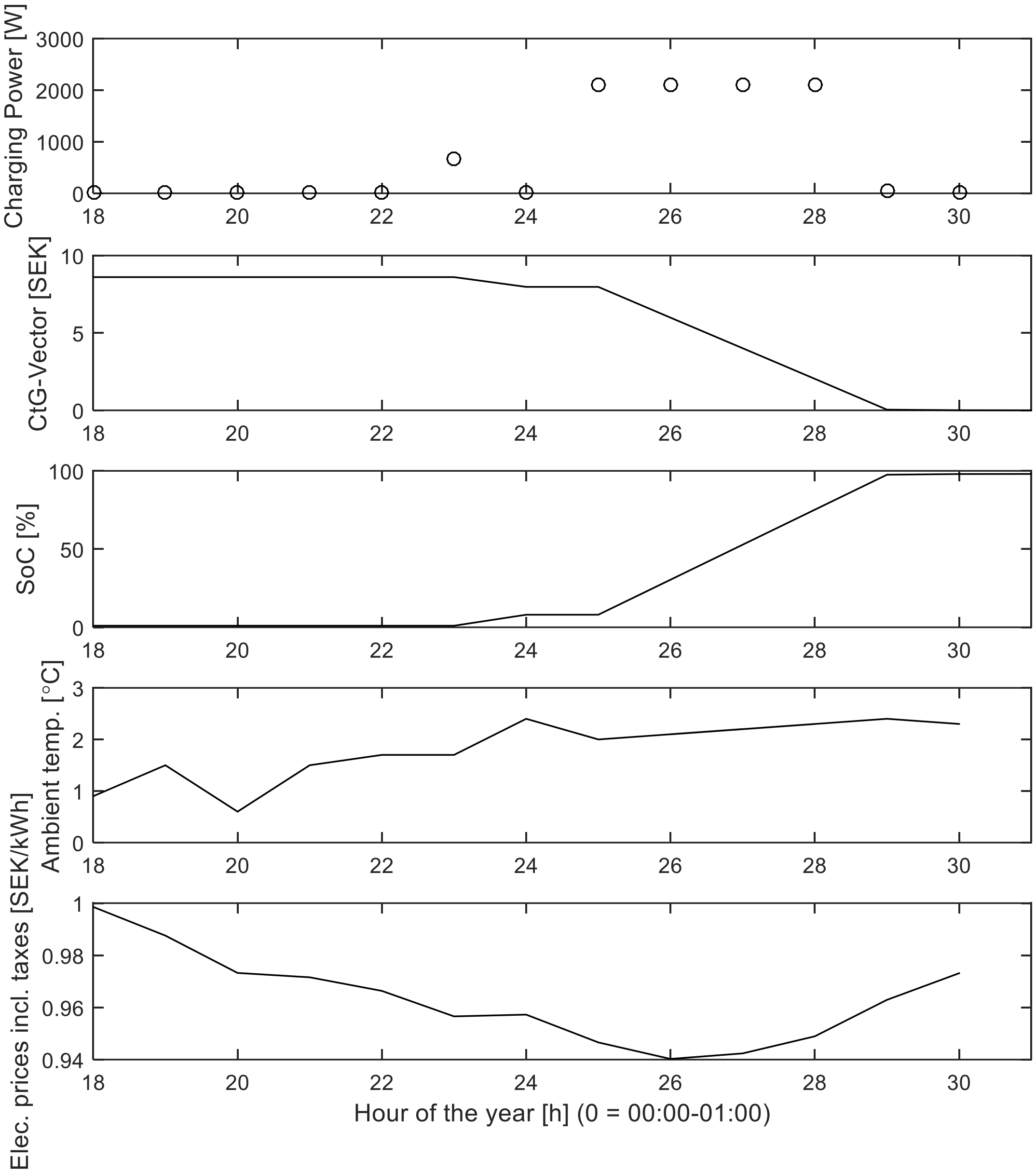

Figure 34: Charging powers and other data for the first night of 2014. Please note that the ambient temperature is not taken into account in the simulations or optimization runs in this thesis.

In Figure 34 beginning from the upmost plot the following can be seen:

1. The charging power for each hour P(t)=[0 0 0 0 0 660 0 2100 2100 2100 2100 40 5]. (Yes, this is somewhat suboptimal and will be discussed in detail in Chapter 7)
2. The CtG-vector, displaying the momentary CtG for each hour. Mainly decreasing. Reaching zero in the end as it should
3. Momentary SoC for each hour. Zero in the beginning, climbing very close to 100% in the end, as it should.
4. Ambient temperature, readily available for future use.
5. Electricity prices for each hour.

As expected, the vehicle is charged when the electricity prices are low.

Figures 35 and 36 show the charging powers for 2013 and 2014.

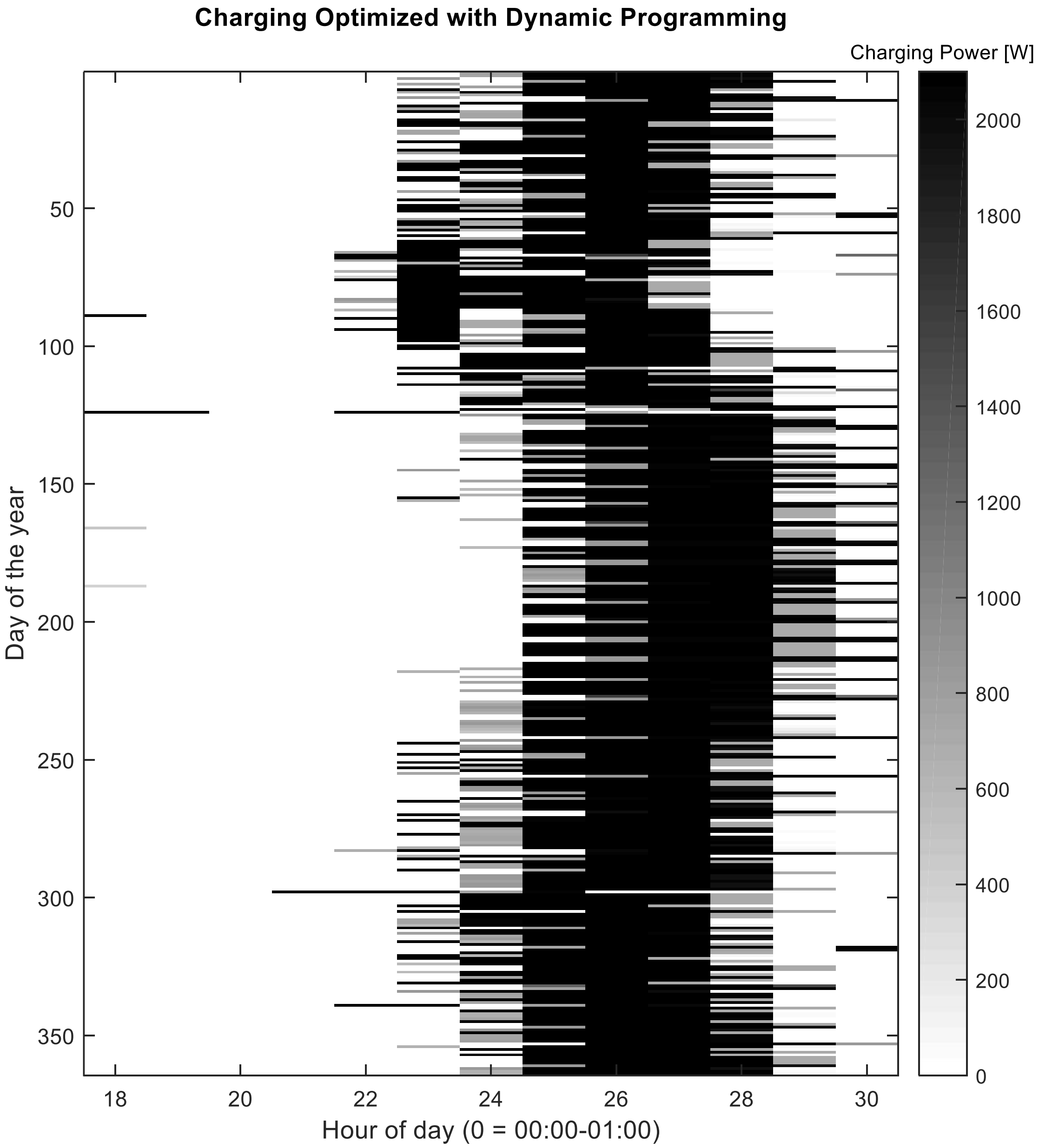

Figure 35: Charging powers for 2013.

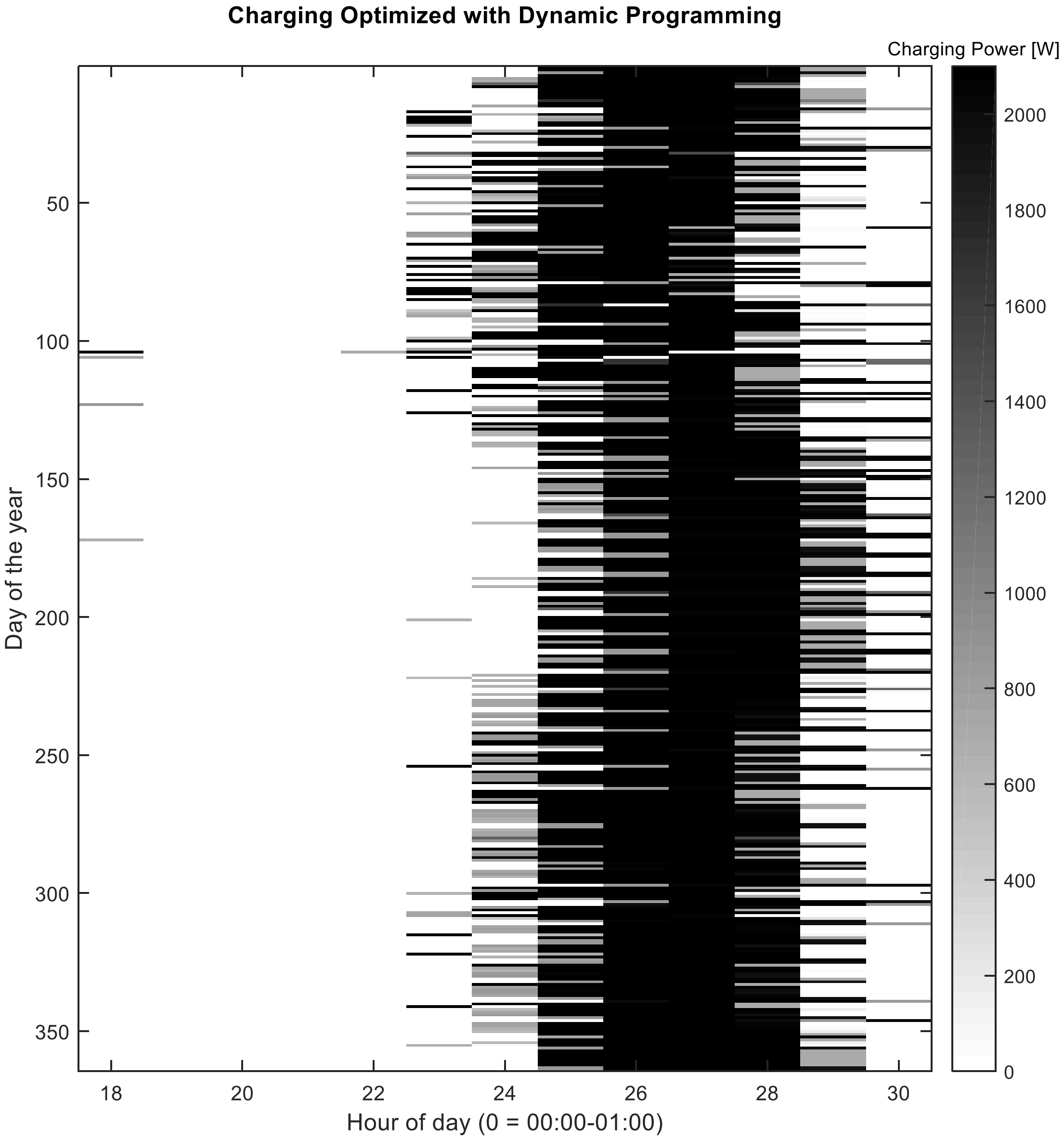

Figure 36: Charging powers for 2014.

From the plots it can be seen that many charging sessions begin at hour 01:00-02:00 (hour 25). Many charging sessions don't begin at full power. At 02:00-03:00 (hour 26) most charging sessions are at full power. At 03:00-04:00 (hour 27) almost every charging sessions is at full power.

7 Dynamic programming boundary issues

During the adaptation of the DP framework, making it solve the charging scheduling problem, some issues surfaced. The DP algorithm made suboptimal choices, for example often saving a small charging event for the last hour, even if electricity prices were steadily increasing.

This issue was not that difficult to understand and try to correct once it had been identified. The main challenge was identifying the issue. Debugging the matrices involved, that are combined again and again in dynamic programming, was not easy.

This chapter begins with a section describing in detail what is wrong with the optimization results. This is followed by a formal description of the problem, a short review of related research, and finally some suggestions on how to mitigate the issues.

7.1 Issues introduction

The problem at hand is dynamic programming with a limited set of predetermined discrete control signals and interpolation, one state and one control signal. The DP algorithm is to choose the control signal with the cheapest cost-to-go. The problem is that a control signal with an unrealizable CtG value can be chosen. The cause of this is that the interpolation function returns numerically correct values, that can't be put into effect, since the control signals needed doesn't belong to the limited set of predetermined control signals.

Example: Looking to get above 97% SoC (where cost-to-go is 0), one might end up at 96,999% somewhere in the end, close to $t = N$. SoC stays there until the last hour, when the final state constraint must be fulfilled.

Why? Because the smallest nonzero control signal (charging power) might be 100 W. Then it will be the cheapest to do nothing, 0 W, because interpolations says that 0 W has the smallest cost-to-go. The algorithm thus fails to take action even if the electricity price (and realizable cost-to-go) increases.

An example will follow. For the first charging session (the first "night) of 2014:

> The optimal choice of charging powers are (handpicked, see section 9.2.10):
> [0 0 0 0 0 705 0 2100 2100 2100 2100 0 0] giving the cost 8.608500 SEK.
>
> DP results in:
> [0 0 0 0 0 660 0 2100 2100 2100 2100 40 5] giving the cost 8.608837 SEK.

Even though the differences in charging powers are clear, the effect on cost is very small.

Generally, this problem doesn't only concern interpolations for the extra grid points adjacent to the zero CtG boundary, but also (at least) every control signal with the chance to cross the boundary.

7.2 Formal issues description

Following is a formalized version of the issues with the DP implementation. See Figure 37 for a situation overview.

Notation:

- $t \in \{0, 1, ..., N\text{-}1\}$ [h] The number of the current hour.
- $C_{t,SoC}$ [SEK] The cost-to-go for a certain hour t and state of charge level SoC.
- SoC_{lim} [%] The state of charge level that should be met or exceeded at the end of hour N-1.
- SoC_{step} [percentage points] The difference in state of charge between two adjacent cost-to-go matrix grid points.
- $SoC \in \{0, SoC_{step}, 2SoC_{step}, ..., 100\}$ [%] The discrete SoC values in the grid and CtG matrix. Every grid point along a horizontal line in the CtG matrix have the same SoC value.
- X_t Extra grid point at time t, used e.g. when finding the optimal trajectory.
- S_t State of charge for X_t.
- $P \in \{P_1, P_2,..., P_k,..., P_n\} = \{0, P_{min}, ..., :P_{max}\}$ [kW] The limited predetermined set of discrete charging powers.
- e(t) [SEK/kWh] The electricity price at hour t.
- $P_k \cdot 1 \cdot e(t) = P_k \cdot e(t)$ [SEK] The cost of using charging power number k for the entire hour t. Power times time is energy. Energy times energy price is cost.

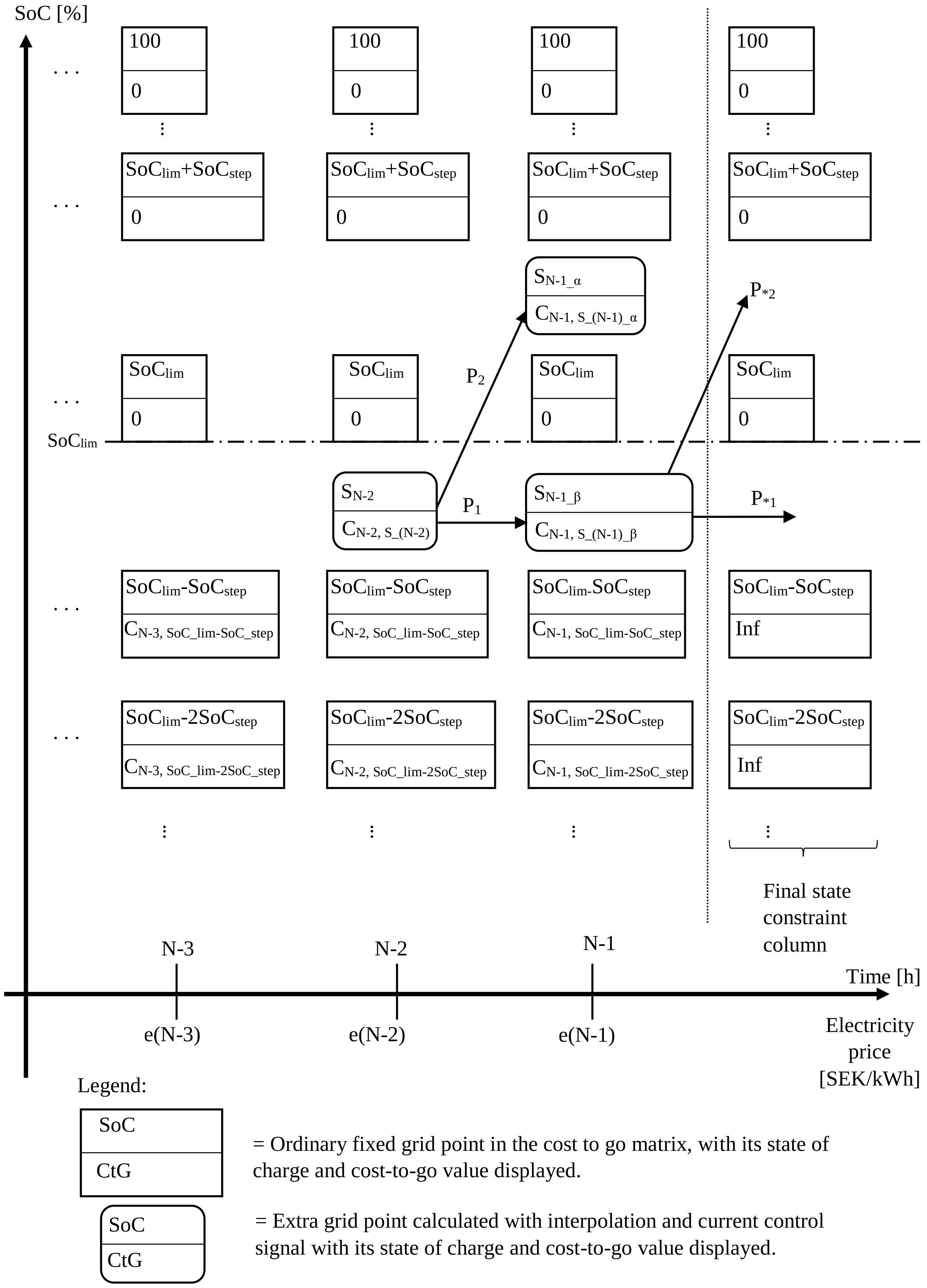
SoC [%]
100
0
SoC$_{lim}$+SoC$_{step}$
0
S$_{N-1\_α}$
C$_{N-1, S\_(N-1)\_α}$
P$_{*2}$
P$_2$
SoC$_{lim}$
0
SoC$_{lim}$
S$_{N-2}$
C$_{N-2, S\_(N-2)}$
P$_1$
S$_{N-1\_β}$
C$_{N-1, S\_(N-1)\_β}$
P$_{*1}$
SoC$_{lim}$-SoC$_{step}$
C$_{N-3, SoC\_lim-SoC\_step}$
C$_{N-2, SoC\_lim-SoC\_step}$
C$_{N-1, SoC\_lim-SoC\_step}$
Inf
SoC$_{lim}$-2SoC$_{step}$
C$_{N-3, SoC\_lim-2SoC\_step}$
C$_{N-2, SoC\_lim-2SoC\_step}$
C$_{N-1, SoC\_lim-2SoC\_step}$
Inf
Final state constraint column
N-3
N-2
N-1
Time [h]
e(N-3)
e(N-2)
e(N-1)
Electricity price [SEK/kWh]
Legend:
SoC
CtG
SoC
CtG

= Ordinary fixed grid point in the cost to go matrix, with its state of charge and cost-to-go value displayed.

= Extra grid point calculated with interpolation and current control signal with its state of charge and cost-to-go value displayed.

Figure 37: Choosing between P_1 and P_2.

Let's observe when the algorithm chooses between P_1 and P_2. Assume

$$e(N-2) < e(N-1)$$

where the price increase is small, e.g. 10%. Remember

$$P_1 = 0 \text{ and } P_2 = P_{min}$$

If the extra grid point X_{N-2} has a S_{N-2} very close to (but smaller than) SoC_{lim} and therefore a very small

$$C_{N-2,S_{N-2}}$$

based upon interpolation of ordinary fixed grid points above and below, where

$$C_{N-2,S_{N-2}} << P_2 \cdot e(N-2)$$

the following will occur. Choose the smallest between

$$P_2 \cdot e(N-2) + C_{N-1,S_{N-1_\alpha}} \tag{30}$$

and

$$P_1 \cdot e(N-2) + C_{N-1,S_{N-1_\beta}} \tag{31}$$

$$\Rightarrow$$

i.e. between

$$P_2 \cdot e(N-2) \tag{32}$$

and

$$C_{N-1,S_{N-1_\beta}} \tag{33}$$

Since

$$C_{N-1,S_{N-1_\alpha}} = 0 \ \& \ P_1 = 0 \tag{34}$$

the value of equation (31) becomes

$$C_{N-1,S_{N-1_\beta}}$$

and will be based on and calculated solely by interpolating between the cost-to-go values of the fixed grid points above and below, valued

$$0 \text{ and } C_{N-1,SoC_{lim}-SoC_{step}}$$

Thus

$$C_{N-1,S_{N-1_\beta}}$$

positioned very close to the point valued zero will become very small. And equation (31) will be chosen by the DP algorithm. The problem is that this promised cost-to-go can't be realized.

For the next hour, N-1, P_{*2} has to be chosen because the final state constraint will lead to the interpolated CtG value of inf for P_{*1}. And since

$$e(N-2) < e(N-1)$$

the result is a higher cost than expected, and an increase in the cost-to-go value of the optimal trajectory. We clearly have a suboptimal solution.

This problem also exists (at least) for all $P_{k \neq 1}$ that can cross the SoC_{lim} border into the zero CtG area, for any time except N-1, in the CtG matrix.

Interpolation, see equation (27), using the currently used notation, becomes

$$C_{N-1,S_{N-1}} = C_{below} + \frac{C_{above} - C_{below}}{SoC_{above} - SoC_{below}} (S_{N-1} - SoC_{below}) \qquad (35)$$

"Above" and "below" are references to the values of the adjacent CtG grid points over and under the point for which an interpolated CtG is sought.

7.3 Current research

Guzzella and Sciarretta (2013, p. 374) discusses some aspects of *"infeasible states or inputs"*. That is, how infinite cost together with an interpolation scheme can be problematic. They also mention the article *On Implementation of Dynamic Programming for Optimal Control Problems with Final State Constraints* by Sundström, Ambühl and Guzzella (2010). This article details how interpolation can lead to that DP uses infeasible grid points, i.e. from which the final state constraint cannot be met. When these grid points are included in the calculation and not specially considered, the found solution deteriorates.

This is related to the problem at hand in this thesis. Interpolation leading to choices of suboptimal inputs/controls signals. Suboptimal because they lead to points being chosen in the grid from which the promised cost-to-go can’t be realized since there is only a limited set of control signals to choose from.

7.4 Solutions

A number of ways to mitigate the issues will now be presented. See also the "Future work" section in Chapter 9.

7.4.1 Negative cost-to-go values

Introduce negative cost-to-go values instead of zero for SoC levels above SoC_{lim}. This way power arrows passing the zero CtG boundary get "rewarded" for the distance travelled past the boundary. The negative costs could be based on how much energy above the zero CtG level the battery holds at the end of the charging session, and the electricity price at that moment. The negative costs could be introduced in the final cost column at SoC levels above the zero CtG SoC level.

This method is questionable from a formal and theoretical standpoint. And even if it removes some unwanted issues, running optimizations indicate that it seems to lead to a higher total cost than no change at all.

The higher total cost might be a result of that the DP algorithm with this modification rewards charging the battery above SoC_{lim}, but the total cost calculation does not take into account the value of SoC levels above SoC_{lim} at the end of the charging session.

7.4.2 Change the interpolation function

It is important to remember that the interpolation function:

- is called when the CtG is built up.
- is called when finding the optimal state trajectory.
- gives an answer to the question of what it will cost to get to the end from a (future) point in the grid which is under consideration to be chosen.

The issue might be addressed in the following manner:

- Change the interpolation function, and thus interfere in the cost-to-go calculations.
- Do this when making the cost-to-go matrix and or finding the optimal state trajectory.
- Force the cost-to-go values to be based on the limited predetermined control signal set, and minimal future electrical energy price, if the boundary (e.g. SoC = 97%) can be crossed.

In detail, this method can be realized in the following way. When there is a power arrow that has the ability to cross the zero CtG boundary, the interpolation function will not return the result from the interpolation calculation, instead it will return a special value.

This special value is based on:

1. the lowest possible available discrete charging power that reaches across the boundary.
2. the lowest possible future electricity price.

These two values are multiplied, and returned as the CtG for the extra grid point at said SoC level at the said future point in time.

Thus note, the modified interpolation function can be used when

a) the CtG matrix is being calculated.
b) finding the optimal control trajectory.

Running optimizations show that method b) solves the issue described earlier, which suboptimally waited for the very last hour to reach above the boundary. Furthermore, method b) actually lowers total cost.

Running optimizations for entire years, the following has been tested [see a) and b) above]:

v00) No modification of the interpolation algorithm.
v01) b)
v10) a)
v11) a) and b)

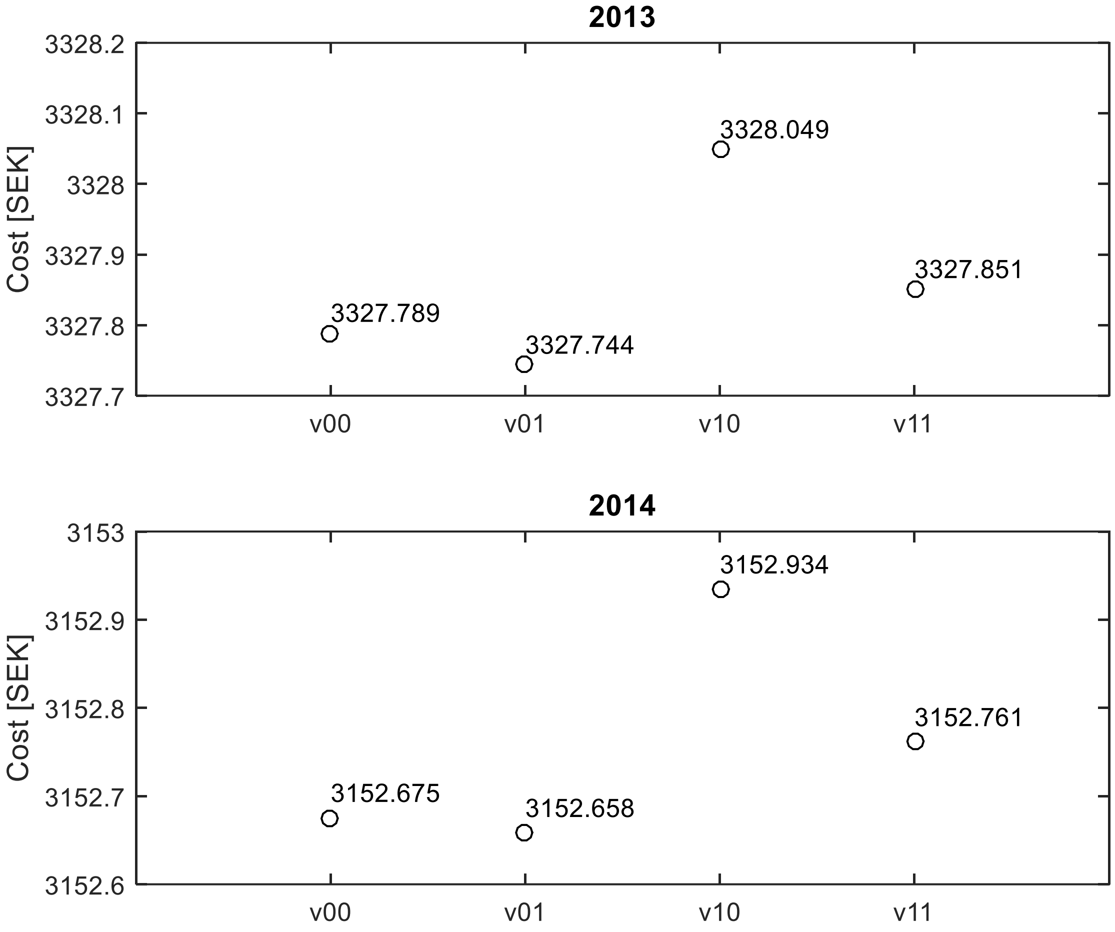

Figure 38: The total cost of charging a vehicle including all taxes for 2013 and 2014 in SEK., using different modifications of the interpolations algorithm.

As can be seen in Figure 38, b) does reduce the total cost for both 2013 and 2014. But only with fractions of a krona. (Please note that these results are based on optimizations with specific settings, see Appendix A. Changing the settings, e.g. grid size, the set of charging powers etc., might give different results.)

The reasons that the v01 modifications doesn't reduce the total cost more might be:

- Even though the modification b) removes some suboptimal manners, it actually results in a higher charging cost for some charging sessions.
- When the modification reduces cost for a day, the reduction is very small.

The modification v01 also seems to introduce some new kind of suboptimal behavior in the algorithm. As an illustration, the issues with the first charging session (the first "night) of 2014 will be repeated and supplemented:

> The optimal choice of charging powers are (handpicked, see section 9.2.10):
> [0 0 0 0 0 705 0 2100 2100 2100 2100 0 0] giving the cost 8.608500 SEK.
>
> DP results in:
> [0 0 0 0 0 660 0 2100 2100 2100 2100 40 5] giving the cost 8.608837 SEK.
>
> DP with v01 modification yields:
> [0 0 0 0 0 660 0 2100 2100 2100 2100 45 0] giving the cost 8.608786 SEK.

Again, clear differences in charging power but small effects on cost. Clearly some issues remain even with the v01 modification.

7.4.3 Add an extra row to the grid

To mitigate the issues related to crossing the boundary, an extra row could be introduced into the grid, and thus also into the CtG matrix, creating something like a buffer zone. Placed a very small distance (e.g. 1e-14) below the SoC_{lim} row, this new row will make the uniform grid nonuniform, and hopefully help with the interpolation issues. The buffer zone should be so small that extra grid points extremely rarely end up in it.

Original uniform vertical spacing of the CtG matrix:
socGrid = [socMin:socStep:socMax]

New nonuniform vertical spacing of the CtG matrix:
socGrid = [socMin:socStep:socFinal-1, socFinal-1e-14, socFinal:socStep:socMax]
Where e.g.:

- socMin = 0
- socMax = 100
- socStep = 1

Running the optimization, as before except for changing socGrid, the first charging session (the first "night) of 2014 now becomes:
[0 0 0 0 0 750 0 2100 2100 2090 2065 0 0] giving the cost 8.608910 SEK.

The problems with the last hours are clearly gone, but other problems evidently still persist.

Running the optimization for the entire year of 2014 results in a total cost of 3152.846 SEK, only beating v10 in the previous section. Thus adding this extra row gives a total cost for 2014 that is more expensive than the unmodified option v00, leaving the v01 modification in the previous section as the cheapest method.

But perhaps something different could be achieved by modifying socStep? See Table 4.

socStep [percentage points]	**Cost [SEK]**	**Power for hour t [W]**													**Total energy usage [Wh]**
		18	**19**	**20**	**21**	**22**	**23**	**24**	**25**	**26**	**27**	**28**	**29**	**30**	
Optimal															
Handpicked	8.608500	0	0	0	0	0	705	0	2100	2100	2100	2100	0	0	9105
With an extra row															
1	8.608910	0	0	0	0	0	750	0	2100	2100	2090	2065	0	0	9105
0.5	8.608910	0	0	0	0	0	750	0	2100	2100	2090	2065	0	0	9105
0.25	8.608910	0	0	0	0	0	750	0	2100	2100	2090	2065	0	0	9105
0.125	*8.608500*	*0*	*0*	*0*	*0*	*0*	*705*	*0*	*2100*	*2100*	*2100*	*2100*	*0*	*0*	*9105*
0.0625	8.610920	0	0	0	0	0	705	0	2100	2100	2100	2000	0	100	9105
0.0313	8.611164	0	0	0	0	5	725	15	2100	2100	2100	1965	0	95	9105
Modification v00															
1	8.608837	0	0	0	0	0	660	0	2100	2100	2100	2100	40	5	9105
0.5	8.608625	0	0	0	0	0	700	5	2100	2100	2100	2095	0	5	9105
0.25	8.608621	0	0	0	0	0	705	0	2100	2100	2100	2095	0	5	9105
0.125	8.608698	0	0	0	0	0	715	0	2100	2100	2100	2085	0	5	9105
0.0625	8.608813	0	0	0	0	0	730	0	2100	2100	2100	2070	0	5	9105
0.0313	8.613366	0	0	0	0	0	705	0	2100	2100	2100	2100	0	5	9110
Modification v01															
1	8.608786	0	0	0	0	0	660	0	2100	2100	2100	2100	45	0	9105
0.5	8.608606	0	0	0	0	0	700	5	2100	2100	2095	2100	5	0	9105
0.25	8.608603	0	0	0	0	0	705	0	2100	2100	2095	2100	5	0	9105
0.125	8.608745	0	0	0	0	0	715	0	2100	2100	2085	2100	5	0	9105
0.0625	8.608958	0	0	0	0	0	730	0	2100	2100	2070	2100	5	0	9105
0.0313	8.613366	0	0	0	0	0	705	0	2100	2100	2100	2100	0	5	9110

Table 4 Changing socStep for different modifications of the DP routine.

Keep in mind that socStep = 1 is the default setting for all other DP optimization runs in this thesis.

Notable results are:

- With an extra row:
    - No difference between socStep = 1, 0.5 and 0.25.
    - Achieves the optimal result for socStep = 0.125.
    - Solution deteriorates for socStep smaller than 0.125.
- Modification v00:
    - Cost initially decrease as socStep gets smaller and smaller, then for 0.125 and 0.0625 it increases.
    - For 0.0313 it reaches close to optimal solution, only the 5 W charge the last hour as an disturbance. Note that the total energy usage here pops up to 9110 Wh, which might happen since the DP algorithm aims at an interval of SoC, clearly increasing total cost.
- Modification v01:
    - Cost initially decrease as socStep gets smaller and smaller, then for 0.125 and 0.0625 it increases.
    - For 0.0313 it reaches close to optimal solution, surprisingly getting a 5 W charge the last hour. That result has been double checked. Note that the total energy usage here pops up to 9110 Wh, which might happen since the DP algorithm aims at an interval of SoC, clearly increasing total cost.

Without doubt something is at play here, making the DP results suboptimal in all cases but one. The "extra row" modification beats v00 and v01 by getting the optimal result for socStep = 0.125. When socStep becomes this small, computation time for one night is around 80 seconds on a modern notebook, 8 times longer than optimizing a charging night with socStep = 1. (This is no surprise since 1/0.125 = 8.)

8 Discussion

This chapter synthesizes and analyzes all knowledge covered in this thesis. Beginning with a thorough discussion regarding the measured charging profiles, followed by a comparison of the simulations and optimizations results. Then comes a list of general recommendations, followed by discussions on "the power gap", Swedish energy taxation, and thesis methodology.

8.1 Charging profiles

A number of charging profiles have been recorded. This involves a wealth of factors that now will be discussed in detail.

8.1.1 Ambient temperature

It is notable that the ambient temperature differences between charging session 1 and 2 didn't render any noticeable differences in total energy usage. The reason for this might be that the vehicle, because of time constraints, wasn't given enough time to fully adapt to the ambient temperature. Only two hours of cooling down in charging session 1, and no cooling down at all in charging session 2.

8.1.2 Thermal battery aspects

First, let's conclude that while the charging sessions in this thesis were executed in rather cold weather, the temperatures are representative for the charging location, having an average yearly temperature of approximately 8.13°C.

This thesis hasn't been able to point out the existence or energy usage of battery preheating. But extra energy costs and low performance of batteries in cold weather will be a new aspect for vehicle consumers, used to ICE vehicles, to handle. Even though an ICE has reduced fuel efficiency in low temperature situations, refilling a vehicle with liquid fossil fuel is actually cheaper in cold weather, since fuel is sold at a price per volume and not weight.

Looking at the summary of the charging sessions in Table 1 in section 4.6 Summary, it is clear that the charging sessions with the higher charging currents have the lowest total energy consumptions. Looking at the numbers from the Volvo V60 PHEV specifications, the opposite is mostly true.

The reasons for this might be the cold weather, and that the lower the current was, the more the battery heating blanket had to work in the charging sessions, since the charging process in itself didn't generate as much heat. And on the other hand, perhaps no cooling was needed in the high current charging sessions, because of the cold ambient temperature. The numbers in the vehicle specifications on the other hand, could be the results of charging with cooling activated for the higher charging currents.

8.1.3 Ramp down

The ramp downs in some of the higher current charging sessions, are evidence that charging profiles and charging optimization could become more complex as charging power increases to higher and higher levels. The ramp down of the 13 A charging profile shows some resemblance to the fast charging charging profile in Bai and Lukic (2013). One explanation might be that heat issues limit the maximum charging power.

From another viewpoint, it is strange that not all charging sessions have a ramp down, since this was anticipated in section 3.1.3 Lithium-ion batteries. One explanation of why the ramp down is close to invisible in the charging sessions using smaller currents, is illustrated in Figure 40. This is a magnification of the lower part of Figure 39. The smaller the initial charging current, the less visible the change from CC to CV is in charging power usage.

Looking at Figure 40, it is possible that the 13 A charging maps onto curve C, the 10 A charging onto curve D (ramp down visible in charging session 1, but not charging session 2) and the 6 and 8 A charging currents may be positioned between curve D and C_{cutoff}, making the transition between CC and CV even more difficult to spot.

It might also be possible that different charging currents create other proportions between the durations of CC and CV, this could further smooth out the power usage change in the phase transition.

Yet another explanation, mentioned in section 8.1.2 Thermal battery aspects, could be that the lower charging currents use an electric heating blanket during the charging session, this would further smooth out the charging phase change from CC to CV.

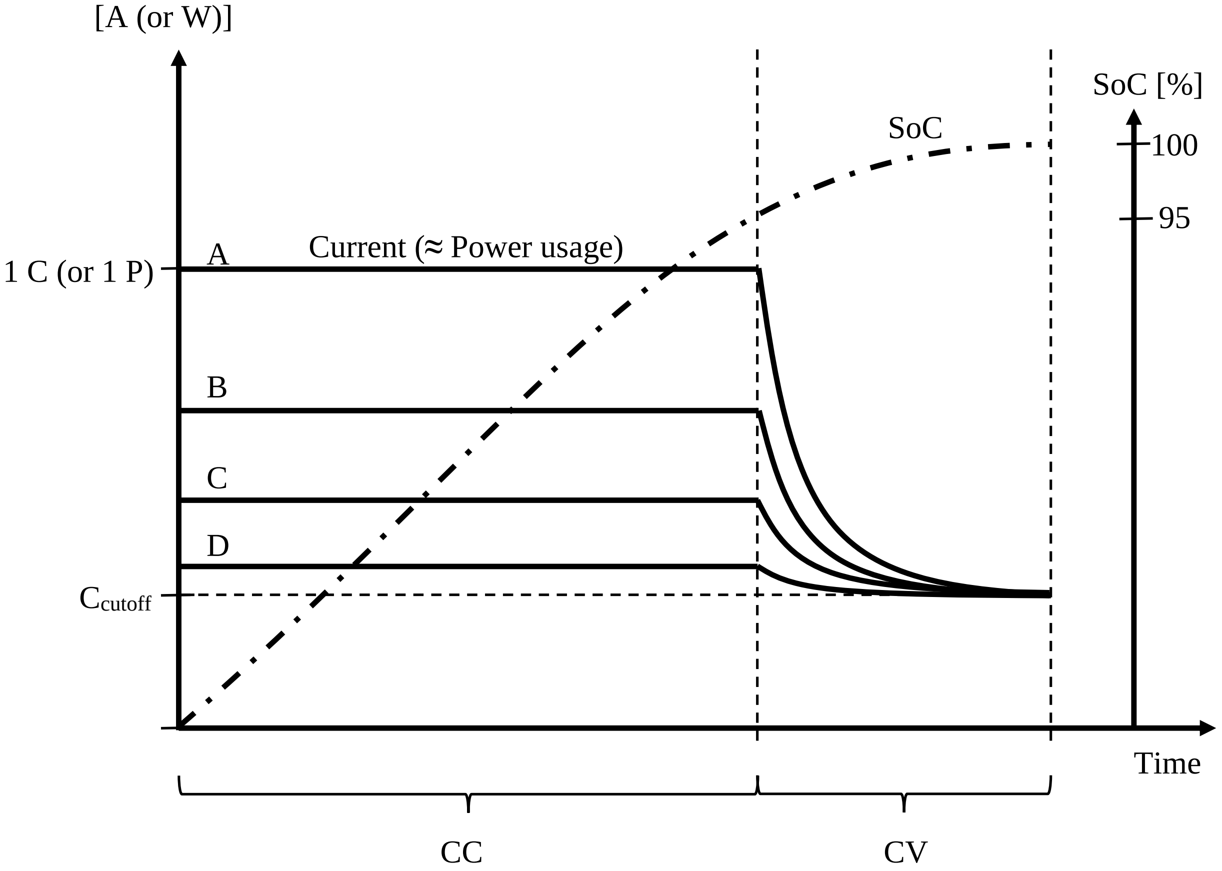

Figure 40: Charging current ramp downs for different charging currents. Please note that this is a somewhat simplified figure. In reality, total charging time will vary with the charging current.

In summary, future studies of vehicle charging, that model charging currents over 10 A, can't assume that the charging profile is a simple rectangle. This relates to the criticism in Pashajavid and Golkar (2014, p. 199) of studies that assume constant charging profile versus time.

8.1.4 Battery capacity available to the driver

Marra, et al. (2010) claims that drivers of PHEV usually have access to 60% of their true rated battery capacity, the number given for EVs is 80%. In the case of the Volvo V60 PHEV, that would mean 6.72 kWh available capacity, assuming a full SoH for the Volvo V60 PHEV. Assuming a full SoH is reasonable since the Volvo V60 PHEV has a low mileage, 20 000 km.

Since the lowest recorded total charging energy usage in this thesis is approximately 9.4 kWh, that would mean a charging efficiency of at best 71.5%. That is much lower than what usually is quoted for Li-ion batteries. Probably Volvo has chosen to give the V60 PHEV driver access to much more than 60%, perhaps somewhere between 70% and 80%.

Tesla Motors (n.d.) states a 92% round-trip DC efficiency of their Li-ion battery Powerwall. Round-trip efficiency is the ratio of total energy output (discharge) divided by total energy input (charge). In this case there are no discharge losses, but instead AC to DC rectifier efficiency losses when charging.

A 90% charging efficiency would mean that 9.4 kWh spent charging saved 8.46 kWh of energy in the battery, representing approximately 75.6 % of the battery's quoted 11.2 kWh capacity.

It is also possible that in the figure 9.4 kWh some other and higher losses than the assumed 10% (=100%-90%) did occur, such as:

- preconditioning and postconditioning of the battery
- the need to heat or cool the battery during charging
- heat developing when charging the battery, in the battery, cables, or electronics (e.g. in the AC/DC converter).

All these factors may push down the calculated 75.6% level further, but hardly to 60%.

8.1.5 Measurements versus specifications

While the total energy usage data doesn't match that well between the charging sessions and the specifications, the charging durations line up reasonable well for 6 and 10 A, the only currents available in both data sets. This indicates that some faulty assumptions might have been made calculating the energy usage from the specifications.

Looking at Table 1, comparing the charging sessions and the calculated values from the specifications, the total energy consumption data has a better fit, the lower the charging current is. As is shown in section 8.1.3 Ramp down, the charging current is not constant, especially for the higher charging currents. Thus the energy usage calculated from the specifications has been exaggerated by assuming that the charging current is constant. This could be another reason for the big energy consumption mismatch, but perhaps not the only reason, since 10 A charging only has a small, if any, ramp down.

An additional factor is charging current setting versus actual charging current. To lower the risk of blowing a fuse in the electrical service in household, the 10 A setting doesn't actually charge at 10 A. Section 4.5.2 Charging session 2 gives mean charging power at 2114.187 W, representing 9.19 A. That's close to 10% less than 10 A, which is used to approximate the total energy usage, for the charging sessions mentioned in the specifications.

Combining all these factors and adding one:

- ambient temperature
- the possibility of energy usage for heating or cooling the battery
- charging current ramp down
- charging current setting versus actual charging current
- battery SoH for a vehicle that is three years old and has been driven 20 000 km

could probably explain the entire difference in total energy usage between the measurements and those calculated from the specifications.

8.2 Charging cost: simulation vs optimization

[SEK] **Total yearly cost starting charging at**
(Savings [SEK] are in relation to start at 18:00)

	18:00	**01:00**		**Cheapest hour**		**DP**	
Year	**Cost**	**Cost**	**Savings**	**Cost**	**Savings**	**Cost**	**Savings**
2013	3746	3446	300	3434	312	3328	418
2014	3504	3259	245	3252	252	3153	351

Table 5: Comparing results from simulations and optimization runs.

In Table 5 it can be seen that starting the vehicle charging session with a timer at 01:00 offers a sizeable saving compared to the default start at 18:00. Picking the cheapest hour offers very small additional savings. Dynamic programming offers clearly better extra savings.

Looking at the charging powers figures in section 6.6 Results it is evident that DP mostly saves additional money by starting and ending the charging sessions with low power charging. In some cases it also uses discontinuous charging.

8.3 What can be done short term?

A general simplified recommendation for vehicle owners would be to start their vehicle's charging so that it is midway at approximately 03:00.

The simulations show that around 250-300 SEK could be saved each year by starting the vehicle charging at 01:00 instead of 18:00. Given an assumed lifetime of 10 years for a charging station, and zero interest etc., that results in a budget of 2500 - 3000 SEK. Note that this is an amount that can be spent on top of what the charging station, that has to be bought to be able to charge the vehicle at home anyways, already cost. 2500 - 3000 SEK should be more than enough to include a simple time and timer function in consumer charging stations.

Finding the cheapest hour to start charging for each individual day offers little extra savings compared to using a timer, at approximately 100 SEK extra for 10 years, and would require a much more complex solution than a simple timer, to acquire and process the energy prices daily. This probably leaves no realizable saving.

The additional savings offered by dynamic programming puts the 10 year investment budget at circa 1000 SEK more than the timer option. Assuming that it is free and convenient to download electricity pricing information, for example via the WiFi network of a household, this could be a realizable saving. Cheap consumers Internet routers can be bought for around 500 SEK, and ought to have a processor fast enough to do the DP optimization. Perhaps a function like this could be built into a consumer charging station fitting within the 10 years total extra budget of circa 3500 - 4000 SEK?

8.4 What can be done long term?

If a household has a building energy management system (BEMS), the BEMS probably knows the future electricity prices and might be able to control the charging station and optimize the charging session at little extra cost.

It is also possible that if the full standard suggested in ISO (2013) is implemented, electricity prices are transferred through the charging interface, and the charging planning can be carried out by the vehicle.

Further it has to be considered that electricity prices may rise considerably in Sweden. As a result of e.g. political decisions or market forces. The potential for huge price increases exists, Sweden has among the lowest pre-tax electricity prices in the world. Swedish electricity prices are approximately half of those in Japan and a third of those in Italy (Oilprices.com, 2010).

8.5 Dynamic programming issues

It was surprising to find an issue with dynamic programming not described in any research paper, as far as could be found. While there were some success in mitigating the problems, there are some issues still remaining. However it has also been proven that the deviations are so small that they probably won't influence any of the conclusions drawn in this thesis.

A number of solutions to the issues are described. One particular modification, using specific DP-settings, achieved the optimal solution for a certain test night. The solution in question introduces a buffer zone which perhaps can mitigate the problems with interpolation when crossing the zero CtG boundary.

8.6 The power gap

Power usage in Sweden fluctuates over the year. Power consumption is at its highest during the winter as can be seen in Figure 41 (Nord Pool Spot, n.d.-c).

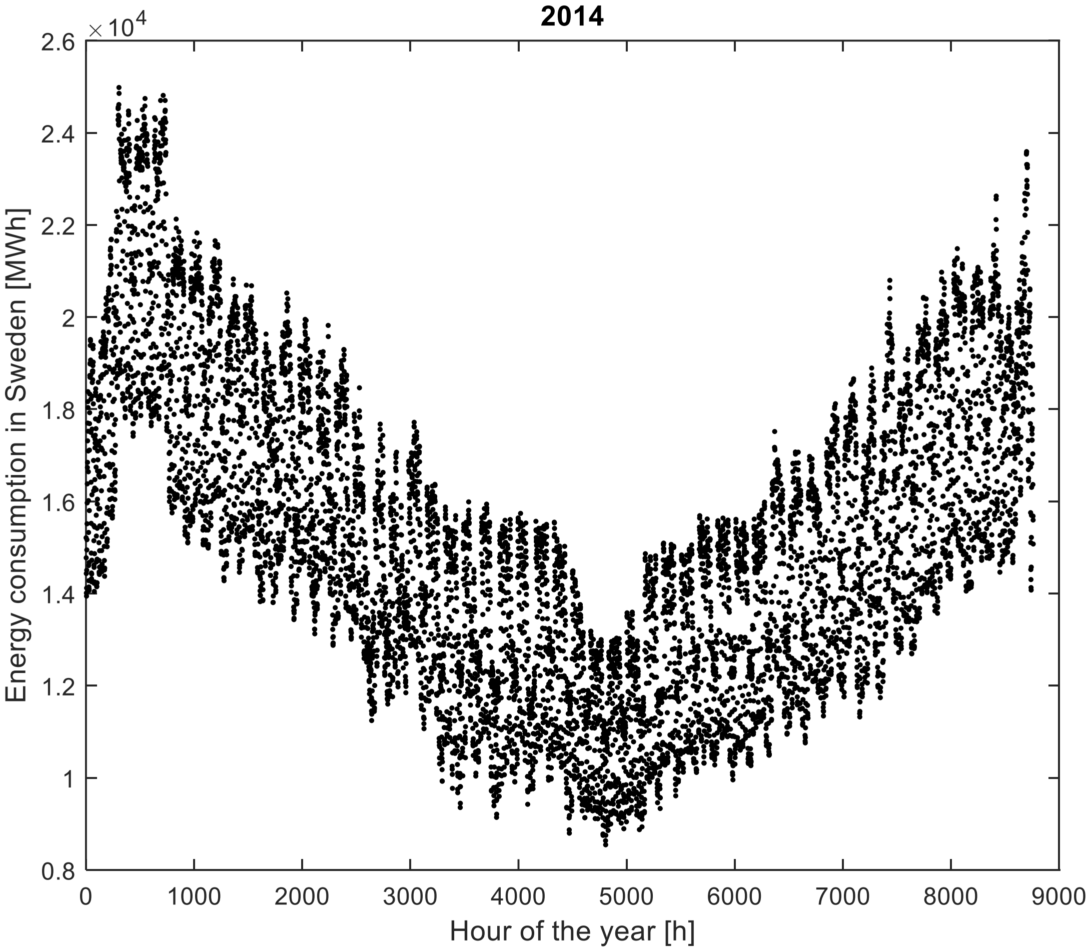

Figure 41: Electric energy usage in Sweden for each hour of 2014.

Similar to energy prices, energy usage also has its daily pattern, see Figure 42.

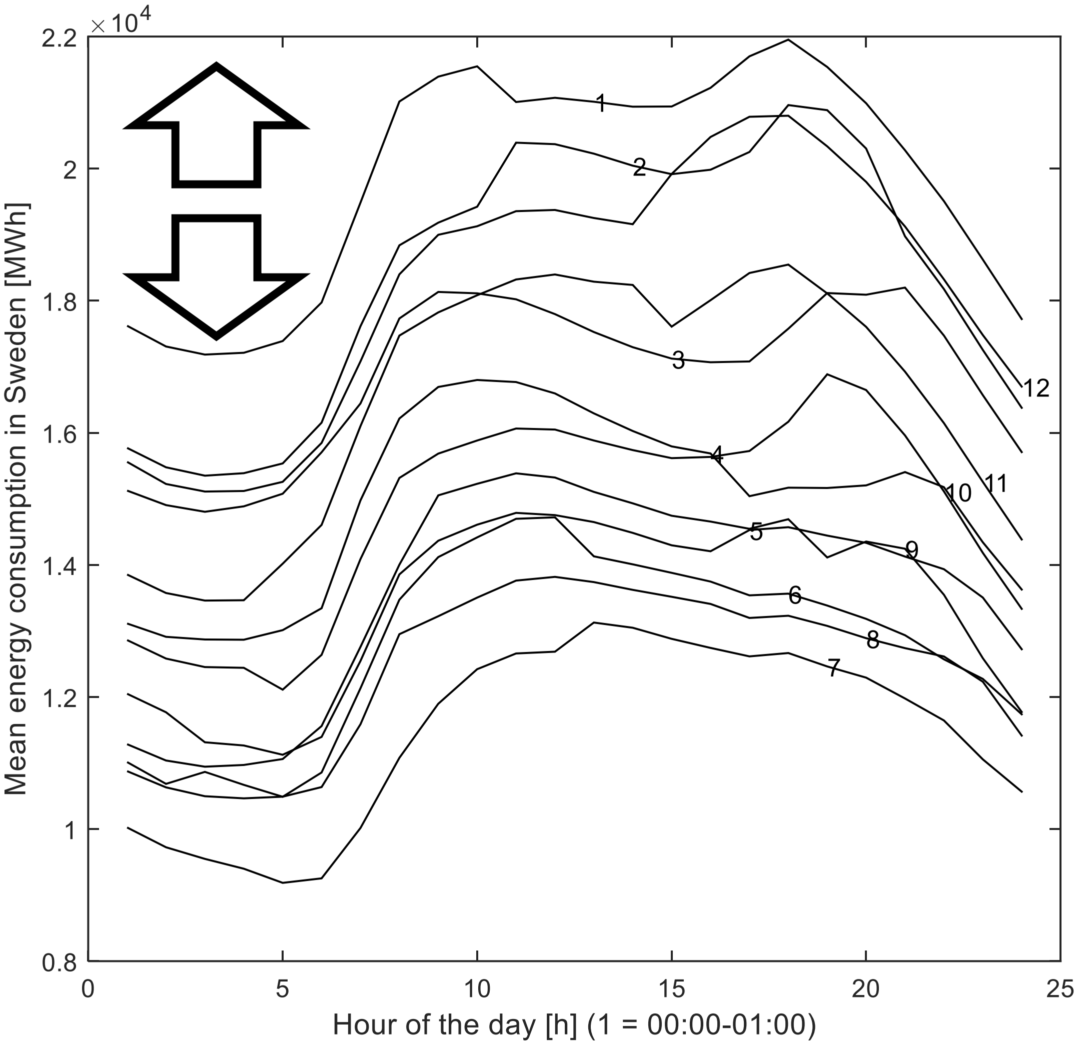

Figure 42: Mean energy consumption for each hour of the day for each month of 2014. The power gap is illustrated with arrows.

Disregarding other issues (such as energy distribution bottlenecks and possible total energy production per year) and only focusing on Figure 42, how large a fleet of PHEVs could the power production capacity in Sweden support?

Assume that the energy production system runs at maximum on the evenings of January (month 1) around 17:00. Further assume that consumers use the charging price optimization methods described in this thesis, thus charging their vehicles mainly between 00:00 and 06:00. Then there is a potential of unused power of approximately 3 GW during the night, even in January, see the arrows in Figure 42. Using the mean power from charging session 2 yields

$$\frac{3\,000\,000\,000}{2114} \approx 1\,419\,111$$

That's 1.4 million vehicles. The total number of registered cars in use in Sweden are 4.401 million (SCB, 2013, p. 200). Thus around 30% of the Swedish car fleet could potentially run on electricity. Looking at other months of the year, the potential is of course even bigger. Disregarding January, almost 50% of the Swedish car fleet could potentially be PHEVs, being charged during the night.

Additionally, this thesis has used a total driving distance of 14 600 km per car per year. In reality, the average driving distance per car per year in Sweden is approximately 12 180 km (SCB, 2013, p. 190), giving headroom for an even larger share of the car fleet to be powered by electricity.

One feature that might be important for this to succeed is to introduce some random variation in the charging station timer. To avoid spikes in power usage at the very start of certain hours with low energy prices, some variation or random delay could be introduced.

To summarize, using electricity pricing as an instrument for decentralized management of aggregated grid loads caused by vehicle charging, should be possible. This is fully in line with Mohsenian Rad, et al. (2010a) and especially Qian, et al. (2011, p. 804), mentioned earlier in Chapter 3.

Note that Sarabi and Kefsi (2014) on the other hand, describes how to centrally plan vehicle charging with dynamic programming, a related but completely different approach.

8.7 Swedish energy taxation issues

The total price of electricity (TPoE) in Sweden for households is calculated as

$$\begin{aligned} TotalPriceOfElectricity &= (SpotPrice + EnergyTax \\ &+ TransmissionCharge + SpotSurcharge \\ &+ RenewableEnergyCertificateCost) \cdot (1 \\ &+ ValueAddedTax) \end{aligned} \tag{36}$$

Some of these variables vary with time, such as spot price and renewable energy certificate cost. Also, some places in Sweden has been granted lower energy tax. As an illustration, representative values for Linköping in the spring of 2015 is given:

- spot price = 0.25819 [SEK/kWh]
- energy tax = 0.293 [SEK/kWh]
- transmission charge = 0.18 [SEK/kWh]
- spot surcharge = 0.02 [SEK/kWh]
- renewable energy certificate cost = 0.025 [SEK/kWh]
- value-added tax (VAT) = 0.25

With these numbers, the TPoE is 0.9702 [SEK/kWh]. Consequently, taxes constitute a large share of the TPoE paid by households, and as such they have the potential to steer consumers.

As can be seen in Figure 42, power usage in Sweden fluctuate during the day. If peaks could be shaved off, money could be saved by less need of peaking power and load following power plants. Furthermore, this might also be good for the environment since these two types of power plants often use fossil fuels, especially with an international outlook.

Thus, if high prices are seen as a sign of high demand, and a control mechanism to make consumers move their energy usage to points in time with lower prices, it is important that the changes in the spot (market) electricity price fully filters through to the consumers. So what happens if the price of electricity doubles in our example above? Will the consumer have a strong incentive to move their consumption in time by e.g. investing in charging stations with timers?

With a doubled spot price the TPoE becomes 1.293 [SEK/kWh]. An increase with 33% compared to earlier. If the spot price of electricity triples, the price increase in TPoE is only 67%.

As to better incentivize consumers to time shift their energy consumption, the taxes on electricity in Sweden have to move away from a per energy unit basis, and move towards per spot price cost basis. A simple solution would be

$$\begin{aligned} &TotalPriceOfElectricity \\ &\quad = SpotPrice \cdot (1 + FlexibleEnergyTax) \cdot (1 \\ &\quad + ValueAddedTax) \end{aligned} \tag{37}$$

The flexible energy tax could be chosen, on say a daily basis, to give exactly the same total tax revenue as the current tax regime.

By letting the TPoE closely follow the spot price by this formula, electricity pricing would be a much stronger instrument for decentralized management of aggregated grid loads caused by vehicle charging and other household and business activities.

8.8 Method

Total replicability of this thesis is difficult without e.g. finding a vehicle in the exact same condition, and running the exact same Matlab implementation of dynamic programming, on the exact same Matlab version. Nevertheless, replicability is kept high by e.g.:

- describing the vehicle in detail and how to totally deplete the battery.
- extensive descriptions of the simulations and dynamic programming implementation.
- an inclusion of the parameters used to run the dynamic programming algorithm.
- a thorough description on how to import the electricity pricing.

Reliability is also good, since few outside factors exist. Some might be the ambient temperature surrounding the vehicle and the temperature of the vehicle and battery itself.

Validity is rated as high since few hard contradictions has been found during the thesis work, most data line up as can be expected, especially regarding cost saving potential using different methods. The only disorders are how ambient temperature could not be shown to have an impact on vehicle charging energy usage.

While the dynamic programming didn't deliver perfect results, it has been shown that the deviations from perfect results are very small for the first night of 2014. Assuming this is a representative result, for the entire year, the total incurred loss due to suboptimal optimization for 2014 would be approximately 0.1 SEK. This cost is negligible seen from a consumer's perspective.

9 Conclusions

During this master's thesis, a number of vehicle charging measurements have been executed, and a lot of Matlab code have been written to implement charging simulation and optimization.

9.1 Key findings and main conclusions

Key findings are:

- For charging currents up to 10 A the charging profile looks more or less like a rectangle. Charging at 13 A seems to result in some kind of ramp down in the end, perhaps caused by heat or the charging algorithm used to charge Li-ion batteries. This behavior is likely to become even more pronounced as charging currents increase beyond 13 A. Surprisingly ambient temperature had no pinpointable impact on the charging profiles.
- There exist true realizable cost savings by controlling charging sessions with a simple timer. A general simplified recommendation for vehicle owners would be to start their vehicle's charging so that it is midway at approximately 03:00. For the Volvo V60 PHEV this means starting charging at 01:00 every night. A somewhat larger saving is probably also realizable by using known future energy prices to plan the charging session.

Moving the charging session start from 18:00 to the cheapest point in time, i.e. around 01:00, will probably have a very low impact on the lifestyle of the people living in a household, if any it is positive. Positive since during the night statistically most people are asleep, and not involved in activities that might compete for power usage with the vehicle charging.

Further, it should be possible to use electricity pricing as an instrument for decentralized management of aggregated grid loads caused by vehicle charging. The Swedish electrical grid should be able to handle a fleet of 1.5 million chargeable vehicles all year round.

It's worth noting that there isn't any consensus on electric vehicles being the dominant means of transportation in the future. Perhaps there will be no single dominant power source, like the internal combustion engine dominates today. Verhelst (2014) discusses a wealth of options, and arrives at the conclusion that the vehicles of the future will use synthesized (non-bio) methanol and internal combustion engines.

That said, the combination of household batteries such as the Tesla Powerwall and ever larger fleets of chargeable vehicles, are sure to make charging cost and energy optimizing an interesting subject for years to come.

9.2 Future work

Following is a list of possible extensions of the research in this thesis.

9.2.1 Immediate accessible range

It is open to discussion what consumers are willing to accept regarding immediate accessible range in pure electric vehicles. Will consumers accept having their vehicles charged for example between 02:00 and 06:00? This might mean that their vehicle lacks the range to get to a hospital if a health issue should arise at midnight.

9.2.2 The buffer battery

The Tesla Powerwall and other solutions for household buffer batteries will need further research. A buffer battery can be charged when prices are low. The popularity might depend upon battery prices, levels of efficiency, and how much TPoE varies during the day. As has been mention, TPoE variation in Sweden could be increased considerably.

9.2.3 Battery state of health impact on charging energy consumption

Battery SoH ought to have an impact on charging energy consumption. Measuring charging energy usage on two vehicles, prepared exactly the same, charging in the exact same location and ambient temperature, but having different mileage and thus SoH, could be interesting.

9.2.4 Charging indoors and outdoors

To increase the repeatability and record even more reliable charging profiles, it might be a good idea to do the charging sessions indoors. There the ambient temperature will fluctuate less, and be repeatable. One drawback is that the conditions will be less close to an average charging situation in Sweden. Another factor is time. According to preliminary tests done as preparation for this thesis, a vehicle could take up to 24 hours to fully adapt to 20°C if it previously had been out in 0°C. Scheduling proper time, 24 hours more or less, for battery cooling down and general temperature adaption, could also be relevant for doing further charging profile measurements outdoors.

9.2.5 Post charging cooling

When doing a non-logged charging of the Volvo V60 PHEV vehicle indoors at 20°C, the cooling fan ran for quite a while, perhaps 15 minutes, at the end of the charging session. This was probably to cool off the battery since charging to fully charged can generate a lot of heat. The energy for this cooling probably came from the electrical grid. Similar behavior might have been recorded in charging session 4. When the cooling fan was running the charge indicator light on the vehicle had a solid green light = fully charged. Future work might look into this and also measure how much energy is consumed.

9.2.6 Charging current ramp down

What were the causes of the ramp down seen in charging session 4? What will the charging profile look like charging the vehicle with its maximum 16 A current, perhaps outside on a hot summer's day?

9.2.7 Solving the boundary crossing issues

Here are some further untested ideas how to solve the boundary crossing issues with DP.

One method is to reach fully charged in a completely different way, and thus completely removing the issues caused by the boundary crossing. Instead of targeting an interval of e.g. 97 to 100% SoC, aim for 100% SoC and let the DP algorithm accept charging arrows reaching exactly or passing 100% SoC. Merely calculate when in time 100% is reached, and use that as basis in the CtG calculations of energy usage and energy cost. Christofer Sundström and Mattias Krysander suggested this method.

A third method might be to use "nearest neighbor" instead of interpolation (Guzzella and Sciarretta, 2013, p. 372).

9.2.8 Improvements on the timer started charging session

Could there be additional savings by making the charging vector, Equation (19), have a "soft" starting and ending? In the simulations in this thesis, E_1 is always at full power, and E_i is at the power "that's left". Perhaps money could be saved by default having $E_1=E_i$? That might be a better average fit than the current charging vector for the electricity pricing valley that usually occurs during the night.

9.2.9 Charging efficiency and ambient temperature

Could charging efficiency, which is different for different charging currents, be used to further optimize the charging, and make the modelling even more realistic? Could the ambient temperature, which might also affect charging efficiency, be taken into account?

9.2.10 Optimization made easy

Using DP enables the code and methods in this thesis to be developed and expanded in the future, taking more aspects into account. But solving the optimization problem solved in this thesis could be done much more easily. Automating the algorithm used to get the "handpicked" results, in section 7.1 Issues introduction, is not hard. For every charging session, check how many hours n should be charged at maximum power. Find the n hours with the n cheapest energy prices. That only leaves an hour of charging to place in time, the hour that doesn't charge at maximum power. Place that charging at the hour with the (n+1):th cheapest energy price. That's it!

Appendix

A Dynamic programming settings

These are the standard settings used for the dynamic programming optimization results in this thesis.

```
batteryCapacity 9384
discretizeCostToGoValuesWhenApplicableCostToGoMatrixBuild 0 or 1
discretizeCostToGoValuesWhenApplicableOptimalTrajectoryFind 0 or 1
samplesPerHour 1
yearToOptimize 2013 or 2014
energytax 2.930000e-01
energyTaxFlexible 0
transferFee 1.800000e-01
spotAddedFee 2.000000e-02
energyCertificateFee 2.500000e-02
VATlevel 2.500000e-01
startDay 0
endDay 363
chargingPowerMin 0
chargingPowerMax 2100
chargingPowerStep 5
socMin 1
socMax 100
socStep 1
socInit 1
socFinal 98
chargingStartTime 18
chargingDuration 13
```

B Brennenstuhl PM 231 E power meter

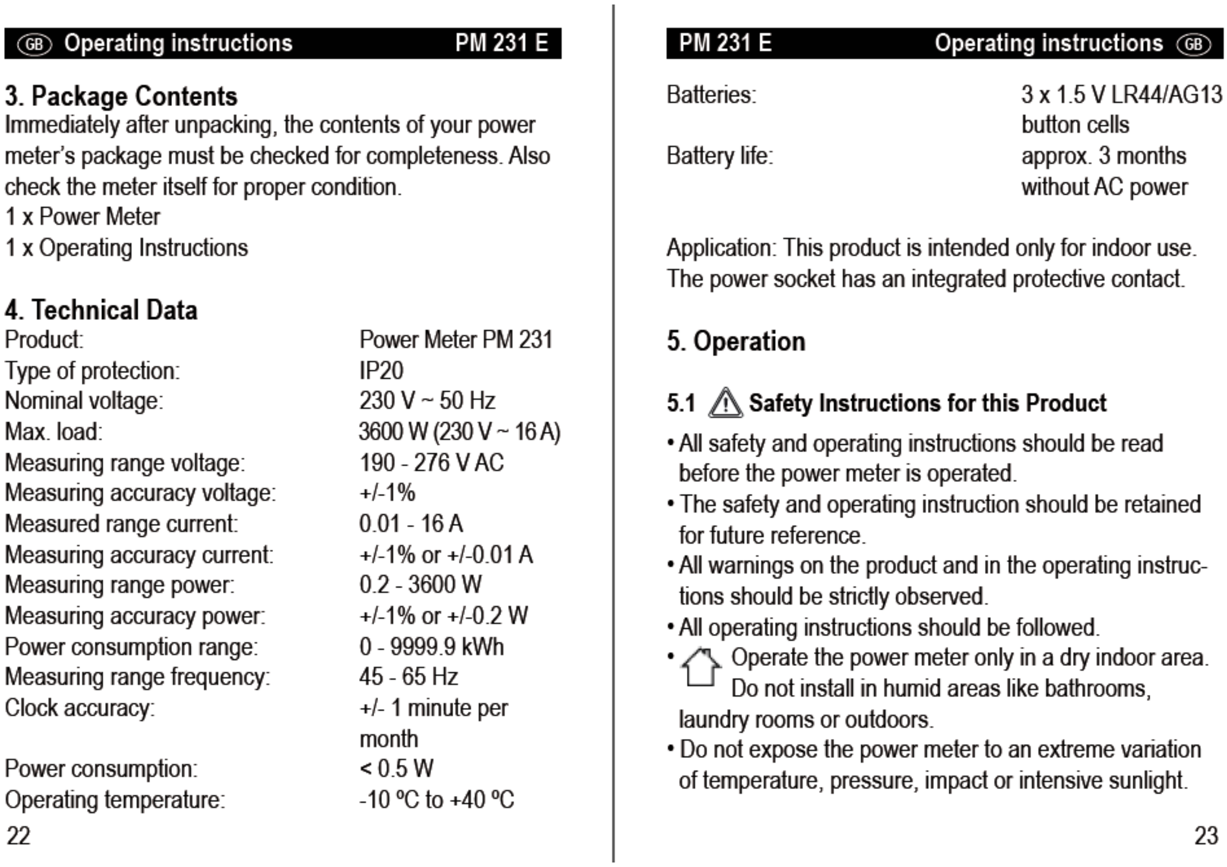

(GB) Operating instructions PM 231 E

3. Package Contents

Immediately after unpacking, the contents of your power meter's package must be checked for completeness. Also check the meter itself for proper condition.

1 x Power Meter
1 x Operating Instructions

4. Technical Data

Product:	Power Meter PM 231
Type of protection:	IP20
Nominal voltage:	230 V ~ 50 Hz
Max. load:	3600 W (230 V ~ 16 A)
Measuring range voltage:	190 - 276 V AC
Measuring accuracy voltage:	+/-1%
Measured range current:	0.01 - 16 A
Measuring accuracy current:	+/-1% or +/-0.01 A
Measuring range power:	0.2 - 3600 W
Measuring accuracy power:	+/-1% or +/-0.2 W
Power consumption range:	0 - 9999.9 kWh
Measuring range frequency:	45 - 65 Hz
Clock accuracy:	+/- 1 minute per month
Power consumption:	< 0.5 W
Operating temperature:	-10 ºC to +40 ºC
Batteries:	3 x 1.5 V LR44/AG13 button cells
Battery life:	approx. 3 months without AC power

22

PM 231 E Operating instructions (GB)

Application: This product is intended only for indoor use. The power socket has an integrated protective contact.

5. Operation

5.1 ⚠ Safety Instructions for this Product

- All safety and operating instructions should be read before the power meter is operated.
- The safety and operating instruction should be retained for future reference.
- All warnings on the product and in the operating instructions should be strictly observed.
- All operating instructions should be followed.
- ⌂ Operate the power meter only in a dry indoor area. Do not install in humid areas like bathrooms, laundry rooms or outdoors.
- Do not expose the power meter to an extreme variation of temperature, pressure, impact or intensive sunlight.

23

C Electricity prices import routine

This is a part of the electricity pricing import routine, responsible for handling summer time issues.

```
case 2013
spotPriceArrayNoNan(1:2138) = spotPriceArrayIncludingNan(1:2138);
spotPriceArrayNoNan(2139)=spotPriceArrayIncludingNan(2138);
spotPriceArrayNoNan(2140:7179)=spotPriceArrayIncludingNan(2140:7179);
spotPriceArrayNoNan(7180)=spotPriceArrayIncludingNan(7181);
spotPriceArrayNoNan(7181:8760)=spotPriceArrayIncludingNan(7182:8761);

case 2014
offsetSummer2Winter=-24; %när blir det sommartid detta året jämfört med 2013,
offset i timmar
offsetWinter2Summer=-24; %när blir det vintertid detta året jämfört med 2013,
offset i timmar
spotPriceArrayNoNan(1:(2138+offsetSummer2Winter)) =
spotPriceArrayIncludingNan(1:(2138+offsetSummer2Winter));
spotPriceArrayNoNan(2139+offsetSummer2Winter)=spotPriceArrayIncludingNan(2138+offse
tSummer2Winter);
spotPriceArrayNoNan((2140+offsetSummer2Winter):(7179+offsetWinter2Summer))=spotPric
eArrayIncludingNan((2140+offsetSummer2Winter):(7179+offsetWinter2Summer));
spotPriceArrayNoNan(7180+offsetWinter2Summer)=spotPriceArrayIncludingNan(7181+offse
tWinter2Summer);
spotPriceArrayNoNan((7181+offsetSummer2Winter):(8760))=spotPriceArrayIncludingNan((
7182+offsetSummer2Winter):(8761));
```

D Volvo V60 PHEV specifications

All measurements was done on the Volvo V60 PHEV:

- with the registration plate: MHP509.
- with the vehicle identification number (VIN): YV1GWAA50D1084646.
    - The "D" in the VIN-number indicates model year 2013, matching a pre-production version manufactured in mid-2012.
- that was manufactured 2012 and registered for usage in April/May 2012, according to the Swedish vehicle registry.
- that had mileage of circa 20 000 km.

This is the complete list of specifications for the production version of the vehicle (Volvo Cars, n.d.):

- Hybrid system: PHEV
- Combustion engine: 2.4 l, five cylinder diesel (215 hp, 440 Nm)
- Transmission: 6-speed automatic
- Electric motor / final drive: Synchronous AC (50 kW / 70 hp, 200 Nm) / 9.16
- Battery: Li-ion, 400 V, 11.2 kWh
- Weight compared to ordinary front-wheel drive V60: +300 kg (weight of battery: 150 kg)
- Emissions standard: Euro 5
- $C0_2$ emissions: 48 g/km (NEDC)
- Fuel consumption: 1.8 l/100 km
- Acceleration: 0-100 km/h: 6.1 s
- Top speed: 230 km/h (actively limited)
- Top speed with only electric motor active: 120 km/h (actively limited)
- Length of charging cable: 4.5 m
- Charging times (empty to full):
    - 16 A: 3.5 h
    - 10 A: 4.5 h
    - 6 A: 7.5 h
- Length: 4628 mm
- Width: 1865 mm
- Height: 1484 mm
- Luggage volume: 305 / 1126 l
- Maximum trailer weight: 1800 kg

Bibliography

Andrea, D., 2010. *Battery Management Systems for Large Lithium-Ion Battery Packs*. Norwood: Artech House.

Ashtari, A., Bibeau, E., Shahidinejad, S. and Molinski, T., 2012. PEV Charging Profile Prediction and Analysis Based on Vehicle Usage Data. *IEEE TRANSACTIONS ON SMART GRID*, 3(1), pp. 341-350.

Bai, S. and Lukic, M., 2013. Unified Active Filter and Energy Storage System for an MW Electric Vehicle Charging Station. *IEEE TRANSACTIONS ON POWER ELECTRONICS*, 28(12), pp. 5793-5803.

Batteryuniversity.com, n.d.. *BU-410: Charging at High and Low Temperatures.* [online] Available at: http://batteryuniversity.com/learn/article/charging_at_high_and_low_temperatures [Accessed 2015-01-14T10:29].

Bellman, R.E., 1957. *Dynamic programming.* Princeton: Princeton University Press.

Bertsekas, D.P., 2005. *Dynamic programming and optimal control, Volume 1.* 3rd ed. Nashua, NH: Athena Scientific.

Di Giorgio, A., Liberati, F. and Canale, S., 2013. Electric vehicles charging control in a smart grid: A model predictive control approach. *Control Engineering Practice*, 22, pp. 147-162.

Diallo, D., Benbouzid, M.E.H. and Masrur, M.A., 2013. (Guest Editorial Special Section on) Conditonal Monitoring and Fault Accommodation in Electric and Hybrid Propulsion Systems. *IEEE Transactions on vehicular technology*, 62(3), pp. 962-964.

Gao, S., Chua, K.T., Chan, C.C., Liu, C. and Wu, D., 2011. Optimal Control Framework and Scheme for Integrating Plug-in Hybrid Electric Vehicles into Grid. *Journal of Asian Electric Vehicles*, 9(1), pp. 1473-1481.

Guzzella, L. and Sciarretta, A., 2013. *Vehicle Propulsion Systems – Introduction to Modeling and Optimization.* Third Edition. Berlin, Heidelberg, Germany: Springer-Verlag.

International Standards Office, 2013. *ISO 15118-1:2013 – Road vehicles – Vehicle to grid communication interface –Part 1: General information and use-case definition*. Geneva: ISO.

Jian, L., Xue, H., Xu, G., Zhu, X., Zhao, D. and Shao, Z.Y., 2013. Regulated Charging of Plug-in Hybrid Electric Vehicles for Minimizing Load Variance in Household Smart Microgrid. *IEEE TRANSACTIONS ON INDUSTRIAL ELECTRONICS*, 60(8), pp. 3218-3226.

Jiang, T., Putrus, G., Gao, Z., Conti, M., McDonald, S. and Lacey, G., 2014. Development of a decentralized smart charge controller for electric vehicles. *Electrical Power and Energy Systems*, 61, pp. 355-370.

Kumar, K.N., Cheah, P.H., Sivaneasan, B., So, P.L. and Wang, D.Z.W., 2012. Electric Vehicle Charging Profile Prediction for Efficient Energy Management in Buildings. In: IEEE Singapore Sect., *2012 10th International Power & Energy Conference (IPEC)*. Ho Chi Minh City, Vietnam, 2012-12-12. Piscataway, NJ USA, Ho Chi Minh City, Vietnam: IEEE *(Country of Publication:* USA).

Lindergren, P., 2014. *Meeting with the CEO of Chargestorm Patrik Lindergren in Norrköping.* [conversation] (Personal communication, 2014-12-03).

Lindergren, P., 2015. *Email from the CEO of Chargestorm Patrik Lindergren.* [email] (Personal communication, 2015-05-05).

Madrid C., Argueta J. and Smith J., 1999. *Performance characterization – 1999 Nissan Altra-EV with lithium-ion battery*, Southern California EDISON, September 1999 [Report from corporation].

Maleki, H., Al Hallaj, S., Selman, R., Dinwiddie, R.B. and Wang, H., 1999. Thermal Properties of Lithium-Ion Battery and Components. *Journal of The Electrochemical Society*, 146(3), pp. 947-954.

Marra, F., Træholt, C., Larsen, E. and Wu, Q., 2010. Average behavior of battery-electric vehicles for distributed energy studies. In: IEEE Power and Energy Society: *Innovative Smart Grid Technologies Conference Europe (ISGT Europe).* Gothenburg, Sweden, 2010-10-11/2010-10-13. S.l.: IEEE.

Marra, F., Yang, G.Y., Træholt, C., Larsen, E., Nygaard Rasmussen, C. and You, S., 2012. Demand Profile Study of Battery Electric Vehicle under Different Charging Options. In: IEEE Power and Energy Society, *General Meeting 2012.* San Diego, Ca, USA, 2012-06-22/2012-06-26. S.l.: IEEE.

Mendoza A. and Argueta J., 2000. *Performance characterization - GM EV1 - Panasonic lead acid battery*, Southern California EDISON, April 2000 [Report from corporation].

Mohsenian-Rad, A.H., Wong, V.W.S., Jatskevich, J., Schober, R. and Leon-Garcia, A., 2010a. Autonomous Demand-Side Management Based on Game-Theoretic Energy Consumption Scheduling for the Future Smart Grid. *IEEE TRANSACTIONS ON SMART GRID*, 1(3), pp. 320-331.

Mohsenian-Rad, A.H. and Leon-Garcia, A., 2010b. Optimal Residential Load Control With Price Prediction in Real-Time Electricity Pricing Environments. *IEEE TRANSACTIONS ON SMART GRID*, 1(2), pp. 120-133.

Nord Pool Spot, n.d.-a. *Day-ahead market - Nord Pool Spot*. [online] Available at: http://www.nordpoolspot.com/How-does-it-work/Day-ahead-market-Elspot-/ [Accessed 2015-05-12T18:09].

Nord Pool Spot, n.d.-b. *elspot-prices_2013_hourly_sek.xls* and *elspot-prices_2014_hourly_sek.xls* price area: SE3. [online] Available at: http://www.nordpoolspot.com/historical-market-data/ [Accessed 2015-05-12T18:15].

Nord Pool Spot, n.d.-c. consumption-se-areas_2014_hourly.xls. [online] Available at: http://www.nordpoolspot.com/historical-market-data/ [Accessed 2015-05-14T16:23].

Oilprice.com, 2010. *How Different Energy Sources Create Electricity Price Differences Between Countries*. [online] Available at: http://oilprice.com/Energy/Energy-General/How-Different-Energy-Sources-Create-Electricity-Price-Differences-Between-Countries.html [Accessed 2015-06-02T19:30].

Pashajavid, E. and Golkar, M.A., 2014. Non-Gaussian multivariate modeling of plug-in electric vehicles load demand. *Electrical Power and Energy Systems*, 61, pp. 197-207.

PluginCars.com, 2014. *Buying Your First Home EV Charger*. [online] 2014-10-24 Available at: http://www.plugincars.com/quick-guide-buying-your-first-home-ev-charger-126875.html [Accessed 2014-12-17T18:21].

Qian, K., Zhou, C., Allan, M. and Yuan, Y., 2011. Modeling of Load Demand Due to EV Battery Charging in Distribution Systems. *IEEE TRANSACTIONS ON POWER SYSTEMS*, 26(2), pp. 802-810.

Sarabi, S. and Kefsi, L., 2014. Electric Vehicle Charging Strategy based on a Dynamic Programming Algorithm. In: IEEE, *2014 IEEE International Conference on Intelligent Energy and Power Systems (IEPS).* Kyiv (Kiev), Ukraine, 2014-06-02/2014-06-06. S.l.: IEEE.

SCB, 2013. *Transporter och kommunikationer - Statistisk Årsbok 2013*. [pdf] SCB. Available at: http://www.scb.se/statistik/_publikationer/OV0904_2013A01_BR_11_A01BR1301.pdf [Accessed 2015-05-14T08:50].

Sheikhi, A., Bahrami, S., Ranjbar, A.M. and Oraee, H., 2013. Strategic charging method for plugged in hybrid electric vehicles in smart grids; a game theoretic approach. *Electrical Power and Energy Systems*, 53, pp. 499-506.

SMHI, n.d.. *SMHI öppna data, Lufttemperatur, timvärde, Malmslätt.* [online] Available at: http://opendata-download-metobs.smhi.se/explore/?parameter=0# [Accessed 2015-05-12T17:02].

Sundström, O., Ambühl, D., Guzzella, L., 2010. On Implementation of Dynamic Programming for Optimal Control Problems with Final State Constraints. *Oil & Gas Science and Technology-Revue de l'IFP*, 65(1), pp. 91-102.

Telsa Motors, n.d. *Powerwall Tesla Home Battery.* [online] Available at: http://www.teslamotors.com/powerwall [Accessed 2015-05-10T16:50].

Volvo Cars, n.d.. *Volvo V60 Plug-in Hybrid.* [online] Available at: http://www.volvocars.com/se/campaigns/hybrid/pages/v60-plugin-hybrid.aspx [Accessed 2015-01-20T15:29].

Verhelst, S., 2014. Future vehicles will be driven by electricity, but not as you think [Point of View]. *Proceedings of the IEEE*, 102(10), pp. 1399-1403.

Weiller, C., 2011. Plug-in hybrid electric vehicle impacts on hourly electricity demand in the United States. *Energy Policy*, 39, pp. 3766-3778.

Upphovsrätt

Detta dokument hålls tillgängligt på Internet – eller dess framtida ersättare –från publiceringsdatum under förutsättning att inga extraordinära omständigheter uppstår.

Tillgång till dokumentet innebär tillstånd för var och en att läsa, ladda ner, skriva ut enstaka kopior för enskilt bruk och att använda det oförändrat för icke-kommersiell forskning och för undervisning. Överföring av upphovsrätten vid en senare tidpunkt kan inte upphäva detta tillstånd. All annan användning av dokumentet kräver upphovsmannens medgivande. För att garantera äktheten, säkerheten och tillgängligheten finns lösningar av teknisk och administrativ art.

Upphovsmannens ideella rätt innefattar rätt att bli nämnd som upphovsman i den omfattning som god sed kräver vid användning av dokumentet på ovan be-skrivna sätt samt skydd mot att dokumentet ändras eller presenteras i sådan form eller i sådant sammanhang som är kränkande för upphovsmannens litterära eller konstnärliga anseende eller egenart.

För ytterligare information om Linköping University Electronic Press se för-lagets hemsida http://www.ep.liu.se/

Copyright

The publishers will keep this document online on the Internet – or its possible replacement – from the date of publication barring exceptional circumstances.

The online availability of the document implies permanent permission for anyone to read, to download, or to print out single copies for his/hers own use and to use it unchanged for non-commercial research and educational purpose. Subsequent transfers of copyright cannot revoke this permission. All other uses of the document are conditional upon the consent of the copyright owner. The publisher has taken technical and administrative measures to assure authenticity, security and accessibility.

According to intellectual property law the author has the right to be mentioned when his/her work is accessed as described above and to be protected against infringement.

For additional information about the Linköping University Electronic Press and its procedures for publication and for assurance of document integrity, please refer to its www home page: http://www.ep.liu.se/.

© Markus Knutfelt 2015